https://www.mdc-berlin.de/de/veroeffentlichungstypen/clinical-journal-club

Als gemeinsame Einrichtung von MDC und Charité fördert das Experimental and Clinical Research Center die Zusammenarbeit zwischen Grundlagenwissenschaftlern und klinischen Forschern. Hier werden neue Ansätze für Diagnose, Prävention und Therapie von Herz-Kreislauf- und Stoffwechselerkrankungen, Krebs sowie neurologischen Erkrankungen entwickelt und zeitnah am Patienten eingesetzt. Sie sind eingeladen, uns beizutreten. Bewerben Sie sich!

The milky appearance of the patient's urine was concerning for chyluria, which was confirmed by identification of elevated urinary chylomicron and triglyceride levels. Chyluria results from abnormal communication between the lymphatic and urinary systems. Possible causes are lymphatic filariasis, congenital lymphatic malformations, post-traumatic lymphatic malformations, and lymphatic compression by tumors. After further work up, a chyluria due to a lymphatic–urinary fistula was diagnosed in this patient.

A 56-year-old woman presented to the emergency department with a 3-week history of leg swelling. On physical examination, pitting edema in both legs was seen and a urine sample was collected. Laboratory studies were notable for a low serum albumin level and a very elevated urinary protein-to-creatinine ratio. Which of the following diagnostic tests is most likely to explain the appearance of the patient's urine?

Urinary chylomicron and triglyceride levels

Urine culture

Urine microscopy for dysmorphic red cells

Urine microscopy for white cell casts

Urine protein electrophoresis

Lungenarterienembolie).
Dabei handelt es sich um eine lebensbedrohliche Verstopfung eines Blutgefäßes in der Lunge. Meistens wird sie durch ein Blutgerinnsel verursacht, das aus einer tiefen Bein- oder Beckenvenenthrombose über den Blutkreislauf in die Lunge geschwemmt wird.

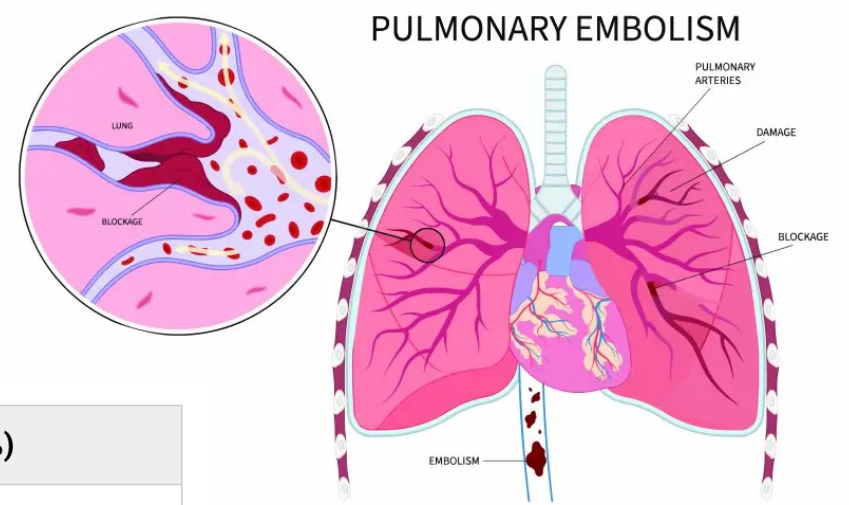

Typische Symptome
- Plötzlich einsetzende Atemnot
- Brustschmerzen, die sich beim tiefen Einatmen verschlimmern
- Herzrasen und innere Unruhe
- Schwindel, Schwäche oder Ohnmacht
- Selten: Blutiger Husten

	niedrig (< 1 %)	**mittel (3–15 %)**	**hoch (> 15 %)**
Schock oder Hypotonie	nein	nein	ja (-> Therapie)
RV-Dysfunktion	nein	nein/ja*	möglich
Troponin erhöht	nein	nein/ja*	möglich
Therapie	frühe Entlassung	stationäre Behandlung	Thrombolyse oder Embolektomie

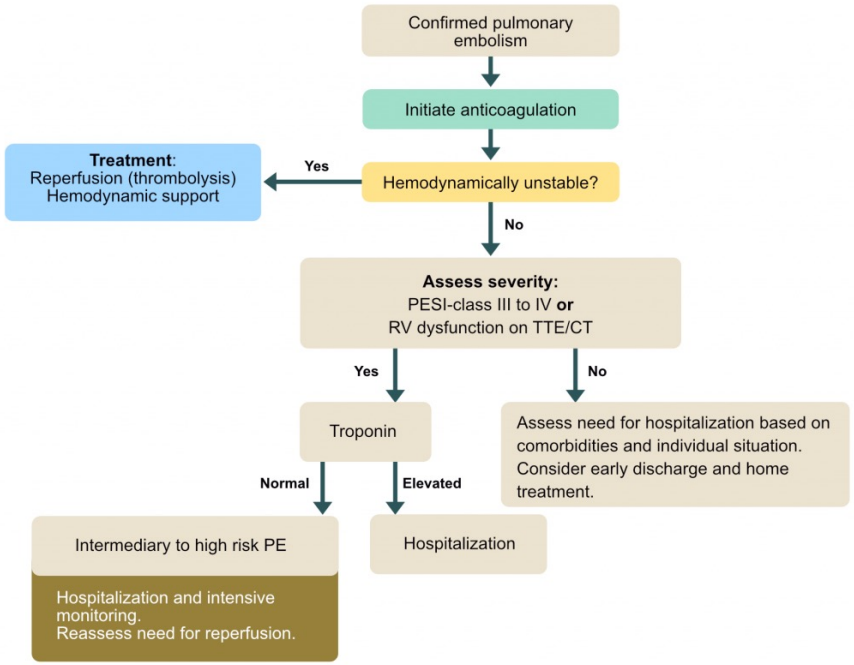

EKOS™-Systems

Das **EKOS™ Endovascular System** (von Boston Scientific) ist ein minimalinvasives Medizinsystem zur **ultraschallgestützten, kathetergeführten Thrombolyse** (Auflösung von Blutgerinnseln).

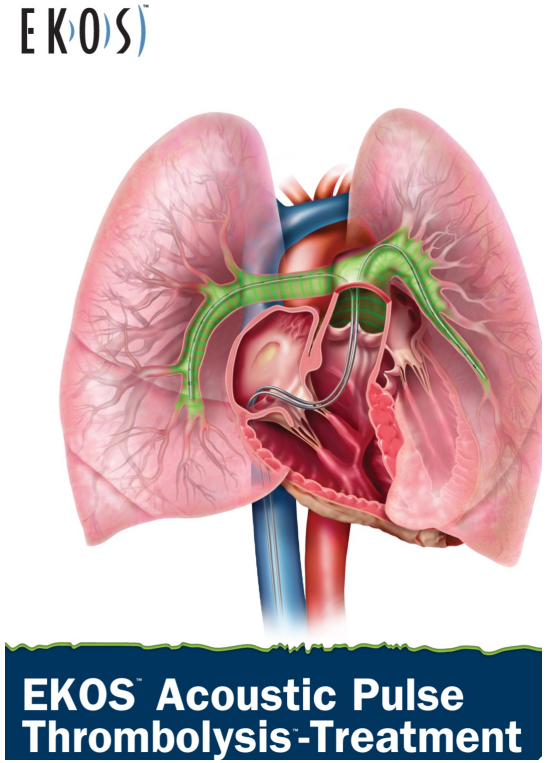

Funktionsweise (Acoustic Pulse Thrombolysis™)

Das System kombiniert die lokale Verabreichung eines Medikaments (Thrombolytikum wie t-PA) mit hochfrequentem Ultraschall mit niedriger Energie:

1.Katheter-Platzierung: Der Infusionskatheter wird direkt im Blutgerinnsel positioniert.

2.Ultraschall-Kern: Ein spezieller Draht mit Ultraschall-Sendern wird in den Katheter eingeführt.

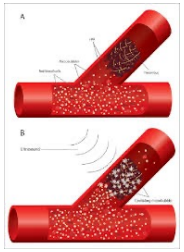

3.Fibrin-Auflockerung: Die Ultraschallwellen lockern das Fibringerüst des Gerinnsels mechanisch auf.

4.Effiziente Lyse: Das Medikament dringt tiefer in den Thrombus ein und erreicht mehr Rezeptoren.

Wichtigste Vorteile

•**Geringere Medikamentendosis**: Benötigt bis zu 90 % weniger Thrombolytika als eine klassische systemische Infusion über die Vene.

•**Minimiertes Blutungsrisiko**: Durch die extrem reduzierte Dosis sinkt die Gefahr schwerer systemischer Blutungen (z. B. Hirnblutungen) drastisch.

•**Schnelligkeit**: Führt oft schon innerhalb weniger Stunden zu einer signifikanten Reduktion der Thrombuslast.

Ultrasound-Facilitated, Catheter-Directed Fibrinolysis for Acute Pulmonary Embolism

Whether anticoagulation alone is an adequate treatment for acute, intermediate-risk pulmonary embolism is uncertain. We conducted a multinational, adaptive-design trial with blinded outcome adjudication. Patients with intermediate-risk pulmonary embolism (with a ratio of right ventricular end-diastolic diameter to left ventricular end-diastolic diameter of ≥1.0 and an elevated troponin level) were eligible if they had at least two indicators of cardiorespiratory distress (systolic blood pressure of ≤110 mm Hg, a heart rate of ≥100 beats per minute, or a respiratory rate of >20 breaths per minute). Patients were randomly assigned to undergo ultrasound-facilitated, catheter-directed fibrinolysis with alteplase plus anticoagulation (the intervention group) or anticoagulation alone (the control group) according to prespecified treatment protocols. The primary outcome was a composite of pulmonary embolism–related death, cardiorespiratory decompensation or collapse, or symptomatic recurrence of pulmonary embolism within 7 days.

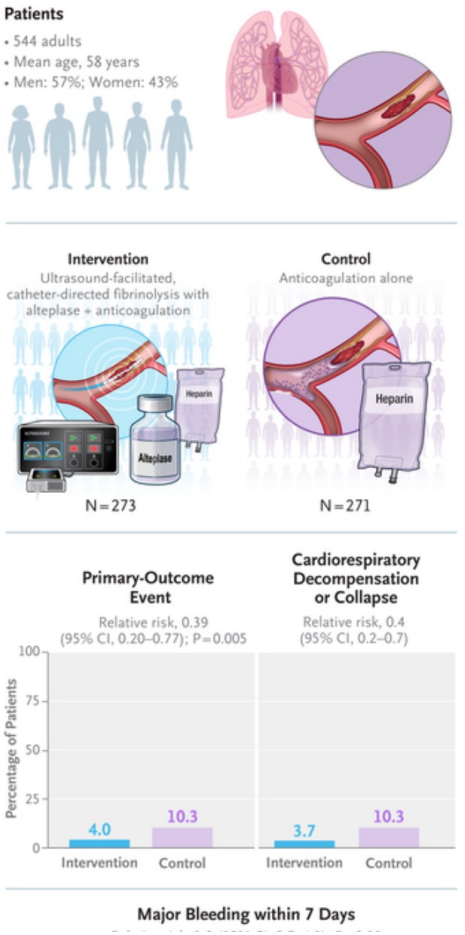

For patients who present with hemodynamic instability, the consensus is that early thrombus removal by means of systemically administered fibrinolysis, percutaneous catheter-directed interventions, or surgical embolectomy is indicated. On the other hand, the appropriate treatment strategy for patients whose condition appears to be stable but who have evidence of right ventricular dysfunction and clinical or laboratory signs that suggest a risk of cardiorespiratory decompensation remains unclear. In a large, randomized, controlled trial, intravenous fibrinolytic therapy prevented hemodynamic collapse in patients with intermediate-risk pulmonary embolism, but at the cost of an increased risk of major hemorrhage and stroke.

High-frequency, low-power ultrasound energy may potentiate fibrinolytic effects; the use of a device that administers such energy as adjunctive therapy with catheter-delivered tissue-type plasminogen activator (alteplase) may allow for lower doses of alteplase and a shorter duration of infusion while maintaining efficacy. Ultrasound-facilitated, catheter-directed fibrinolysis has been associated with early recovery of right ventricular function. To date, however, evidence has been lacking from randomized, controlled trials of the effect of this intervention, or of any other catheter-directed treatment, on relevant clinical outcomes in patients with acute pulmonary embolism, as compared with current usual care. We conducted the Higher-Risk Pulmonary Embolism Thrombolysis (HI-PEITHO) trial to assess whether ultrasound-facilitated, catheter-directed fibrinolysis combined with anticoagulation improves patient outcomes as compared with anticoagulation alone.

Patients, Randomization, and Trial Interventions

Adult patients 18 to 80 years of age with acute, intermediate-risk pulmonary embolism in at least one main or proximal lobar pulmonary artery as confirmed by computed tomographic pulmonary angiography were eligible if they presented with a ratio of right ventricular end-diastolic diameter to left ventricular end-diastolic diameter of 1.0 or higher and abnormal cardiac troponin levels and met at least two criteria for cardiorespiratory distress (systolic blood pressure of ≤110 mm Hg, tachycardia with a heart rate of ≥100 beats per minute, or tachypnea with a respiratory rate of >20 breaths per minute or hypoxemia) within the 6-hour window preceding randomization. Patients with persistent hemodynamic instability were excluded.

Patients were randomly assigned in a 1:1 ratio to undergo ultrasound-facilitated, catheter-directed fibrinolysis with alteplase plus anticoagulation (the intervention group) or to receive the current usual care, which is anticoagulation alone (the control group).

Outcome Measures

The primary outcome was a composite of pulmonary embolism–related death, cardiorespiratory collapse or decompensation, or nonfatal, symptomatic recurrence of pulmonary embolism, as confirmed by computed tomographic angiography, within 7 days after randomization.

Deeply buried in the supplement, I discovered what the patients actually received.

Pulmonary Embolism (PE)

The FDA recommended dose for PE is 100 mg infused intravenously over 2 hours. Parenteral anticoagulation should be started near the end of, or immediately following, the infusion when the partial thromboplastin time or thrombin time is equal to or lower than twice normal.

Intervention

Patients with bilateral proximal thrombus had two infusion catheters placed, one into each pulmonary artery. Alteplase (recombinant tissue-type plasminogen activator) was administered as a bolus of 2 mg per catheter, followed by infusion of 1 mg per catheter per hour for seven hours, for a total dose of 9 mg for unilateral therapy and 18 mg for bilateral therapy. The alteplase dose could be reduced, or the infusion stopped, in case of bleeding during the infusion. The sheath could be removed no earlier than one hour following infusion completion, with manual compression for hemostasis.

Patients in both treatment arms received initial anticoagulation with subcutaneous weight-adjusted low molecular weight heparin at a twice-daily dose regimen, or therapeutic doses of intravenous unfractionated heparin guided by activated partial thromboplastin time (aPTT) measurements as per locally established anticoagulation protocols. For patients in the intervention arm, this regimen was followed up to initiation of the procedure. During and up to four hours following ultrasound-facilitated catheter-directed fibrinolysis, intravenous unfractionated heparin was infused at a rate of 300-600 U per hour, with the exact dose determined by the treating physician. Subsequently, patients in the intervention arm were transitioned to full therapeutic-dose parenteral anticoagulation with twice-daily subcutaneous low molecular weight heparin or unfractionated heparin. Transition to oral anticoagulation occurred at least 24 hours after the end of fibrinolytic infusion for patients in the intervention arm and at least 24 hours after randomization in the control (anticoagulation-only) arm. Anticoagulant treatment was to continue for at least 3 months.

Characteristic	Intervention (N=273)	Control (N=271)	Standardized Difference†
			percent
Demographic data			
Age — yr	58.2±13.6	58.2±13.4	0.2
Female sex — no. (%)	114 (41.8)	118 (43.5)	3.6
Clinical status			
Body-mass index‡	32.9 ± 8.5	33.4 ± 8.2	5.0
Frailty index§	1.9 ± 0.7	1.9 ± 0.7	2.0
Duration of symptoms (current episode) — days¶	3.5 ± 3.3	3.9 ± 3.5	12.5
Dyspnea — no. (%)	254 (93.0)	242 (89.3)	13.2
Chest pain — no. (%)	87 (31.9)	101 (37.3)	11.4
Syncope — no. (%)	67 (24.5)	64 (23.6)	2.2
Tachycardia — no. (%)‖	210 (76.9)	215 (79.3)	5.8
Prolonged hypotension — no. (%)	4 (1.5)	6 (2.2)	5.6
Tachypnea — no. (%)**	118 (43.2)	142 (52.4)	18.4
Hypoxemia — no. (%)	135 (49.5)	130 (48.0)	3.0
National Early Warning Score††	6.0±1.9	6.0±1.9	2.2
Concomitant ultrasound-confirmed, lower-extremity deep-vein thrombosis — no. (%)			
Yes	107 (39.2)	109 (40.2)	2.1
No	82 (30.0)	86 (31.7)	
Ultrasound not performed	84 (30.8)	76 (28.0)	
Imaging findings			
Bilateral pulmonary embolism — no. (%)‡‡	251 (91.9)	262 (96.7)	20.6
RV:LV ratio§§	1.6±0.5	1.5±0.4	12.5
Medical history — no. (%)			
Congestive heart failure			
Yes	4 (1.5)	9 (3.3)	12.2
No	267 (97.8)	259 (95.6)	
Unknown	2 (0.7)	3 (1.1)	
Transient ischemic attack or stroke			
Yes	7 (2.6)	11 (4.1)	8.4
No	266 (97.4)	259 (95.6)	
Unknown	0	1 (0.4)	
Current or previous cancer¶¶			
Yes	29 (10.6)	21 (7.7)	10.0
No	236 (86.4)	249 (91.9)	
Unknown	8 (2.9)	1 (0.4)	
Chronic obstructive pulmonary disease			
Yes	13 (4.8)	14 (5.2)	1.9
No	256 (93.8)	247 (91.1)	
Unknown	4 (1.5)	10 (3.7)	

Clinical Efficacy Outcomes

Outcome	Intervention (N=273)		Control (N=271)		Relative Risk (95% CI)†
	no. of patients	*% (95% CI)†*	*no. of patients*	*% (95% CI)†*	
Any primary-outcome event	11	4.0 (2.3–7.1)	28	10.3 (7.2–14.5)	0.39 (0.20–0.77)‡
Components of the primary outcome					
Pulmonary embolism–related death	3	1.1 (0.4–3.2)	1	0.4 (0.1–2.1)	3.0 (0.3–28.5)
Cardiorespiratory decompensation or collapse	10	3.7 (2.0–6.6)	28	10.3 (7.2–14.5)	0.4 (0.2–0.7)
Recurrence of pulmonary embolism	1	0.4 (0.1–2.0)	1	0.4 (0.1–2.1)	1.0 (0.1–15.8)

Cumulative Major Bleeding Events through 30 Days

Event	Intervention (N=271)	Control (N=271)	Relative Risk (95% CI)†	P Value‡
	no. of patients (%)			
Major bleeding according to ISTH criteria				
Within 72 h	10 (3.7)	4 (1.5)	2.5 (0.8–7.9)	0.17
Within 7 days	11 (4.1)	6 (2.2)	1.8 (0.7–4.9)	0.32
Within 30 days	11 (4.1)	8 (3.0)	1.4 (0.6–3.4)	0.64
Moderate-to-severe bleeding within 7 days according to GUSTO criteria	9 (3.3)	4 (1.5)	2.3 (0.7–7.2)	0.26
Ischemic stroke				
Within 7 days	1 (0.4)	0	NE	1.00
Within 30 days	1 (0.4)	0	NE	1.00
Intracranial hemorrhage				
Within 7 days	0	0	NE	1.00
Within 30 days	0	0	NE	1.00

Mortality, Recurrence of Pulmonary Embolism, and Serious Adverse Events through 30 Days

Event	Intervention (N=271)	Control (N=271)	Relative Risk (95% CI)†
	no. of patients (%)		
Death from any cause through 7 days	3 (1.1)	2 (0.7)	1.5 (0.3–8.9)
Outcomes through 30 days			
Death from any cause	5 (1.8)	3 (1.1)	1.7 (0.4–6.9)
Symptomatic recurrence of pulmonary embolism	1 (0.4)	2 (0.7)	0.5 (0.0–5.5)
Any serious adverse event‡	40 (14.8)	44 (16.2)	0.9 (0.6–1.3)§

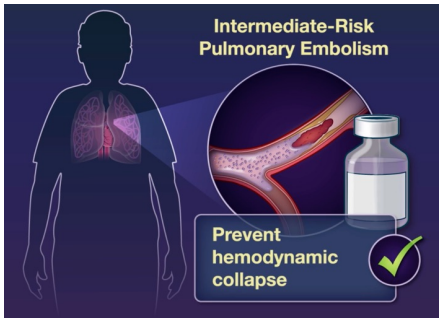

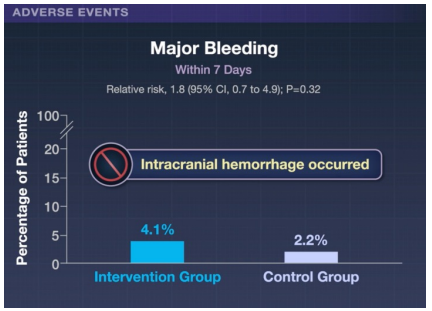

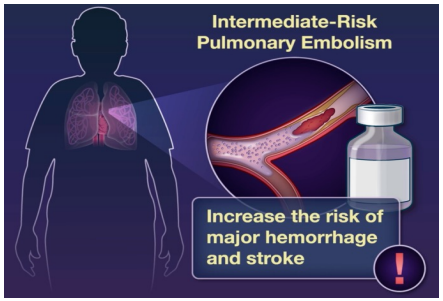

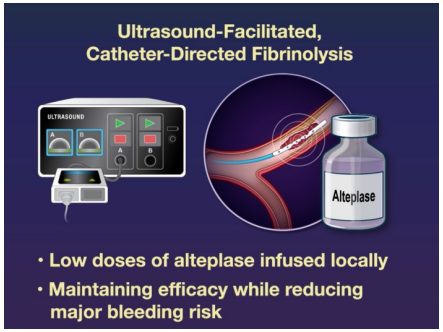

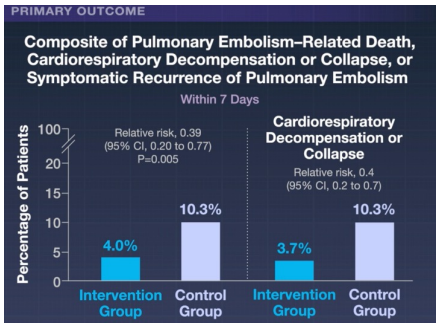

The dose of Alteplase was considerably lower than the dose for PE recommended by the FDA

EDITORIAL | SCIENCE BEHIND THE STUDY

Remuscularizing the Failing Human Heart

Heart failure with reduced ejection fraction remains a progressive and ultimately lethal condition for millions of patients worldwide. Although current therapies prolong survival and reduce symptoms, they do not address the fundamental pathologic substrate: the irreversible loss of cardiomyocytes and their replacement with fibrotic scar. Patients with advanced heart failure — particularly those with ischemic heart faiure — may lose as many as a billion cardiomyocytes, and the annual mortality among patients with advanced heart failure is approximately 50%. Among patients with heart failure of any severity, the inability of the heart to regenerate muscle and the physiological stress of a dilated failing heart result in a 5-year mortality of approximately 50%. For decades, the notion of replacing lost cells — of truly remuscularizing the human heart — has been a central aspiration of regenerative medicine. Major approaches currently being advanced for cardiac regeneration include unlocking cell division in resident cardiomyocytes, reprogramming of resident cardiac fibroblasts into induced cardiomyocytes, and transplantation of pluripotent stem-cell–derived cardiomyocytes, each with a goal of creating more contractile units.

In the BioVat study, the progenitor cells (cardiomyocytes and supporting stromal cells) are **allogeneic**. They originate from a standardized bank of healthy, human induced pluripotent stem cells (iPSCs) rather than being harvested from each individual patient.

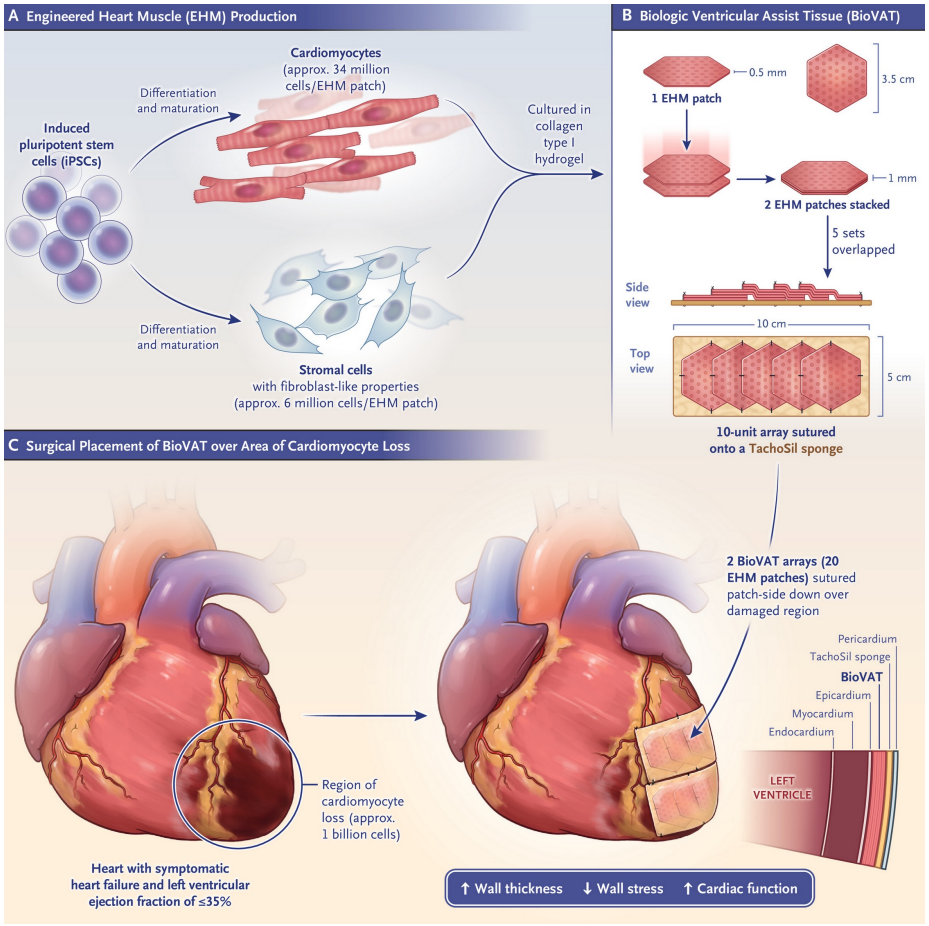

Biologic Ventricular Assist Tissue (BioVAT).

Zimmermann et al. report the experimental use of BioVAT in this issue of the *Journal*.[5] They made hexagonal patches of cardiac muscle from collagen and human induced pluripotent stem cell (iPSC)–derived cardiomyocytes and stromal cells, as described previously[9] (Panels A and B). These patches were surgically sewn onto the surface of damaged, thinned ventricular areas in patients with advanced heart failure. BioVAT placement increased wall thickness in these regions, decreased wall stress, and was followed by some improvement in cardiac function (Panel C).

Biologic ventricular assist tissue (BioVAT):
Thin patches of engineered cardiac muscle made up of stem-cell–derived cardiomyocytes and stromal cells. BioVAT may be surgically attached to the outside of the ventricle where damage has occurred. It may assist in ventricular function by reducing wall stress and increasing cardiac contractility.
Cardiac regeneration
Replacement of lost cardiac muscle with new contractile units, such as beating cardiac muscle cells derived from pluripotent stem cells, replication of existing cardiomyocytes, or conversion of noncardiomyocytes in the heart to cardiomyocytes.
Immunosuppression
The inhibition of unwanted immune responses that, in the context of allotransplantation, would otherwise result in the rejection of a foreign (or histoincompatible) organ or cellular graft. Immunosuppressive drugs are also used to treat autoimmune and inflammatory diseases. These drugs eliminate or block the activity of immune cells and soluble mediators secreted by immune cells (e.g., cytokines and antibodies) that recruit other immune cells. Immunosuppression can also occur as an unwanted side effect of drugs used in chemotherapy and as a consequence of the underlying pathologic process (e.g., cancer).
Induced pluripotent stem cell
A type of pluripotent stem cell derived from a nonpluripotent cell (e.g., an umbilical cord blood–derived hematopoietic stem cell) or an adult somatic cell (e.g., a fibroblast) through the forced expression of stem-cell–associated genes by transfection or transduction.

Stem-Cell–Derived Biologic Ventricular Assist Tissue in Heart Failure

Biologic ventricular assist tissue (BioVAT) is formulated from engineered heart muscle composed of cardiomyocytes and stromal cells derived from allogeneic induced pluripotent stem cells for cardiac remuscularization in patients with heart failure and a reduced left ventricular ejection fraction.
We conducted an open-label, phase 1–2 study of tissue-engineered heart repair by means of BioVAT transplantation. Patients with heart failure and a left ventricular ejection fraction of 35% or less and at least one hypokinetic or dyskinetic left ventricular segment were treated with BioVAT allografts, which consisted of 5, 10, or 20 engineered-heart-muscle units. All the patients received immunosuppression. Safety was assessed as adverse events related to the procedure. The primary efficacy end points were the change from baseline in the target heart-wall thickness, the left ventricular ejection fraction, and the Kansas City Cardiomyopathy Questionnaire–Overall Summary Score (KCCQ-OSS).

Conclusions

In this interim analysis, cardiac remuscularization with BioVAT was associated with an increase in the target heart-wall thickness, left ventricular ejection fraction, and KCCQ-OSS at 3 months; all the patients had at least one adverse event. Longer-term follow-up and further clinical investigation are warranted. (Funded by the German Center for Cardiovascular Research and Repairon; BioVAT-HF ClinicalTrials.gov number, NCT04396899.)

The most prevalent pathologic feature of heart failure with a reduced ejection fraction is a loss of cardiomyocytes in the heart. It is estimated that approximately 1 billion cardiomyocytes are lost in each patient with symptomatic heart failure with a reduced ejection fraction. Cardiac remuscularization by cardiomyocyte transplantation may present a viable measure to address this underlying condition.

The introduction of human embryonic and induced pluripotent stem cells in combination with the advent of robust protocols for their directed differentiation opened the door for applications in cell-based organ repair, with more than 100 registered clinical trials currently under way. Seven trials have been initiated with the goal of repairing the failing heart by transplantation of cardiomyocytes derived from pluripotent stem cells.

We have previously described a case of cardiac remuscularization in a patient who was treated with biologic ventricular assist tissue (BioVAT) consisting of 10 engineered-heart-muscle units derived from allogeneic induced pluripotent stem cells. Here, we report interim data from the phase 1–2 BioVAT-HF study, in which we evaluated the safety and efficacy of epicardial transplantation of BioVAT in patients with symptomatic heart failure with a reduced ejection fraction that was resistant to guideline-directed medical therapy.

Methods

Study Design and Patients

We conducted this open-label, two-part study at two centers in Germany (University Medical Centers Göttingen and Schleswig Holstein, Campus Lübeck) to assess the safety and initial efficacy of tissue-engineered heart repair by surgical BioVAT transplantation in patients with heart failure with a reduced ejection fraction. The study design is shown in Figure S1 in the Supplementary Appendix and the study protocol, both available with the full text of this article at NEJM.org.

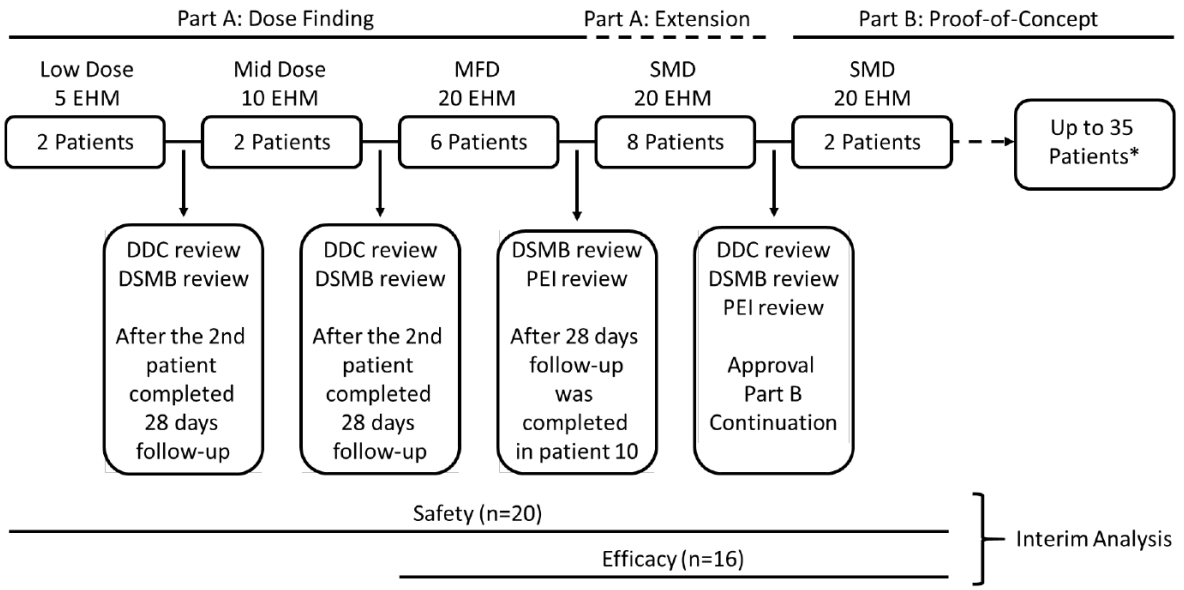

BioVAT denotes Biological Ventricular Assist Tissue, DDC Dose Determining Committee, DSMB Data Safety Monitoring Board, EHM engineered-heart-muscle, PEI Paul-Ehrlich-Institute, MFD maximal feasible dose, SMD safe maximal dose, and VAT Ventricular Assist Tissue.

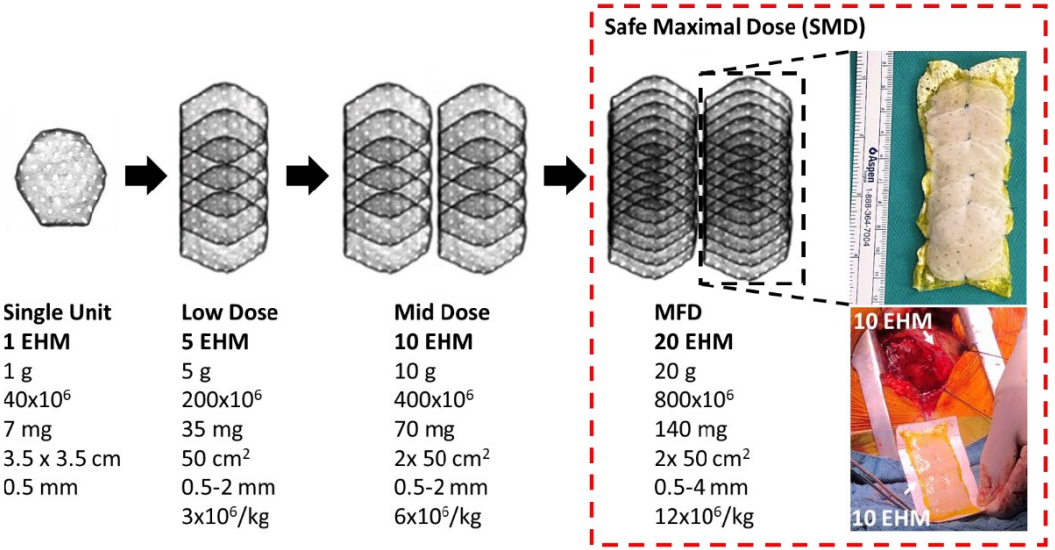

	Single Unit 1 EHM	Low Dose 5 EHM	Mid Dose 10 EHM	MFD 20 EHM
Wet weight:	1 g	5 g	10 g	20 g
Cells:	$40x10^6$	$200x10^6$	$400x10^6$	$800x10^6$
Collagen:	7 mg	35 mg	70 mg	140 mg
Area covered:	3.5 x 3.5 cm	50 cm^2	2x 50 cm^2	2x 50 cm^2
Thickness:	0.5 mm	0.5-2 mm	0.5-2 mm	0.5-4 mm
Dose:		$3x10^6$/kg	$6x10^5$/kg	$12x10^6$/kg

Schematic overview of BioVAT dose levels. Individual engineered-heart-muscle units (single units) are stacked as indicated to cover the surface of a TachoSil sponge (9.5 x 4.8 cm TachoSil, Corza Medical). At the low dose level, 5 engineered-heart-muscle units were sutured using Prolene 5-0 (Johnson & Johnson) to a single TachSil sponge. At the mid dose level, two 5 engineered-heart-muscle units per TachoSil assemblies were transplanted side-by-side. At the high-dose level (prespecified as the maximal feasible dose [MFD]), two 10 engineered-heart-muscle units per TachSil assemblies were transplanted side-by-side. The TachoSil sponge served as a security measure to stop epicardial bleeding, to reduce pericardial adhesions, and to ensure transfer and positioning of the engineered-heart-muscle units directly onto the target epicardium. A demonstration of spontaneous contractility of a single engineered-heart-muscle unit at the time of release for transplantation is shown in **Supplementary Video S1**.

In Part A (dose finding), which was designed to determine a safe maximal dose, we examined BioVAT assembled from 5, 10, and 20 engineered-heart-muscle units (Fig. S2). A minimum of 2 patients who were treated according to each dose level with uneventful follow-up for 28 days was considered as a safety measure (Fig. S3), because preclinical studies that tested intramyocardial injections of cardiomyocytes had identified this time window as particularly sensitive to engraftment arrhythmia. Part B (proof of concept) was designed to be initiated after the determination of a safe maximal dose in Part A and to include a minimum of 5 and a maximum of 30 patients for BioVAT transplantation. An interim analysis was scheduled after a minimum of 15 patients had been treated with the safe maximal dose in Parts A and B. The database lock for the interim analysis was performed on October 6, 2025.

In this interim analysis, we report safety outcomes for 20 patients: 2 treated with the low dose, 2 treated with the middle dose, and 16 treated with the safe maximal dose. We also report effectiveness for the 16 patients treated with the safe maximal dose.

Treatment

All the patients had received guideline-directed medical therapy, including device therapy with an implantable cardioverter–defibrillator (ICD) or cardiac resynchronization therapy with a defibrillator (CRT-D). Single engineered-heart-muscle units were prepared in a hexagonal format from freshly produced cardiomyocytes (34 million) and cryopreserved stromal cells (6 million) derived from induced pluripotent stem cells after suspension in a collagen type I hydrogel, as reported previously.

In the dose-finding cohort, patients received BioVAT assemblies from 5, 10, and 20 engineered-heart-muscle units, which represented dose levels of 0.05, 0.10, and 0.24 engineered-heart-muscle units per kilogram of body weight, respectively. At the point of care, single engineered-heart-muscle units were assembled into the prespecified dose of BioVAT and transplanted onto the target epicardial heart wall through a minimally invasive left lateral thoracotomy with standard off-pump heart exposure (Figure 1A). The engineered-heart-muscle units, which were supported by a TachoSil membrane, were sutured to the epicardium with Prolene 5-0 sutures (Johnson & Johnson) to cover the target area. Immunosuppression was initiated at 4 to 10 days before surgery, but the schedule could be adapted according to recommendations by the International Society for Heart and Lung Transplantation.

A BioVAT Assembly and Transplantation

B Voltage Map from an Electrophysiological Study

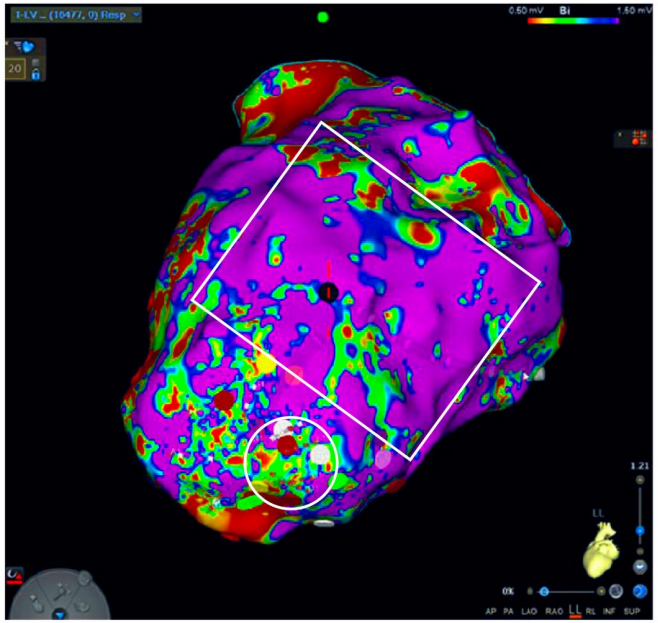

BioVAT Transplantation and Electrophysiological Mapping.

Panel A shows the process of assembly of the biologic ventricular assist tissue (BioVAT) array, including 10 engineered-heart-muscle units on a TachoSil sponge (upper panels) and transplantation onto the epicardium through a left lateral thoracotomy. The bottom left panel shows positioning of the first BioVAT array, constructed from 10 engineered-heart-muscle units, before suturing to the epicardium. The bottom right panel shows completion of suturing of 2 BioVAT arrays, each assembled from 10 engineered-heart-muscle units, onto the target heart wall. Panel B shows the voltage map from an electrophysiological study performed 220 days after BioVAT transplantation (left anterior oblique projection; CARTO, Biosense Webster). The patient was admitted for drug-resistant ventricular tachycardia. The voltage map shows a predominantly healthy myocardium (purple) interspersed with numerous small areas of reduced voltage (green-to-red areas), findings that are consistent with fibrosis commonly observed in nonischemic cardiomyopathy. The white circle indicates the ablation site where termination of the induced ventricular tachycardia was achieved. The white rectangle marks the location of the BioVAT transplant.

Characteristic	All Patients (N=26)
Age — yr	
Mean	59±10
Range	31–77
Male sex — no. (%)	23 (88)
Weight — kg	90±18
Body-mass index†	28.4±4.3
Heart rate — beats/min	68±11
Blood pressure — mm Hg	
Systolic	104±13
Diastolic	69±8
Heart failure–related features	
Duration before recruitment — yr	4.6±4.9
Left ventricular ejection fraction — %	25±7
NYHA classification — no. (%)	
Class II	1 (4)
Class III	25 (96)
Median NT-proBNP (IQR) — ng/liter	1422 (499–2849)
Medical history — no. (%)	
Coronary heart disease	23 (88)
Myocardial infarction	18 (69)
Nonischemic cardiomyopathy	3 (12)
Type 2 diabetes	8 (31)
Hypertension	15 (58)
Dyslipidemia	23 (88)
Atrial fibrillation	10 (38)
Estimated glomerular filtration rate — no. (%)	
≥90 ml/min/1.73 m^2	2 (8)
60–89 ml/min/1.73 m^2	8 (31)
31–59 ml/min/1.73 m^2	16 (62)

Summary of Adverse Events.

Adverse Event	Patients (N=20)
	no. of patients (%)
Any adverse event	20 (100)
Renal or urinary disorder	18 (90)
Infection or infestation	15 (75)
Cardiac disorder	14 (70)
Blood or lymphatic system disorder	10 (50)
Gastrointestinal disorder	7 (35)
Metabolism or nutrition disorder	7 (35)
Investigation†	5 (25)
Serious adverse event	
Any serious event	17 (85)
Immunosuppression	10 (50)
Underlying heart disease	9 (45)
Related to study procedure‡	6 (30)
Concurrent disease	4 (20)
Concomitant medication	2 (10)
Other reason	5 (25)
Death§	
From any cause	3 (15)
From cardiovascular cause	2 (10)
Arrhythmic event after BioVAT transplantation¶	
Ventricular tachycardia	3 (15)
Atrial fibrillation	1 (5)

Primary and Secondary Efficacy End Points, According to Dose.

End Point	At Baseline	At 3 Months	Latest Time Point†
Primary efficacy end points			
Low dose and middle dose: 5 to 10 engineered-heart-muscle units			
Target heart-wall thickness — mm; no. of patients	5.0±1.7; 3	8.3±1.5; 3	5.0; 1
Left ventricular ejection fraction — %; no. of patients	31±5; 4	32±5; 4	35±5; 3
KCCQ-OSS — points; no. of patients‡	58±29; 4	51±13; 4	41±8; 3
Safe maximal dose: 20 engineered-heart-muscle units			
Target heart-wall thickness — mm; no. of patients	6.4±1.1; 11	10.8±1.8; 10	8.6±1.1; 5
Left ventricular ejection fraction — %; no. of patients	24±5; 16	28±7; 12	31±5; 8
KCCQ-OSS — points; no. of patients‡	60±18; 16	61±15; 12	68±18; 5
Secondary efficacy end points			
Low dose and middle dose: 5 to 10 engineered-heart-muscle units			
NYHA classification — no./total no. (%)§			
Class II	0	1/4 (25)	1/3 (33)
Class III	4/4 (100)	3/4 (75)	2/3 (67)
Six-minute walk distance — m; no. of patients	403±93; 4	381±174; 4	356±167; 3
Peak maximal oxygen uptake — ml/kg/min; no. of patients	15.3±6.0; 4	12.6±2.8; 4	14.1; 2
Hand-grip strength — kg; no. of patients	40.7±8.6; 4	34.5±11.2; 4	39.1±14.2; 3
EQ-VAS — points; no. of patients¶	46±20; 4	50±14; 4	39; 2
Medication adherence — points; no. of patients‖	6±0; 4	6±0; 4	6; 2
Safe maximal dose: 20 engineered-heart-muscle units			
NYHA classification — no./total no. (%)§			
Class I	0	0	1/8 (12)
Class II	1/16 (6)	6/12 (50)	6/8 (75)
Class III	15/16 (94)	6/12 (50)	1/8 (12)
Six-minute walk distance — m; no. of patients	387±84; 16	411±92; 11	390±102; 8
Peak maximal oxygen uptake — ml/kg/min; no. of patients	12.5±5.0; 10	13.3±2.6; 6	12.7±3.8; 6
Hand-grip strength — kg; no. of patients	38.6±8.7; 15	32.4±10.1; 12	34.6±12.4; 8
EQ-VAS — points; no. of patients¶	58±16; 16	60±13; 12	71±11; 5
Medication adherence — points; no. of patients‖	5.7±0.7; 16	5.6±0.8; 11	6±0; 5

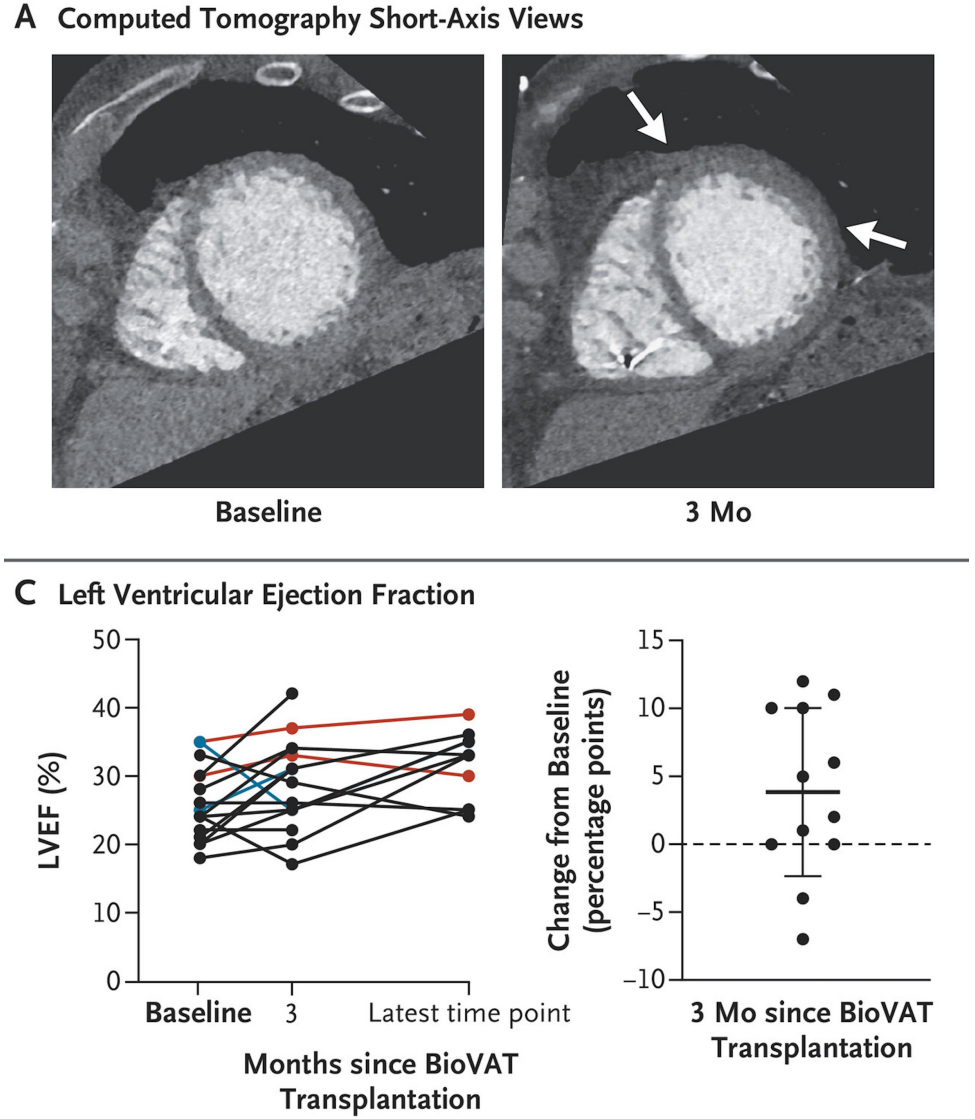

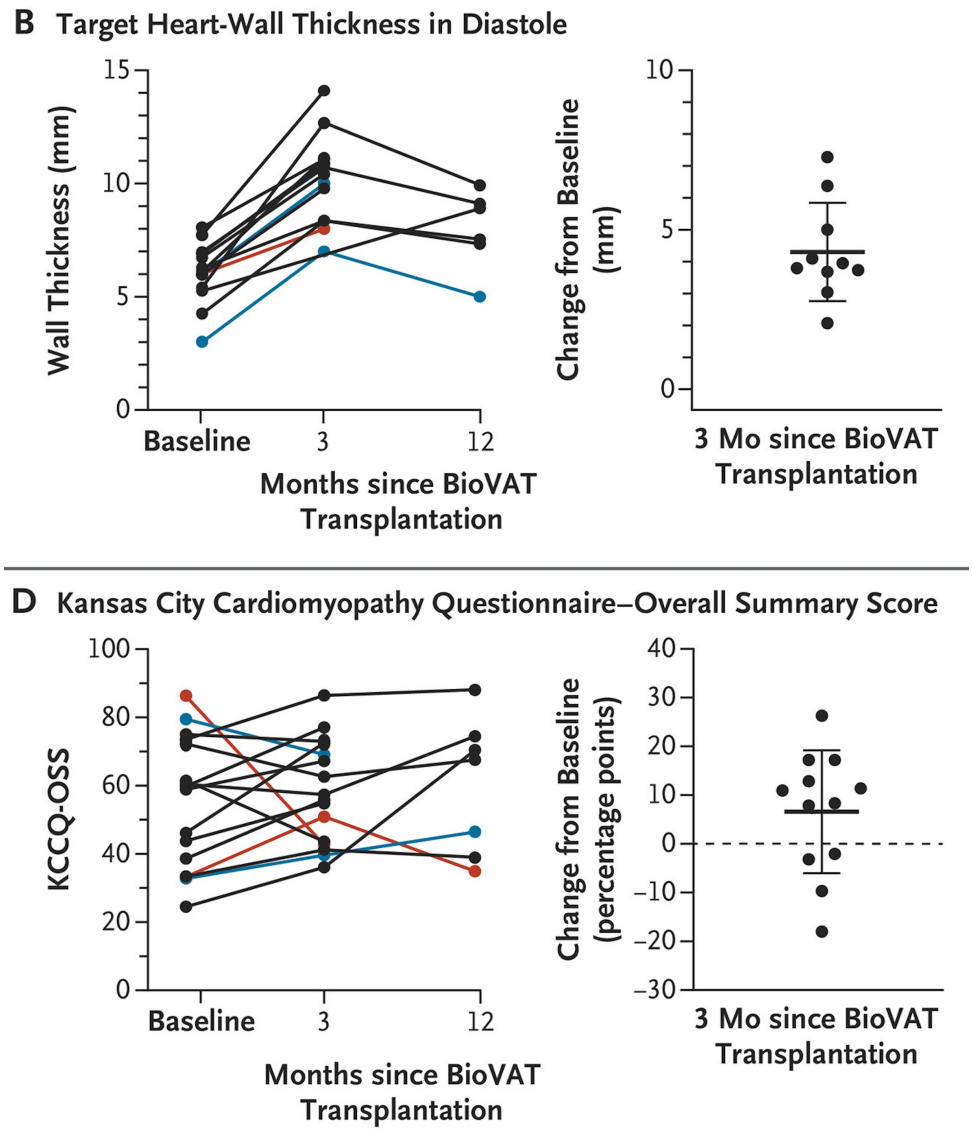

Panel C shows the left ventricular ejection fraction (LVEF) at baseline, at 3 months, and at the latest time point after transplantation for all the study patients (mean, 22 months; range, 6 to 52) (at left), as well as a summary of the change in the left ventricular ejection fraction at the time of the prespecified 3-month interim analysis in patients who were treated with the safe maximal dose (at right). Panel D shows the Kansas City Cardiomyopathy Questionnaire–Overall Summary Score (KCCQ-OSS) at baseline and at 3 months and 12 months after transplantation for all the study patients (at left), as well as a summary of the change in the KCCQ-OSS at the time of the prespecified 3-month interim analysis in patients treated with the safe maximal dose (at right). In Panels B, C, and D, all available data are from patients who were treated with BioVAT formulated from 5 engineered-heart-muscle units (red curvess), 10 engineered-heart-muscle units (blue curves), and 19 or 20 engineered-heart-muscle units (black curves) at a minimum follow-up of 3 months. In these panels, the black horizontal bar indicates the mean change from baseline, and the I bars indicate the standard deviation.

Discussion

All the study patients had symptomatic heart failure with a reduced left ventricular ejection fraction of 35% or less that was refractory to guideline-directed medical therapy. The dose-finding part of the study identified BioVAT assembled from 20 engineered-heart-muscle units as the safe maximal dose.

Of the 20 patients who underwent BioVAT transplantation, all had adverse events. Three patients had five episodes of ventricular tachycardia, which were believed to be unrelated to the BioVAT transplantation according to data obtained by epicardial mapping. The transplant recipients had increases in measures of the target heart-wall thickness in diastole, the left ventricular ejection fraction, and quality of life at the prespecified 3-month interim analysis.

The 3-month interim analysis time point was prespecified to inform the design of a subsequent phase 3 trial. The data that were obtained provide safety and effectiveness information for the use of BioVAT assembled from 20 engineered-heart-muscle units. Conceptually, adding contractile heart muscle to a hypocontractile area may support both systolic and diastolic function. Moreover, target heart-wall thickening will reduce stress on the heart wall, according to Laplace's law. Both effects may contribute to reverse remodeling of the left ventricle.

All the patients had adverse events, although only 3 of 20 patients had ventricular tachycardia, episodes that were possibly unrelated to the BioVAT transplant, and no treated patients had ventricular fibrillation. In alignment with the proposed mode of action, BioVAT transplantation resulted in increases in the target heart-wall thickness, left ventricular ejection fraction, and quality of life.

Zanidatamab (Handelsname: **Ziihera®**) ist ein neuartiger, bispezifischer monoklonaler Antikörper, der gezielt zur Behandlung bestimmter **HER2-positiver Krebserkrankungen** eingesetzt wird. Seit Anfang 2026 ist das Medikament auf dem deutschen Markt verfügbar.

Hauptindikation

Das Medikament ist als Monotherapie für Erwachsene mit einem **biliären Karzinom (Gallengangskrebs oder Gallenblasenkrebs)** zugelassen. Die Zulassung gilt für Fälle, die:

•**Inoperabel**, lokal fortgeschritten oder metastasiert sind.

•Einen nachgewiesenen, stark ausgeprägten **HER2-positiven Tumorstatus (IHC 3+)** aufweisen.

•Bereits mindestens eine vorherige systemische Krebstherapie (Chemotherapie) erhalten haben.

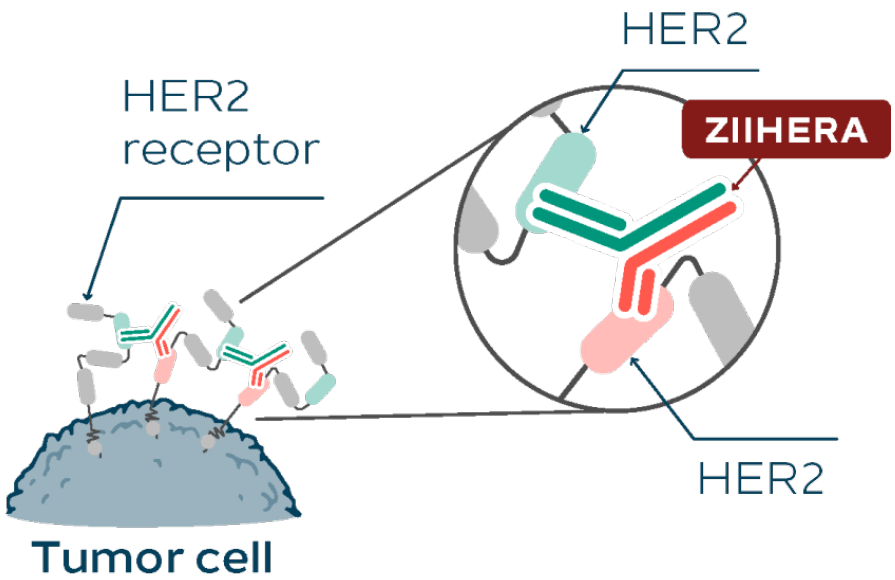

Approximately 15% to 25% of advanced esophageal adenocarcinomas overexpress or test positive for Human Epidermal Growth Factor Receptor 2 (HER2). However, the exact rate varies dramatically depending on the specific histological subtype and anatomical location of the cancer

Tislelizumab (Handelsname **Tevimbra**), einen modernen Arzneistoff aus der Gruppe der **Monoklonalen Antikörper**. Es handelt sich dabei um einen sogenannten **Immuncheckpoint-Inhibitor (PD-1-Inhibitor)**, der in der Krebsmedizin (Onkologie) eingesetzt wird.

Wirkungsweise

Der Wirkstoff blockiert gezielt den PD-1-Rezeptor auf den T-Zellen des körpereigenen Immunsystems. Krebszellen nutzen diesen Rezeptor normalerweise, um sich vor der Immunabwehr zu tarnen. Durch die Blockade von Tislelizumab wird diese Tarnung aufgehoben und das Immunsystem kann die Tumorzellen wieder erkennen und bekämpfen.

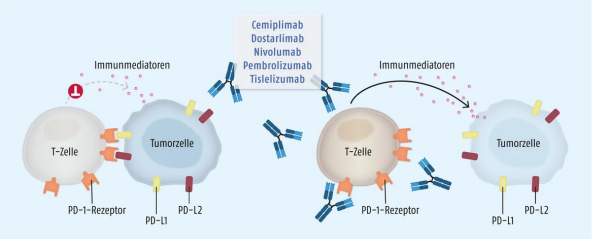

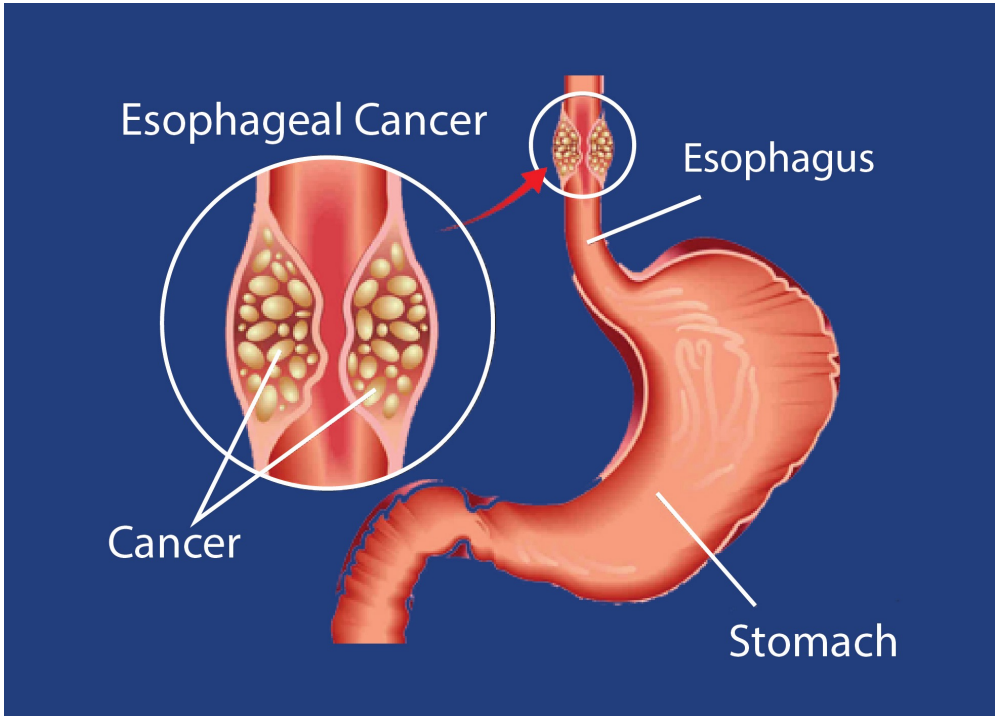

Zanidatamab with and without Tislelizumab in HER2-Positive Gastroesophageal Cancer

Zanidatamab, a dual human epidermal growth factor receptor 2 (HER2)–targeted bispecific antibody, plus chemotherapy both with and without tislelizumab (anti–programmed death 1), showed encouraging efficacy and safety as first-line therapy in phase 2 studies involving patients with HER2-positive gastroesophageal adenocarcinoma.

In an open-label, phase 3 trial, we randomly assigned, in a 1:1:1 ratio, patients with previously untreated, centrally confirmed HER2-positive advanced gastroesophageal adenocarcinoma to receive zanidatamab and tislelizumab plus chemotherapy, zanidatamab plus chemotherapy, or trastuzumab plus chemotherapy. The two primary end points were progression-free survival and overall survival.

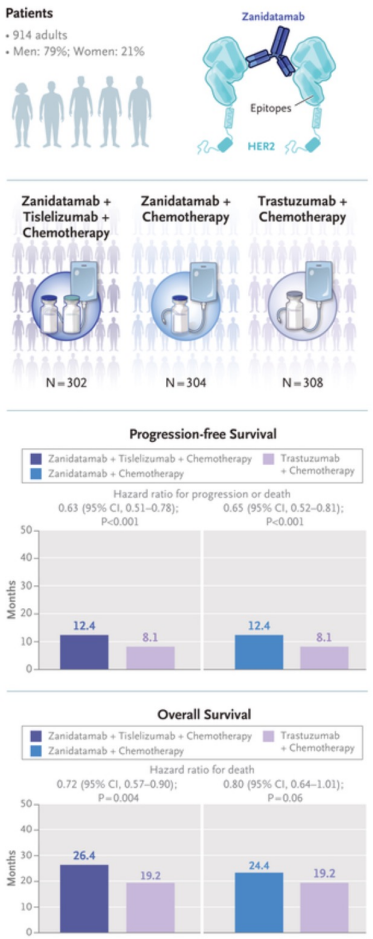

For more than a decade, the standard first-line therapy for these patients was platinum-based chemotherapy plus the HER2-targeted monoclonal antibody trastuzumab. More recently, the addition of pembrolizumab, a programmed death 1 (PD-1) inhibitor, to trastuzumab plus chemotherapy prolonged survival among patients with a programmed death ligand 1 (PD-L1) combined positive score of 1 or more. However, outcomes in this patient population remain modest, with a median progression-free survival of approximately 10 months and a median overall survival of 20 months.

Zanidatamab is a bispecific IgG1-like antibody that binds to extracellular domains 2 and 4 on HER2 in the trans configuration. This biparatopic binding enables zanidatamab to crosslink neighboring HER2 proteins, leading to receptor clustering. In preclinical studies, zanidatamab elicited antibody-mediated internalization and subsequent degradation of HER2, reduced downstream signaling, and promoted immune-mediated cytotoxicity through complement-dependent cytotoxicity and antibody-dependent cellular cytotoxicity and phagocytosis. Zanidatamab showed antitumor activity in both HER2 high– and HER2 low–expressing cell lines.

Tislelizumab is a PD-1 inhibitor engineered to minimize Fcγ receptor binding on macrophages, thereby limiting antibody-dependent cellular phagocytosis and potentially limiting acquired resistance. In the phase 3 RATIONALE-305 trial, tislelizumab plus chemotherapy significantly prolonged overall survival among patients with HER2-negative advanced gastric or gastroesophageal junction adenocarcinoma.

Methods

Trial Design and Patients

In this international, open-label, randomized, active-comparator, phase 3 trial, we enrolled patients (≥18 years of age) who had histologically confirmed, unresectable, locally advanced, recurrent or metastatic, HER2-positive adenocarcinoma of the stomach, gastroesophageal junction, or esophagus. HER2-positivity was defined as an IHC score of 3+ or as an IHC score of 2+ with ISH-positive status. Patients had to have an Eastern Cooperative Oncology Group (ECOG) performance-status score of 0 or 1 (range, 0 to 5, with higher numbers indicating greater disability). Enrollment was based on HER2 status as assessed at a central laboratory. PD-L1 expression was retrospectively assessed with the use of the VENTANA SP263 assay and the tumor area positivity (TAP) score, an approach consistent with the RATIONALE-305 trial. Patients were randomly assigned, in a 1:1:1 ratio, to receive zanidatamab and tislelizumab plus chemotherapy, zanidatamab plus chemotherapy, or trastuzumab plus chemotherapy.

End Points

The two primary end points were progression-free survival, as assessed by blinded independent central review according to the Response Evaluation Criteria in Solid Tumors, version 1.1, and overall survival.

Characteristic	Zanidatamab + Tislelizumab + Chemotherapy (N=302)	Zanidatamab + Chemotherapy (N=304)	Trastuzumab + Chemotherapy (N=308)
Age			
Median (range) — yr	63 (22–81)	62.5 (25–87)	64 (21–84)
Distribution — no. (%)			
<65 yr	163 (54.0)	174 (57.2)	162 (52.6)
≥65 yr	139 (46.0)	130 (42.8)	146 (47.4)
Sex — no. (%)			
Male	244 (80.8)	244 (80.3)	238 (77.3)
Female	58 (19.2)	60 (19.7)	70 (22.7)
Race or ethnic group — no. (%)†			
White	122 (40.4)	115 (37.8)	120 (39.0)
Asian	167 (55.3)	168 (55.3)	166 (53.9)
Black	1 (0.3)	3 (1.0)	1 (0.3)
American Indian or Alaska Native	3 (1.0)	5 (1.6)	9 (2.9)
Other or multiple	4 (1.3)	3 (1.0)	6 (1.9)
Not reported or unknown	5 (1.7)	10 (3.3)	6 (1.9)
Geographic region — no. (%)‡			
Asia	159 (52.6)	163 (53.6)	165 (53.6)
European Union or North America	95 (31.5)	91 (29.9)	93 (30.2)
Rest of the world	48 (15.9)	50 (16.4)	50 (16.2)
ECOG performance-status score — no. (%)§			
0	121 (40.1)	134 (44.1)	120 (39.0)
1	180 (59.6)	170 (55.9)	188 (61.0)
2	1 (0.3)	0	0
Primary tumor site — no. (%)			
Stomach	208 (68.9)	204 (67.1)	226 (73.4)
Esophagus	20 (6.6)	39 (12.8)	22 (7.1)
Gastroesophageal junction	74 (24.5)	61 (20.1)	60 (19.5)
Extent of disease — no. (%)			
Locally advanced unresectable	18 (6.0)	9 (3.0)	9 (2.9)
Metastatic	284 (94.0)	295 (97.0)	299 (97.1)
Previous gastrectomy — no. (%)	51 (16.9)	43 (14.1)	56 (18.2)
Measurable disease — no. (%)	280 (92.7)	280 (92.1)	283 (91.9)
HER2 status — no. (%)¶			
IHC 2+ and ISH-positive	51 (16.9)	51 (16.8)	52 (16.9)
IHC 3+	251 (83.1)	251 (82.6)	255 (82.8)
Other or missing data	0	2 (0.7)	1 (0.3)
PD-L1 status — no. (%)‖			
TAP score <1%	90 (29.8)	108 (35.5)	98 (31.8)
TAP score ≥1%	187 (61.9)	178 (58.6)	188 (61.0)
Missing data	25 (8.3)	18 (5.9)	22 (7.1)
Choice of chemotherapy backbone — no. (%)**			
Capecitabine plus oxaliplatin	273 (90.4)	276 (90.8)	282 (91.6)
Fluorouracil plus cisplatin	29 (9.6)	28 (9.2)	26 (8.4)

Adverse Events.

Event	Zanidatamab + Tislelizumab + Chemotherapy (N=294)††	Zanidatamab + Chemotherapy (N=305)††	Trastuzumab + Chemotherapy (N=302)
	number of patients with event (percent)		
Adverse event of any grade	293 (99.7)	301 (98.7)	297 (98.3)
Grade 3 or 4 event	217 (73.8)	200 (65.6)	203 (67.2)
Grade 5 event	28 (9.5)	25 (8.2)	22 (7.3)
Serious adverse event	172 (58.5)	150 (49.2)	128 (42.4)
Adverse event leading to discontinuation of any drug	134 (45.6)	113 (37.0)	92 (30.5)
Discontinuation of zanidatamab or trastuzumab	39 (13.3)	32 (10.5)	17 (5.6)
Discontinuation of tislelizumab	50 (17.0)	1 (0.3)‡‡	—
Adverse event leading to dose reduction	182 (61.9)	179 (58.7)	178 (58.9)
Adverse event leading to dose interruption	71 (24.1)	72 (23.6)	32 (10.6)
Adverse events of any grade occurring in ≥20% of the patients in any group			
Diarrhea	244 (83.0)	241 (79.0)	161 (53.3)
Nausea	164 (55.8)	166 (54.4)	144 (47.7)
Anemia	139 (47.3)	135 (44.3)	147 (48.7)
Decreased appetite	135 (45.9)	123 (40.3)	109 (36.1)
Vomiting	126 (42.9)	133 (43.6)	100 (33.1)
Hypokalemia	114 (38.8)	100 (32.8)	65 (21.5)
Weight decreased	104 (35.4)	109 (35.7)	65 (21.5)
Neutrophil count decreased	79 (26.9)	71 (23.3)	93 (30.8)
Peripheral sensory neuropathy	78 (26.5)	98 (32.1)	98 (32.5)
Infusion-related reaction	74 (25.2)	77 (25.2)	40 (13.2)
Platelet count decreased	68 (23.1)	63 (20.7)	94 (31.1)
Aspartate aminotransferase increased	63 (21.4)	61 (20.0)	64 (21.2)
Hypoalbuminemia	61 (20.7)	45 (14.8)	58 (19.2)
Fatigue	60 (20.4)	56 (18.4)	45 (14.9)
White-cell count decreased	60 (20.4)	50 (16.4)	62 (20.5)
Palmar–plantar erythrodysesthesia syndrome	54 (18.4)	51 (16.7)	64 (21.2)
Adverse events of grade ≥3 occurring in ≥5% of the patients in any group			
Diarrhea	73 (24.8)	61 (20.0)	39 (12.9)
Hypokalemia	65 (22.1)	57 (18.7)	33 (10.9)
Anemia	46 (15.6)	46 (15.1)	57 (18.9)
Neutrophil count decreased	32 (10.9)	24 (7.9)	36 (11.9)
Decreased appetite	23 (7.8)	20 (6.6)	17 (5.6)
Nausea	23 (7.8)	13 (4.3)	9 (3.0)
Weight decreased	21 (7.1)	19 (6.2)	9 (3.0)
Vomiting	16 (5.4)	11 (3.6)	11 (3.6)
Platelet count decreased	15 (5.1)	13 (4.3)	32 (10.6)
Neutropenia	14 (4.8)	14 (4.6)	17 (5.6)

A **Progression-free Survival with Zanidatamab+Tislelizumab+Chemotherapy vs. Trastuzumab+Chemotherapy**

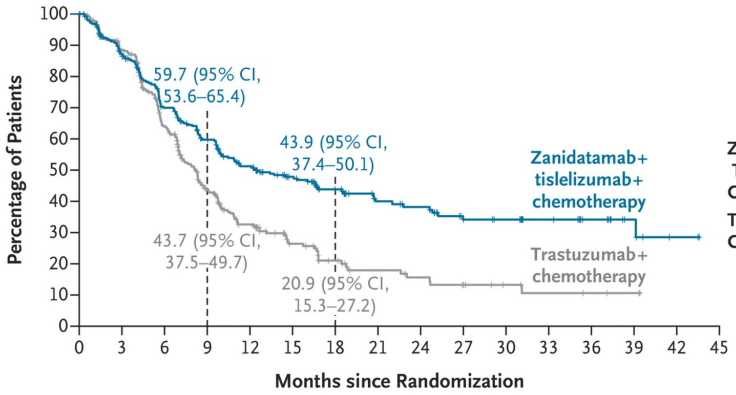

	No. of Events	Median Progression-free Survival (95% CI)
		mo
Zanidatamab+ Tislelizumab+ Chemotherapy	154	12.4 (9.8–18.5)
Trastuzumab+ Chemotherapy	196	8.1 (7.0–8.9)

Hazard ratio for disease progression or death, 0.63 (95% CI, 0.51–0.78)
P<0.001

No. at Risk

Zanidatamab+tislelizumab+ chemotherapy	302	240	183	147	113	90	65	46	42	30	27	20	13	6	2	0
Trastuzumab+chemotherapy	308	247	168	97	63	37	23	16	13	10	6	4	3	2	0	

B **Progression-free Survival with Zanidatamab+Chemotherapy vs. Trastuzumab+Chemotherapy**

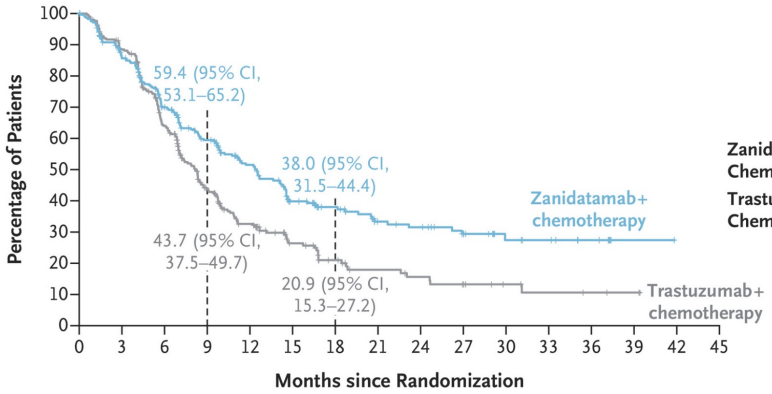

	No. of Events	Median Progression-free Survival (95% CI)
		mo
Zanidatamab+ Chemotherapy	160	12.4 (9.8–14.5)
Trastuzumab+ Chemotherapy	196	8.1 (7.0–8.9)

Hazard ratio for disease progression or death, 0.65 (95% CI, 0.52–0.81)
P<0.001

Progression-free Survival as Assessed by Blinded Independent Central Review.

Panel A shows the Kaplan–Meier estimates of progression-free survival for the comparison of zanidatamab and tislelizumab plus chemotherapy with trastuzumab plus chemotherapy. Panel B shows the Kaplan–Meier estimates of progression-free survival for the comparison of zanidatamab plus chemotherapy with trastuzumab plus chemotherapy. In these analyses, the first event was disease progression in 118 patients in the zanidatamab–tislelizumab–chemotherapy group and in 130 patients in the zanidatamab–chemotherapy group; the first event was death in 36 and 30 patients, respectively. In the trastuzumab–chemotherapy group, the first event was disease progression in 169 patients and death in 27. A total of 148 patients in the zanidatamab–tislelizumab–chemotherapy group, 144 in the zanidatamab–chemotherapy group, and 112 in the trastuzumab–chemotherapy group had their data censored (tick marks). Data were censored for the following reasons: no baseline or postbaseline tumor assessment (for 7 patients in the zanidatamab–tislelizumab–chemotherapy group, for 11 in the zanidatamab–chemotherapy group, and for 8 in the trastuzumab–chemotherapy group), receipt of new anticancer therapy (for 33, 41, and 50 patients, respectively), and missing data for at least two consecutive tumor assessments (for 6, 16, and 8 patients, respectively). The remaining patients were alive and had not had disease progression at the time of the analysis. The estimated percentages of patients who were alive and free from disease progression are shown at 9 months and 18 months.

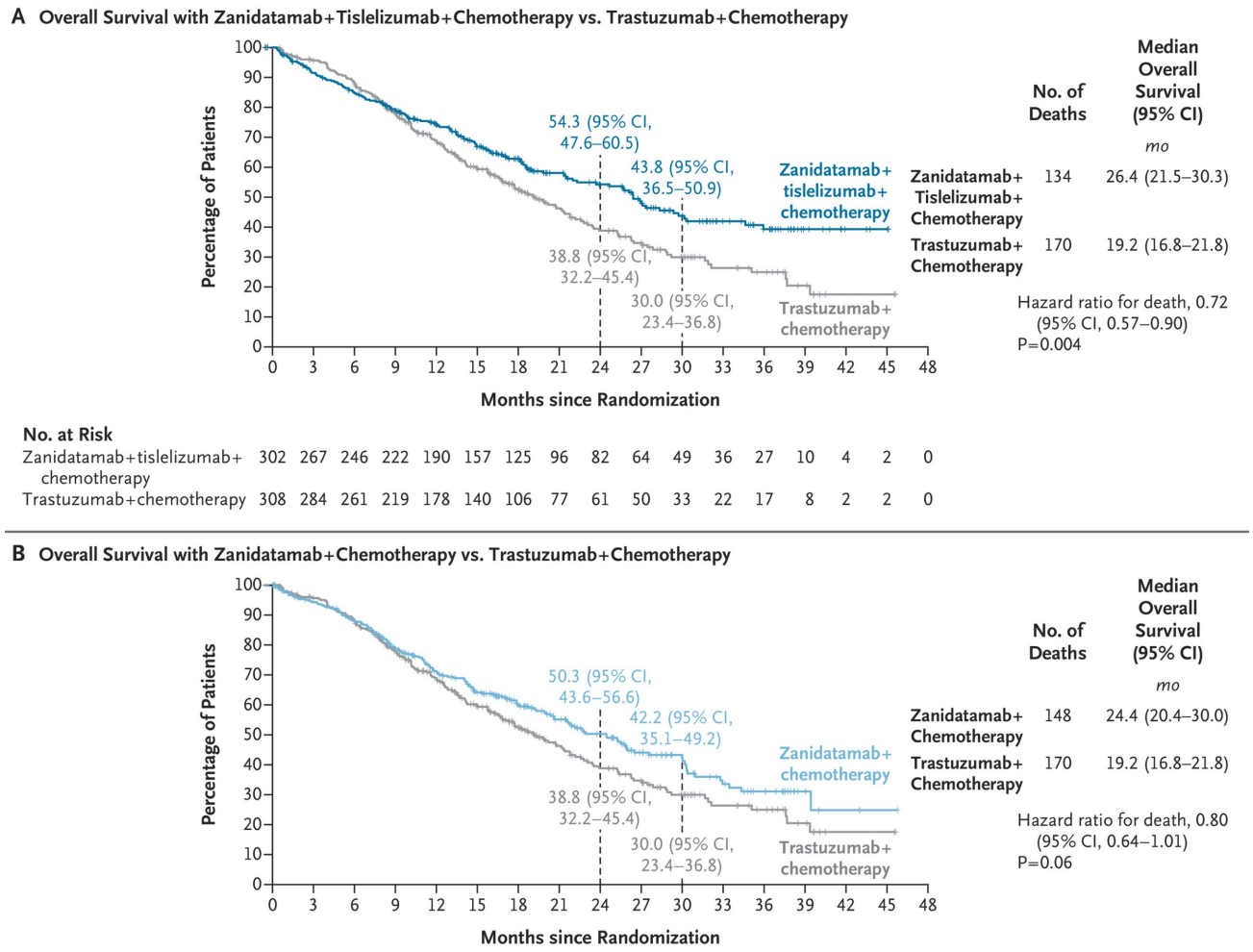

Overall Survival.

Panel A shows the Kaplan–Meier estimates of overall survival for the comparison of zanidatamab and tislelizumab plus chemotherapy with trastuzumab plus chemotherapy. Panel B shows the Kaplan–Meier estimates of overall survival for the comparison of zanidatamab plus chemotherapy with trastuzumab plus chemotherapy. At the time of this first interim analysis, 134 patients in the zanidatamab–tislelizumab–chemotherapy group, 148 patients in the zanidatamab–chemotherapy group, and 170 in the trastuzumab–chemotherapy group had died. A total of 168 patients in the zanidatamab–tislelizumab–chemotherapy group, 156 in the zanidatamab–chemotherapy group, and 138 in the trastuzumab–chemotherapy group had their data censored (tick marks). Data were censored owing to withdrawal of consent (for 20 patients in the zanidatamab–tislelizumab–chemotherapy group, for 16 in the zanidatamab–chemotherapy group, and for 19 in the trastuzumab–chemotherapy group), because of loss to follow-up (for 2, 1, and 1 patient, respectively), and for other reasons (for 1 patient in the zanidatamab–chemotherapy group). The remaining patients were alive at the time of the analysis. The estimated percentages of patients who were alive are shown at 24 months and 30 months. At the time of this first interim analysis, overall survival for the zanidatamab–chemotherapy group did not meet the prespecified criteria for significance as compared with trastuzumab–chemotherapy.

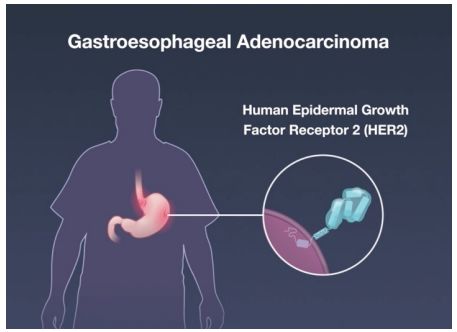
Gastroesophageal Adenocarcinoma
Human Epidermal Growth Factor Receptor 2 (HER2)

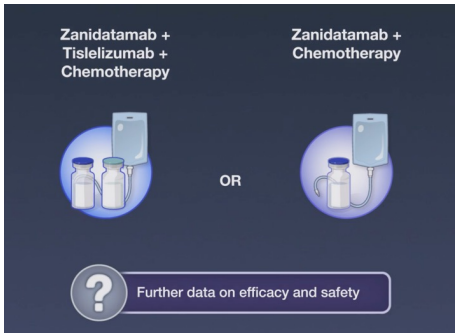
Zanidatamab + Tislelizumab + Chemotherapy
Zanidatamab + Chemotherapy
OR
Further data on efficacy and safety

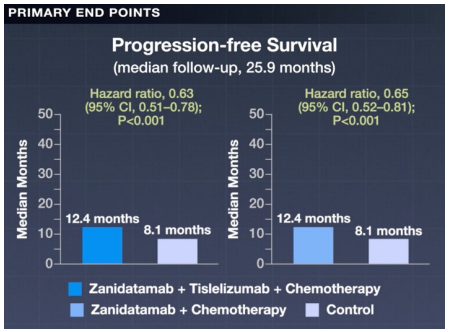
PRIMARY END POINTS
Progression-free Survival
(median follow-up, 25.9 months)
Hazard ratio, 0.63 (95% CI, 0.51–0.78); P<0.001
Hazard ratio, 0.65 (95% CI, 0.52–0.81); P<0.001
Median Months
12.4 months
8.1 months
12.4 months
8.1 months
Zanidatamab + Tislelizumab + Chemotherapy
Zanidatamab + Chemotherapy
Control

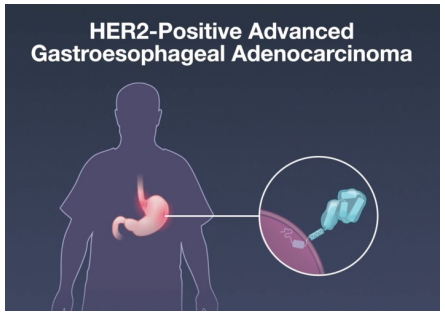
HER2-Positive Advanced Gastroesophageal Adenocarcinoma

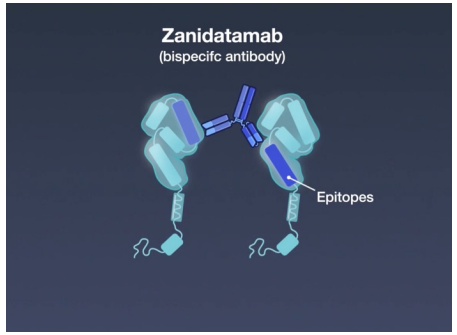
Zanidatamab
(bispecifc antibody)
Epitopes

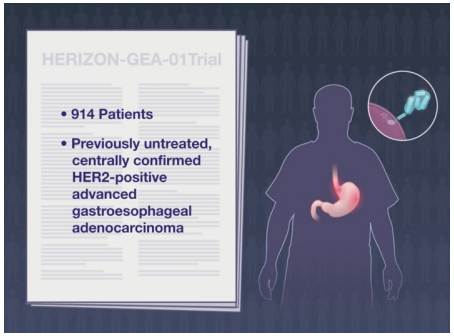
HERIZON-GEA-01Trial
• 914 Patients
• Previously untreated, centrally confirmed HER2-positive advanced gastroesophageal adenocarcinoma

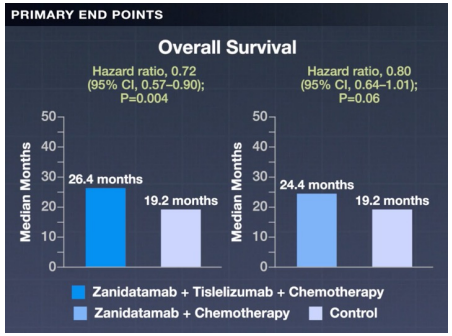
PRIMARY END POINTS
Overall Survival
Hazard ratio, 0.72 (95% CI, 0.57–0.90); P=0.004
Hazard ratio, 0.80 (95% CI, 0.64–1.01); P=0.06
Median Months
26.4 months
19.2 months
24.4 months
19.2 months
Zanidatamab + Tislelizumab + Chemotherapy
Zanidatamab + Chemotherapy
Control

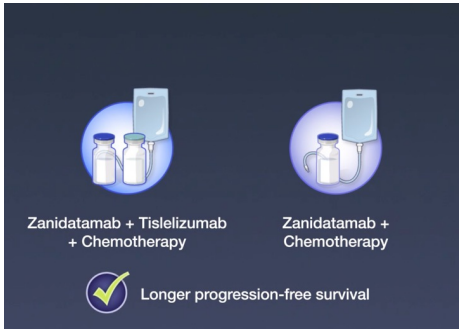
Zanidatamab + Tislelizumab + Chemotherapy
Zanidatamab + Chemotherapy
Longer progression-free survival

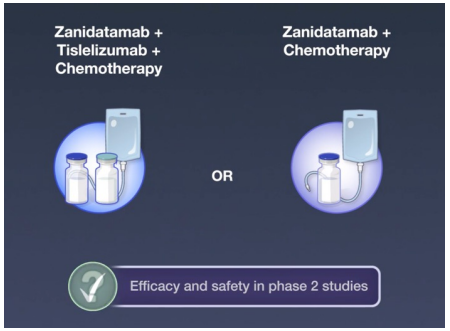
Zanidatamab + Tislelizumab + Chemotherapy
Zanidatamab + Chemotherapy
OR
Efficacy and safety in phase 2 studies

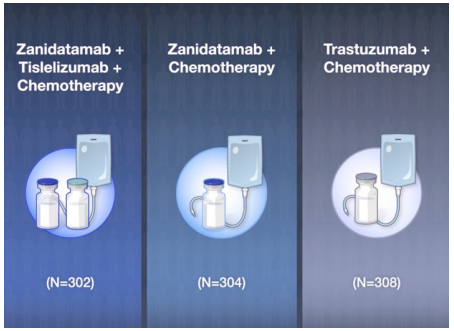
Zanidatamab + Tislelizumab + Chemotherapy
Zanidatamab + Chemotherapy
Trastuzumab + Chemotherapy
(N=302)
(N=304)
(N=308)

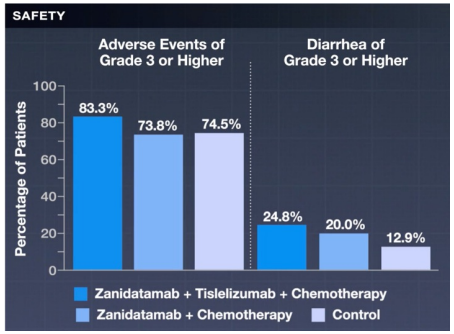
SAFETY
Adverse Events of Grade 3 or Higher
Diarrhea of Grade 3 or Higher
Percentage of Patients
83.3%
73.8%
74.5%
24.8%
20.0%
12.9%
Zanidatamab + Tislelizumab + Chemotherapy
Zanidatamab + Chemotherapy
Control

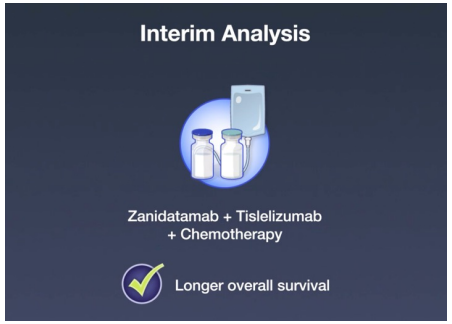
Interim Analysis
Zanidatamab + Tislelizumab + Chemotherapy
Longer overall survival

Die **Chiari-Malformation Typ 1 (CMI)** ist eine meist angeborene Fehlbildung der hinteren Schädelgrube, bei der Teile des Kleinhirns (die Kleinhirntonsillen) durch das Hinterhauptsloch (Foramen magnum) nach unten in den oberen Wirbelkanal rutschen. Da der Schädelknochen in diesem Bereich oft zu klein ist, werden die Nervenstrukturen komprimiert und die Zirkulation des Nervenwassers (Liquor) blockiert.

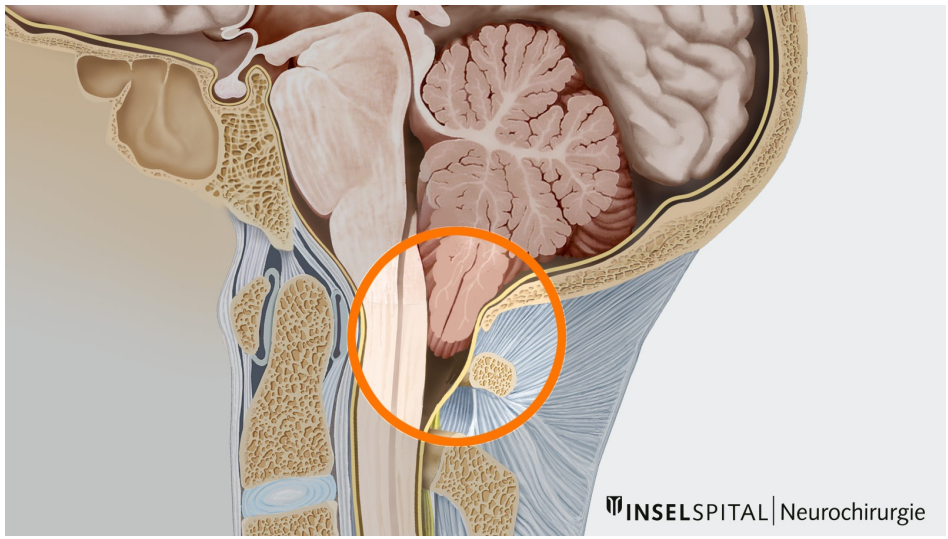

Häufige Begleiterkrankung: Syringomyelie

In vielen Fällen führt der gestörte Nervenwasserabfluss dazu, dass sich Flüssigkeit im Rückenmark ansammelt. Es bildet sich ein Hohlraum (eine sogenannte Syrinx). Diese Syringomyelie kann unbehandelt zu dauerhaften Nervenschäden führen

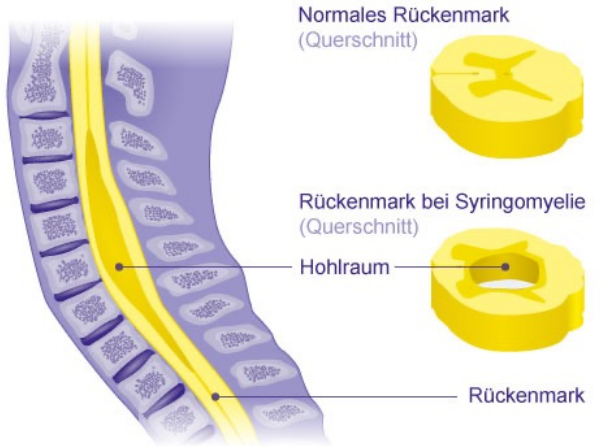

Was ist eine Syringomyelie?
Eine Syringomyelie beschreibt einen flüssigkeitsgefüllten Hohlraum innerhalb des Rückenmarks und tritt oftmals zusammen mit einer CMI auf. Sie kann aber auch durch andere Ursachen bedingt sein: infektiös, entzündlich, traumatisch oder durch einen Hydrocephalus (Wasserkopf) oder eine Raumforderung (z.B. Tumor). Die Syringomyelie im Rahmen einer CMI kommt wahrscheinlich zustande, wenn die CMI zu einem erhöhten Druck im Gehirn führt und daraufhin Hirnwasser in das Rückenmark austritt.

Decompression with or without Duraplasty for Chiari I and Syringomyelia

In children with Chiari type I malformation and syringomyelia, neurosurgical posterior fossa decompression (PFD) provides clinical improvement, but whether duraplasty (incising the dura and placing a dural graft) improves outcomes is unclear.

We conducted a multicenter, cluster-randomized, controlled trial of PFD with duraplasty (PFD-D) as compared with PFD alone. Persons 21 years of age or younger with cerebellar tonsillar ectopia of at least 5 mm and a maximum syrinx diameter of 3.0 to 9.9 mm were enrolled at 38 centers. Centers were cluster-randomized: all the participants within each center underwent the same intervention. The primary outcome was surgical complications within 6 months. Secondary outcomes were clinical improvement, syrinx reduction, and repeat decompression at 10 to 24 months and the change in overall health-related quality of life at 6 to 24 months.

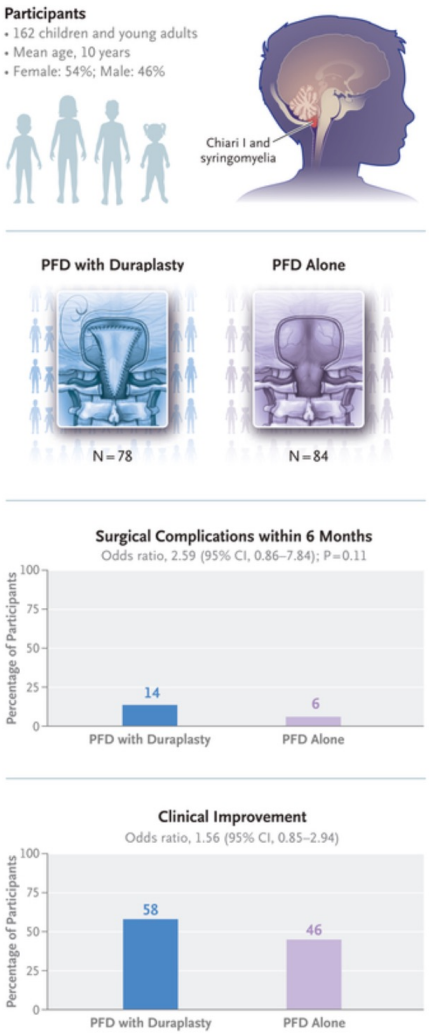

Chiari type I malformation and syringomyelia are closely associated developmental disorders of the craniovertebral junction and spinal cord, respectively. Children with Chiari malformation and syringomyelia may have headaches, cerebellar and cranial nerve dysfunction, pain, hydrocephalus, sensorimotor deficits, and spinal deformity. Posterior fossa decompression (PFD) may provide clinical improvement and reduction of syringomyelia (spinal cord cavitation) on imaging; however, the choice of surgical technique remains controversial.

The standard treatment for Chiari malformation and syringomyelia has been PFD with duraplasty (PFD-D), which includes suboccipital craniectomy (with or without cervical laminectomy), dural opening with intradural microdissection, and placement of an expansile dural graft (Figure 1). The high incidence of cerebrospinal fluid (CSF)–related complications after PFD-D (18.5%; range, 8.3 to 66.7) has prompted many surgeons to perform extradural PFD without duraplasty. Whether PFD alone carries a lower risk of surgical complications than PFD-D or provides effective treatment for clinical symptoms, neurologic deficits, syringomyelia, or quality-of-life impairment with durable effect remains unclear.

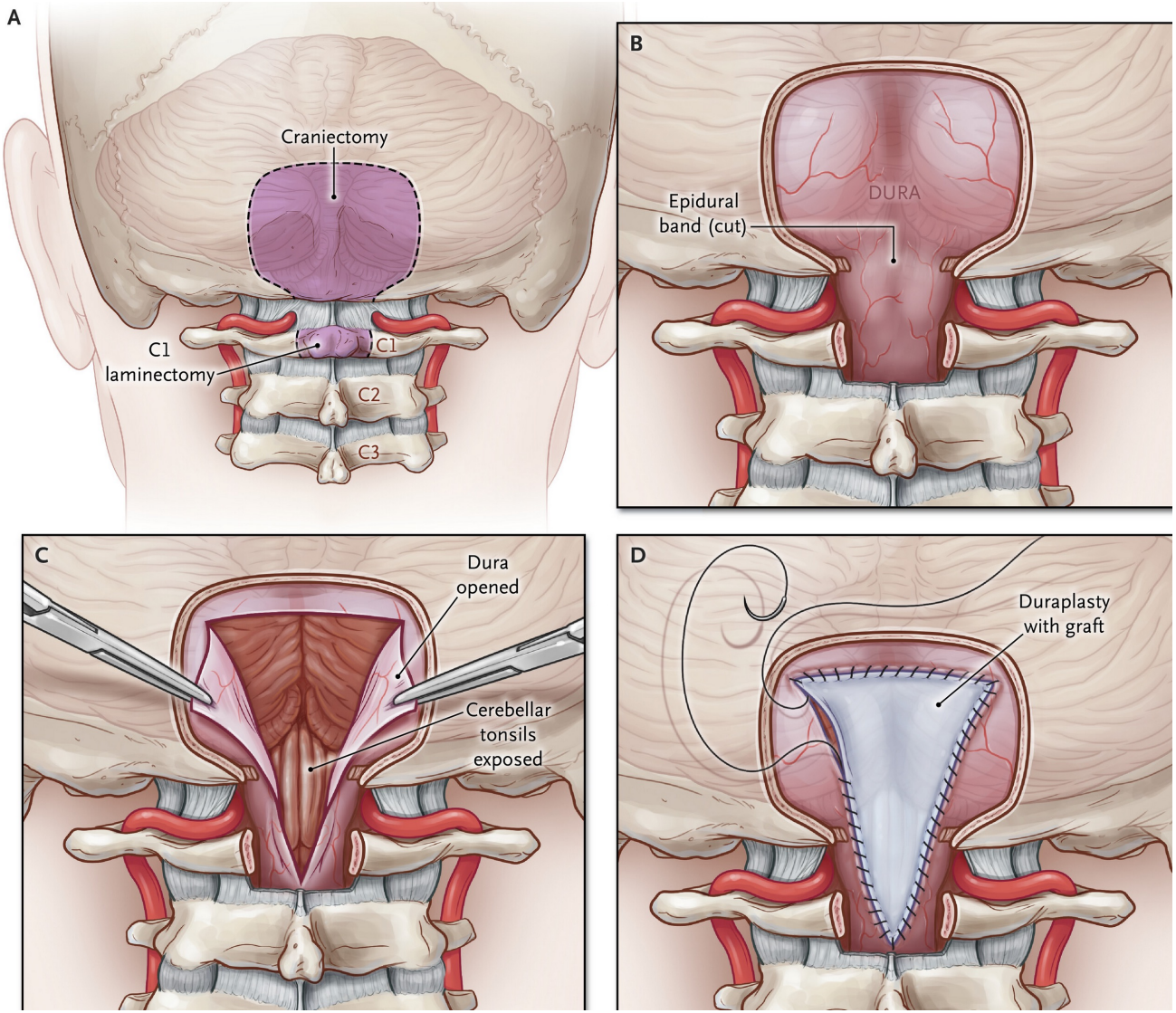

Posterior Fossa Decompression (PFD) and PFD with Duraplasty (PFD-D).

Both PFD and PFD-D begin with a midline posterior suboccipital incision extending from the level of the inion inferiorly. Planned areas of bone removal from the suboccipital region of the skull and C1 lamina are shown for PFD and PFD-D (Panel A). For PFD, after bony decompression, the band-like epidural atlanto-occipital membrane is removed (Panel B). Dural scoring or splitting (without dural opening) may be performed on the basis of intraoperative observations. For PFD-D, the dura is opened sharply, exposing the cerebellar tonsils, brain stem, and upper spinal cord (Panel C). Intradural microsurgical maneuvers (e.g., removal of adhesions and opening of occlusive membranes) are performed as indicated. After microsurgical dissection, the dura is sutured closed in a watertight fashion with the use of an expansile graft with or without a dural sealant according to usual institutional practice (Panel D).

Trial Participants

Participants were 21 years of age or younger with preoperative magnetic resonance imaging (MRI) showing Chiari type I malformation (cerebellar tonsillar ectopia, ≥5 mm) and syringomyelia (maximum anteroposterior diameter of the spinal cord syrinx, 3.0 to 9.9 mm). Among the exclusion criteria were basilar invagination, a clivo-axial angle of less than 120 degrees (the angle between the clivus and the second cervical vertebra, with smaller angles signifying complex craniocervical anomalies), previous PFD-D or PFD, and Chiari malformation and syringomyelia secondary to tumors or other unrelated intracranial pathologic features.

Trial Outcomes

The primary outcome was measured as a binary (yes or no) variable for surgical complications, including clinically significant pseudomeningocele, CSF leak, chemical meningitis, infection, hydrocephalus, shunt malfunction or infection, cervical instability, or cerebellar ptosis within 6 months after initial PFD-D or PFD.

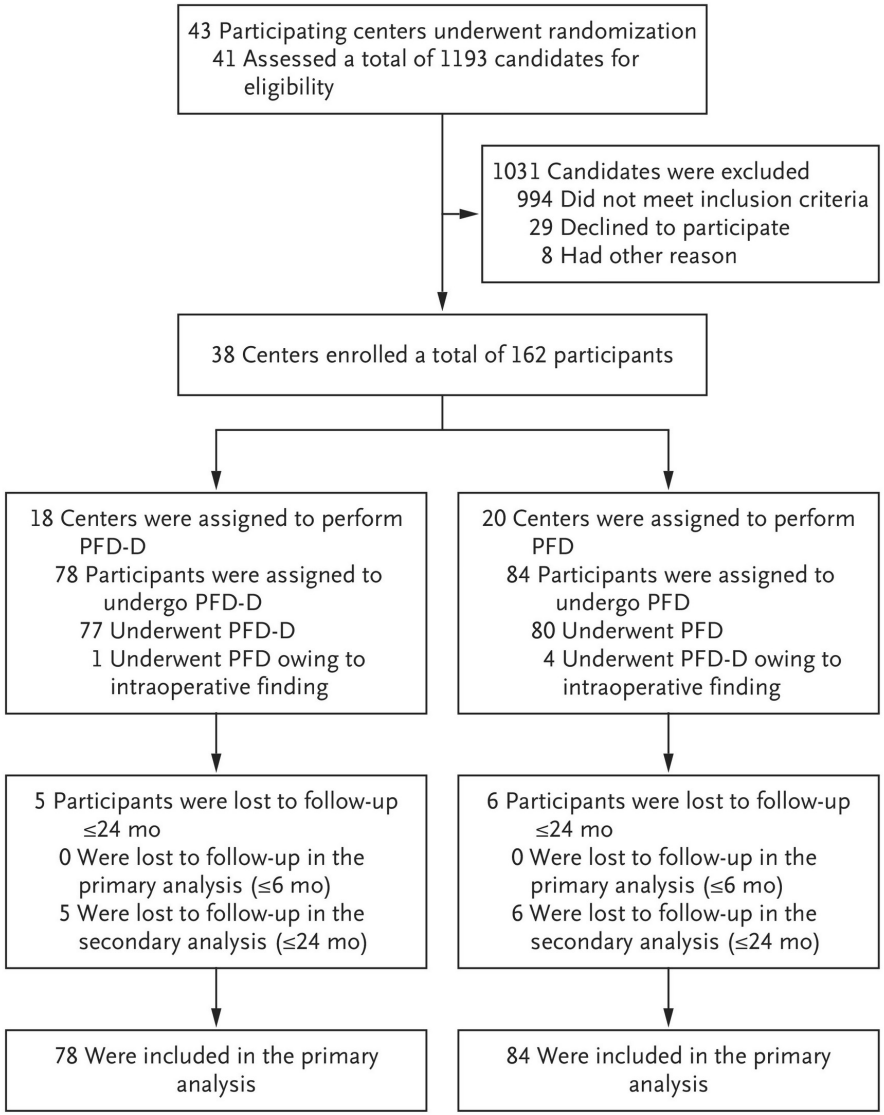

Characteristic	PFD-D (N=78)	PFD (N=84)	Total (N=162)
Age — yr	10.8±5.4	9.9±5.6	10.3±5.5
Sex — no. (%)			
Female	39 (50)	48 (57)	87 (54)
Male	39 (50)	36 (43)	75 (46)
Race or ethnic group — no. (%)†			
Asian, Native Hawaiian, Pacific Islander, American Indian, or Alaska Native	1 (1)	1 (1)	2 (1)
Black	10 (13)	5 (6)	15 (9)
White	58 (74)	73 (87)	131 (81)
More than one race	4 (5)	4 (5)	8 (5)
Unknown or not reported	5 (6)	1 (1)	6 (4)
Hispanic or Latino ethnic group — no. (%)†			
Yes	9 (12)	6 (7)	15 (9)
No	69 (88)	78 (93)	147 (91)
Cerebellar tonsillar ectopia — mm	13.7±4.6	13.9±5.4	13.8±5.0
Maximum diameter of syrinx — mm	5.8±2.1	5.5±2.1	5.6±2.1
Symptoms at presentation — no. (%)‡			
Any	71 (91)	71 (85)	142 (88)
Index headache	52 (67)	52 (62)	104 (64)
Neck pain	26 (33)	21 (25)	47 (29)
Sensorimotor symptoms	37 (47)	26 (31)	63 (39)
Pain in arms, legs, or trunk	14 (18)	15 (18)	29 (18)
Gait ataxia	17 (22)	9 (11)	26 (16)
Duraplasty type — no. of participants§			
Autograft	21	—	
Allograft	6	—	
Xenograft	39¶	—	
Synthetic graft	11	—	

Primary and Secondary Outcomes (Intention-to-Treat Population).

Outcome	PFD-D (N=78)	PFD (N=84)	Treatment Effect: PFD-D vs. PFD (95% CI)
Primary outcome			
Surgical complications within 6 mo — no. (%)	11 (14)	5 (6)	2.59 (0.86 to 7.84)†‡
Secondary outcomes			
Clinical improvement — no. (%)§	45 (58)	39 (46)	1.56 (0.85 to 2.94)†
Syrinx reduction — diameter in mm¶	3.08±2.33	1.22±1.79	1.86 (1.27 to 2.46)‖
Improvement in CHIP health-related quality of life — overall score**	0.07±0.02	0.09±0.02	−0.02 (−0.07 to 0.03)‖

Discussion

This multicenter, cluster-randomized, controlled trial compared PFD-D with PFD alone in terms of surgical complications, clinical improvement, syrinx reduction, treatment durability, and quality of life. No significant difference was observed between PFD-D and PFD alone with respect to the primary outcome of surgical complications within 6 months after surgery. PFD-D was similar to PFD alone in quality of life. Noninferiority of PFD relative to PFD-D was not established for clinical improvement or syrinx regression. The PFD group appeared to have a less robust reduction in syrinx diameter and a higher likelihood of repeat decompression.

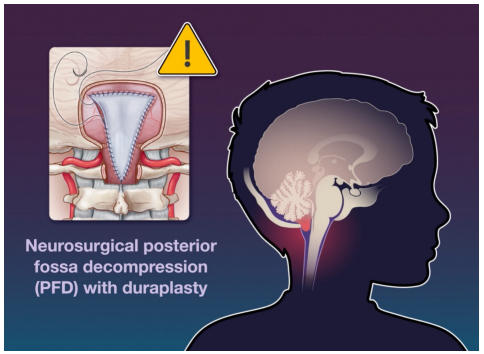

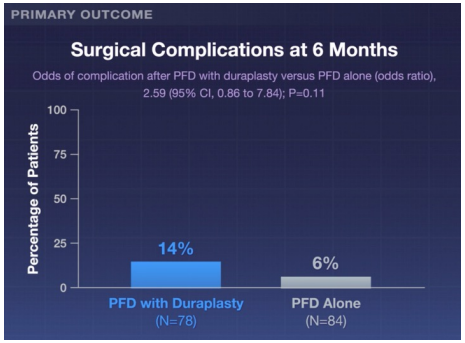

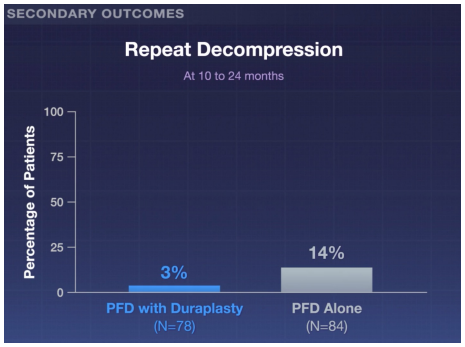

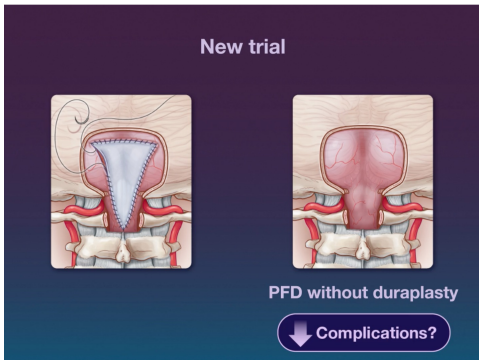

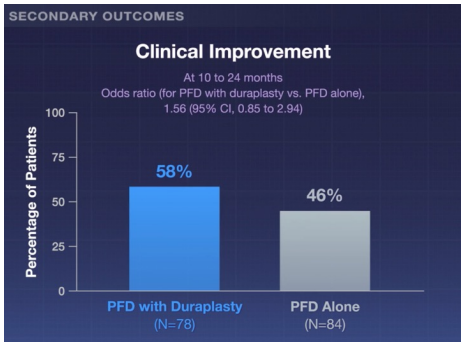

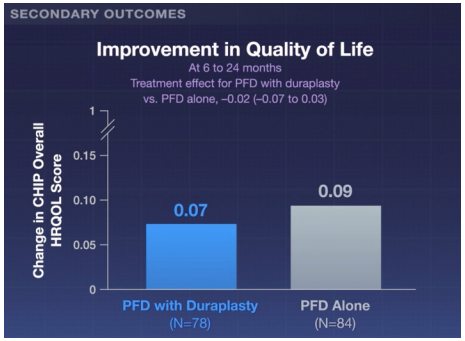

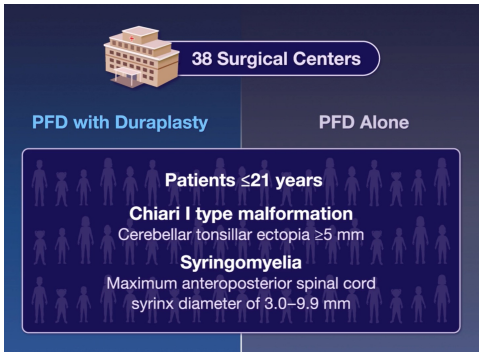

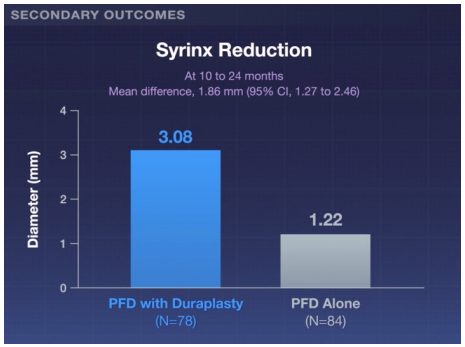

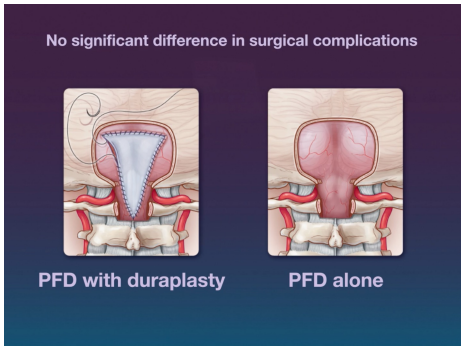

Noninferiority could not be shown

Kala-Azar (auch bekannt als **viszerale Leishmaniose** oder „Schwarzes Fieber“) ist eine lebensgefährliche, von Parasiten verursachte Infektionskrankheit. Unbehandelt verläuft sie in über 95 % der Fälle **tödlich**. Sie wird durch den Stich infizierter Sandmücken übertragen und greift die inneren Organe sowie das Immunsystem an.

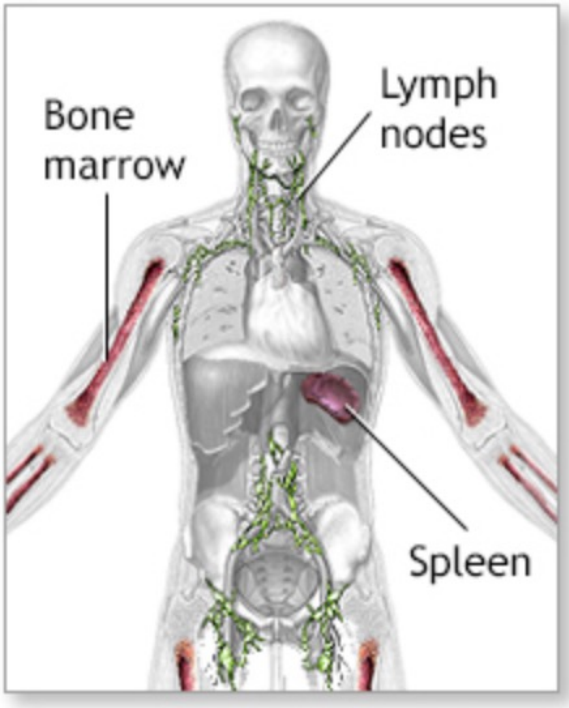

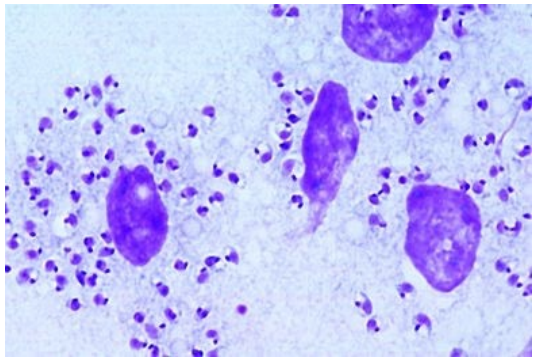

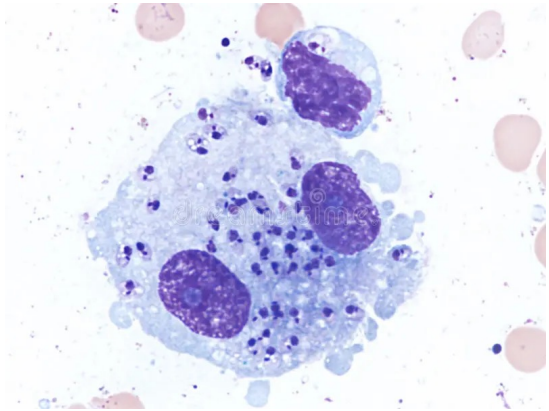

REVIEW ARTICLE

Leishmaniasis

Summary

Leishmaniases comprise clinically distinct diseases caused by the protozoan parasite leishmania, which is transmitted through the bite of infected sand flies. Cutaneous leishmaniasis is the most common form and manifests as a localized skin lesion. Mucosal leishmaniasis causes destructive nose, mouth, and throat lesions. Visceral leishmaniasis is a potentially life-threatening form that results from bloodborne dissemination of the parasites. The number of cases of cutaneous leishmaniasis is increasing, particularly in the Eastern Mediterranean region, and the prevalence of visceral leishmaniasis is decreasing globally. Laboratory diagnosis of the leishmaniases has shifted to the use of molecular methods to test tissue samples (e.g., skin or bone marrow), which can be used to identify infecting species. Treatment is challenged by limited drug choices. A recent advance is the use of combination therapies for visceral leishmaniasis. Two human leishmaniasis vaccines are undergoing preclinical testing or are ready for human testing.

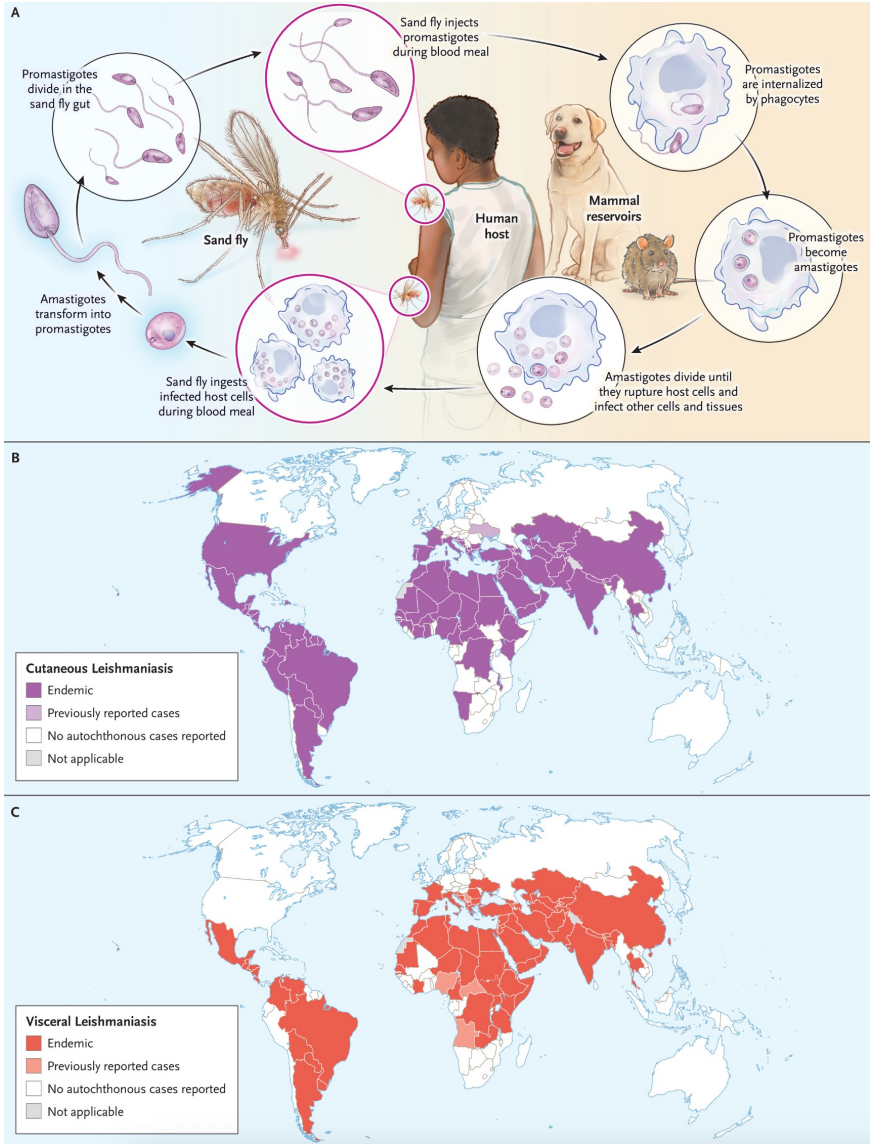

Life Cycle of Leishmania and Disease Distribution.

Panel A shows the life cycle of leishmania. Panels B and C show the geographic distribution of cutaneous leishmaniasis and visceral leishmaniasis in 2024.[9]

Leishmaniasis

- Leishmaniasis is transmitted through the bite of an infected sand fly.
- The number of cutaneous leishmaniasis cases is increasing, particularly in the Eastern Mediterranean region, whereas the number of visceral cases is decreasing globally.
- Most cases of visceral leishmaniasis are asymptomatic, but symptomatic cases are lethal unless they are adequately treated. Visceral leishmaniasis is an opportunistic infection in persons with human immunodeficiency virus (HIV) infection who live in endemic regions.
- Laboratory diagnosis of the leishmaniases has shifted to molecular assessment of tissue samples (e.g., skin and bone marrow), which can be used to identify infecting species.
- Treatment is challenged by limited drug choices. A recent advance is the use of combination therapies for the treatment of visceral leishmaniasis.
- Two leishmaniasis vaccines are undergoing preclinical testing or are ready for testing in humans. Modeling suggests that with a 50% rate of vaccine efficacy, visceral leishmaniasis could be eliminated in 8 to 10 years of vaccine use.

Leishmaniasis Clinical Syndromes and Causative Species.

Leishmania parasites cause diverse diseases with distinct clinical manifestations and outcomes. Selected species are representative examples; this list is not exhaustive.

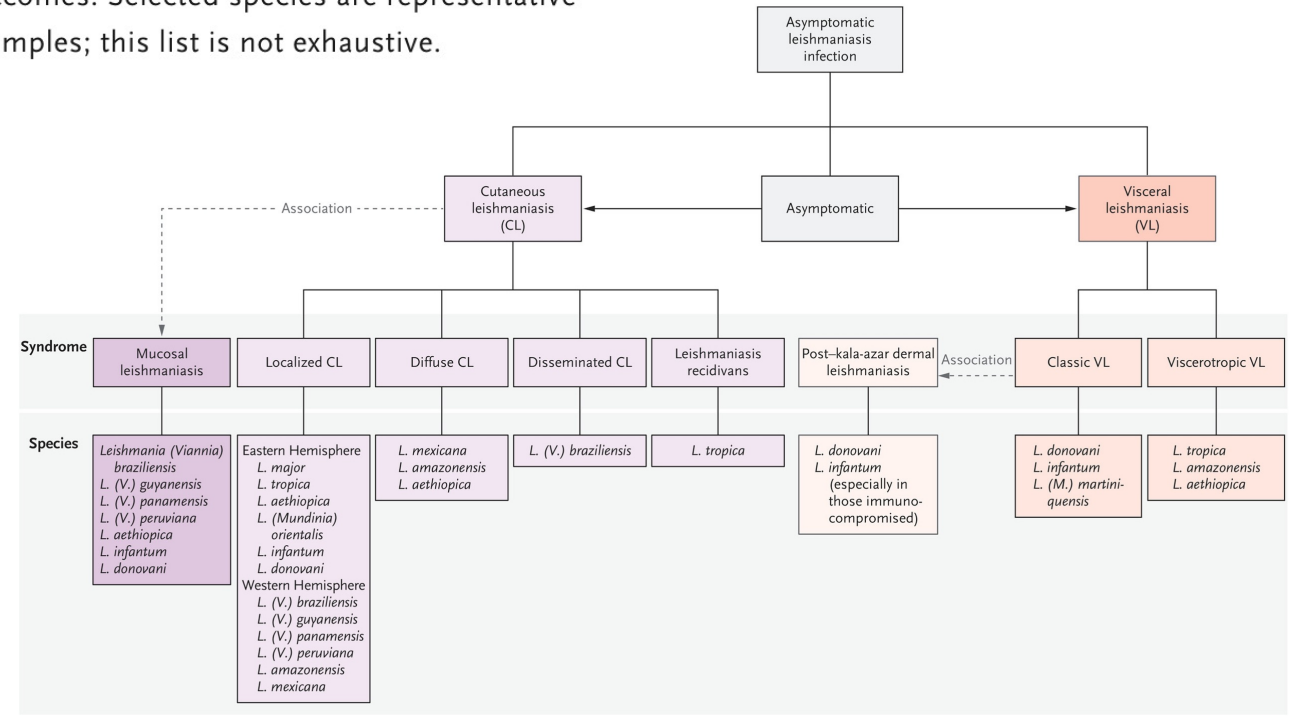

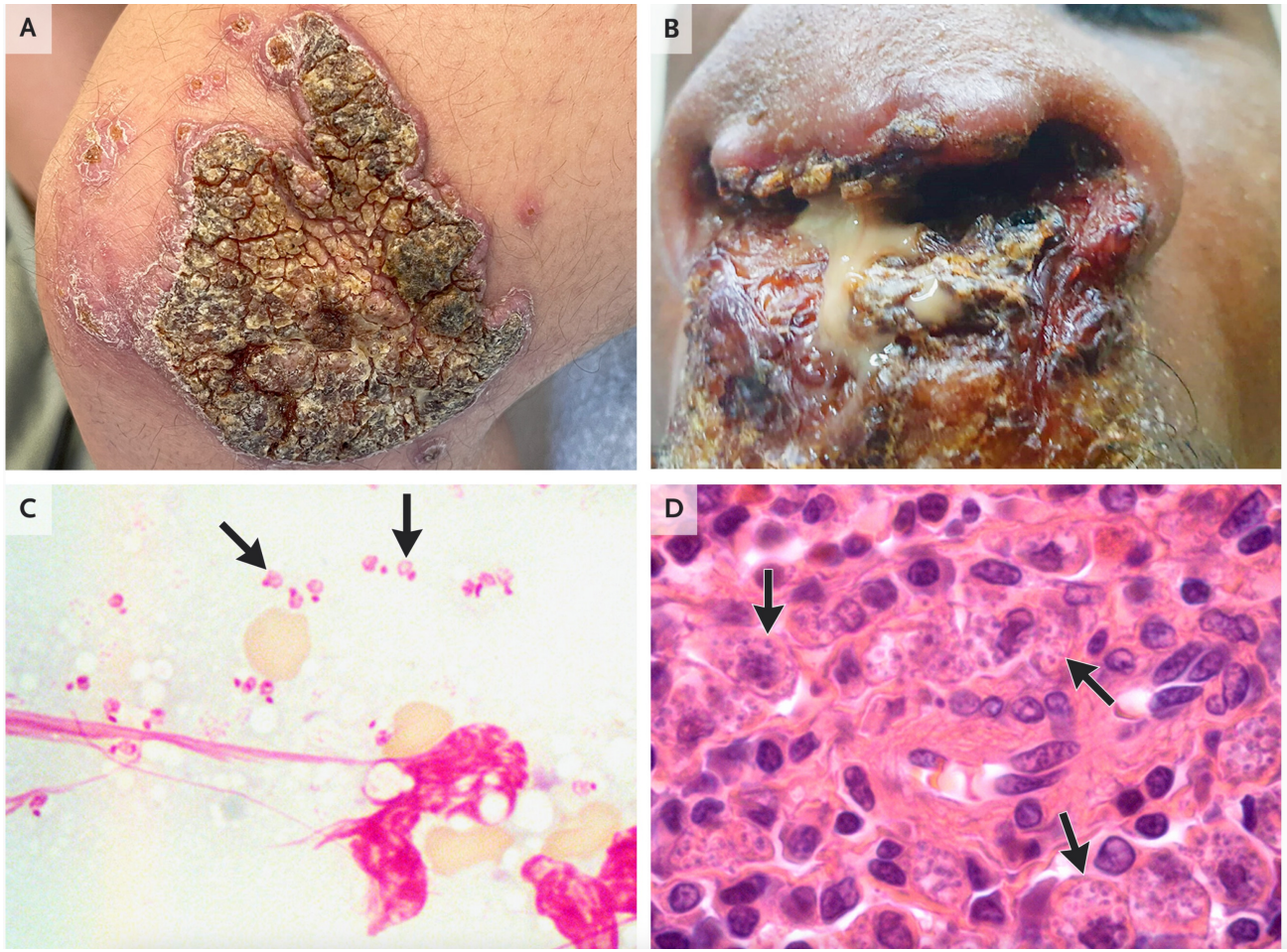

Clinical and Histopathological Manifestations of Leishmaniasis.

Panel A shows a lesion caused by *Leishmania (Viannia) guyanensis*. Panel B shows a mucosal lesion with facial disfigurement. Panel C shows leishmania amastigotes (arrows) on a Giemsa-stained smear of a splenic aspirate. Panel D shows *L. infantum* amastigotes (arrows) in a tissue specimen obtained from an infected spleen stained with hematoxylin and eosin.

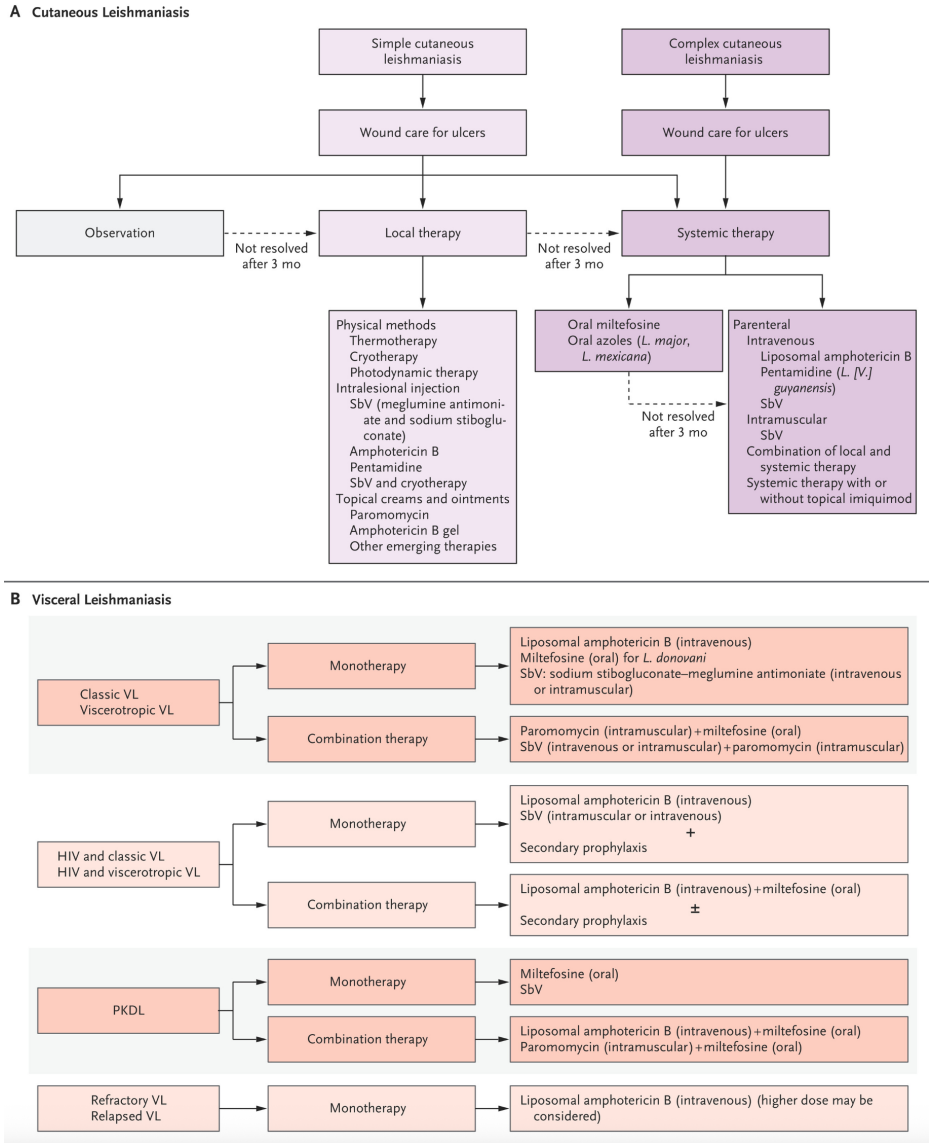

Approach to the Treatment of Cutaneous Leishmaniasis and Visceral Leishmaniasis.

Treatment of leishmaniasis is determined by many factors, such as the clinical type of disease, causative *Leishmania* species, and associated coexisting conditions (e.g., human immunodeficiency virus [HIV]).[51] PKDL denotes post–kala-azar dermal leishmaniasis, and SbV pentavalent antimonial agent.

Cutaneous Leishmaniasis	Mucosal Leishmaniasis	Visceral Leishmaniasis	Visceral Leishmaniasis with HIV Coinfection	Post–Kala-Azar Dermal Leishmaniasis
L-AMB: IV, 3 mg/kg/day, on days 1–5, and 10 or on days 1–5, 8, and 9; higher dose for immunocompromise; OR **Miltefosine:** oral, 2.5 mg/kg/day, divided into 2–3 daily doses for 28 days, up to 150 mg/day (doses >150 mg/day are associated with unacceptable side effects) (FDA-approved); OR **Pentavalent antimonial drugs:** **Meglumine antimoniate†**: IV or IM, 20 mg/kg/day for 10–20 days; or intralesional, 0.5–2 ml of 81 mg/ml every 15 days for up to 3 sessions; OR **Sodium stibogluconate:** IV or IM, 20/mg/kg/day for 10–20 days, or intralesional, 0.5–2 ml of 100 mg/ml, every 15 days for up to 3 sessions‡; OR **Paromomycin:** ointment, twice daily for 10 days, wait 10 days, then reapply for 10 days§; cream, once daily for 20 days¶; OR **Pentamidine isethionate:** IV, either 7 mg/kg, in 2 doses given 48 hr apart (more doses for *L. [V.] braziliensis*), or 4 mg/kg, in 3 doses given every other day; or intralesional, 120 μg/mm^2 on days 1, 3, and 5 (less favored option); OR **Fluconazole:** oral, 200–400 mg/day for 4–6 wk	**L-AMB:** IV, 3 mg/kg/day; total dose, 40–60 mg/kg; OR **Miltefosine:** oral, 2.5 mg/kg/day, divided into 2–3 daily doses for 28 days, up to 150 mg/day (FDA-approved); OR **Pentavalent antimonial drugs:** **Sodium stibogluconate‡**: IV or IM, 20 mg/kg/day, once daily for 28 days; OR **Meglumine antimoniate**: IV or IM, 20 mg/kg/day, once daily for 28–30 days†; OR **Pentamidine isethionate:** IV, 2–4 mg/kg, given on alternate days or 3 times/wk for 15 or more doses (less favored option) **All regimens:** given with or without pentoxifylline, oral, 400 mg every 8 hr for 30 days	**L-AMB:** IV, 3 mg/kg/day, once daily on days 1–5, 14, and 21 (FDA-approved) or once daily for 7 days or once daily for 10–14 days; OR **Miltefosine (for *L. donovani* only):** oral, 2.5 mg/kg/day, once daily for 28 days (FDA-approved for *L. donovani*); OR **Pentavalent antimonial drugs:** **Sodium stibogluconate‡**: IV or IM, 20 mg/kg/day for 28–31 days; OR **Meglumine antimoniate†**: IV, 20 mg/kg/day for 28 days; OR **Sodium stibogluconate‡ plus paromomycin‡:** **East Africa:** sodium stibogluconate, IV or IM, 20 mg/kg/day, plus paromomycin, IM, 15 mg/kg/day for 17 days; OR **Paromomycin‡ plus miltefosine:** **East Africa:** paromomycin, IM, 20 mg/kg/day, plus miltefosine, oral, 2.5 mg/kg/day for 14 days **Indian subcontinent (second-line treatment):** paromomycin, IM, 15 mg/kg/day, plus miltefosine, 2.5 mg/kg/day for 10 days	**L-AMB plus miltefosine (for *L. donovani*):** **East Africa:** L-AMB, IV, total dose of 30 mg/kg, plus miltefosine, oral, 100 mg/day for 28 days **Indian subcontinent:** L-AMB, IV, 30 mg/kg total dose, plus miltefosine, oral, 100 mg/day for 14 days, with or without secondary prophylaxis; OR **L-AMB (for all species):** IV, 3 mg/kg/day, up to total dose of 40 mg/kg; or IV, 5 mg/kg/day, once daily for days 1–4 or 5, day 8 or 10, day 17, and day 24; or IV, 4 mg/kg/day, on days 1–5, 10, 17, 24, 31, and 38, total dose, 40 mg/kg (FDA-approved), and secondary prophylaxis; OR **Pentavalent antimonial drugs (less preferred option):** **Sodium stibogluconate‡ or meglumine antimoniate†**: IV or IM, 20 mg/kg/day, once daily for 28 days, and secondary prophylaxis **Secondary prophylaxis:** **L-AMB:** IV, 3–5 mg/kg, once every 3–4 wk; OR **Pentamidine isethionate:** IV, 4 mg/kg (300 mg for adults), once every 3–4 wk	**L-AMB (usable, but optimal regimen not established):** total dose typically ≥30 mg/kg (e.g., IV, 2.5 mg/kg/day for 20 days); OR **Miltefosine:** oral, 2.5 mg/kg/day, once daily for 12 wk, up to 150 mg/day; OR **Pentavalent antimonial drugs:** **Meglumine antimoniate† or sodium stibogluconate‡**: IV or IM, 20 mg/kg/day, once daily for 30–60 days; OR **Indian subcontinent: L-AMB**, 20 mg/kg (IV, 5 doses of 4 mg/kg, given over the course of 20 days), plus oral allometric miltefosine for 30 days **East Africa: paromomycin,‡** IM, 20 mg/kg for 14 days, plus oral allometric miltefosine for 42 days

* FDA denotes Food and Drug Administration, HIV human immunodeficiency virus, IM intramuscular, IV intravenous, and L-AMB liposomal amphotericin B.

† Meglumine antimoniate is available as an investigational new drug in the United States and can be obtained from Sanofi (https://www.astmh.org/blog/instructions-for-acquiring-glucantime-(meglumine-a).

‡ This drug is not available in the United States. The dose of 20 mg per kg per day of antimony is equal to 75 mg per kg of meglumine antimoniate.

§ This is compounded paromomycin ointment with the contents of paromomycin capsules: 15% paromomycin with 12% methylbenzethonium chloride in paraffin.

¶ This is compounded paromomycin cream with the contents of paromomycin capsules: 15% paromomycin sulfate 15% weight per weight in Aquaphilic with 10% carbamide ointment 67.8% and water 16.67%.[52]

Conclusions and Future Directions

The leishmaniases are a serious global health problem and are designated by the WHO as neglected tropical diseases, even cases that are reported from the southwestern United States due to autochthonous transmission. Several medications, including liposomal amphotericin B, miltefosine, pentavalent antimonial agents, and paromomycin, are used for the treatment of leishmaniasis. However, these treatments have serious drawbacks, including prolonged parenteral administration, poor adherence owing to toxic effects, high cost, limited availability of therapeutic options in various regions, and the emergence of drug-resistant parasites. Promising new oral anti-trypanosomatid compounds, including DNDI-6148, GSK3186899/DDD853651, GSK3494245/DDD01305143, LXE408, and DNDI-0690, are currently in the clinical pipeline of possible drugs for leishmaniasis.

No leishmania vaccine is currently available for humans, despite extensive research; however, two vaccines are under investigation in preclinical or clinical studies.

Bronchial Anthracosis

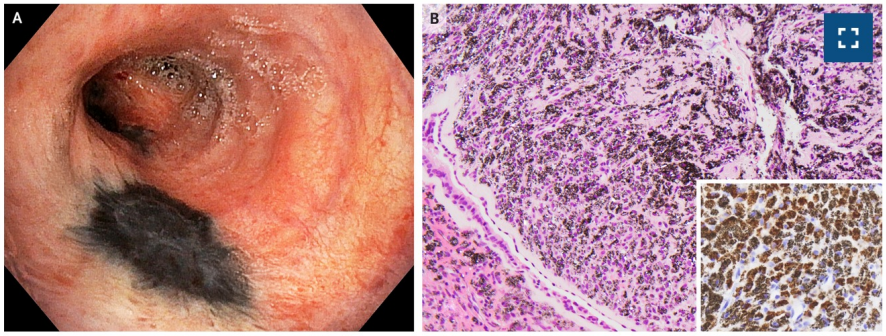

A 77-year-old man undergoing bronchoscopy for evaluation of suspected lung cancer was noted to have black patches on the bronchial mucosa. He had a smoking history of 50 pack-years and a history of pulmonary tuberculosis treated with left upper lobectomy. During bronchoscopy, areas of black discoloration were seen on the mucosa of the left main bronchus and left segmental bronchi (Panel A). A biopsy sample showed ciliated respiratory epithelium with subepithelial accumulation of macrophages containing black pigment (Panel B, hematoxylin and eosin stain). Also noted was the deposition of small, birefringent dust particles of unknown origin, which were thought to possibly be silicates. On immunohistochemical staining, abundant pigment-laden macrophages were identified by their diffuse cytoplasmic positivity for CD68 (Panel B, inset). A diagnosis of bronchial anthracosis — a benign, often incidental finding indicating carbon pigment deposition in the mucosa — was made. Bronchial anthracosis is associated with prolonged exposure to biomass smoke or environmental dust. On further history taking, the patient reported having socialized around open fires for decades of his life in the Middle East, as well as having been exposed to substantial amounts of dust while incarcerated for 10 years. No treatment was recommended for the bronchial anthracosis; subsequent management and follow-up focused on the lung cancer that had been confirmed by computed tomography (CT) and CT-guided biopsy.

Colles' Fracture

A 57-year-old woman with a history of osteopenia presented to the emergency department with left wrist pain after slipping on ice and landing on her palm. Physical examination was notable for swelling, tenderness, and limited movement of the left wrist. There was also dorsal angulation of the distal forearm proximal to the wrist, a finding known as a "dinner fork" deformity owing to its contour, which is similar to that of an upside-down fork (Panel A). A radiograph of the left wrist showed an extraarticular transverse fracture of the distal radius with dorsal displacement of the distal fragment, also known as a Colles' fracture (Panel B [lateral view] and Panel C [frontal view], black arrows). There was also a fracture of the ulnar styloid tip (Panel C, white arrow), which is an avulsion injury that may accompany a Colles' fracture owing to traction at the ligamentous attachment site. A Colles' fracture is a fragility fracture that indicates a diagnosis of osteoporosis in postmenopausal women, regardless of results of bone mineral density testing. Treatment with closed reduction and casting was provided. The patient received dietary education (daily targets of calcium and vitamin D intake) and medication for osteoporosis (calcium, vitamin D, and alendronate), followed by wrist rehabilitation and weight-bearing exercises after cast removal to prevent falls and reinjury. At the 12-week follow-up, the pain and limited mobility had abated. She continues to receive follow-up care.

Case 15-2026: A 64-Year-Old Woman with Fatigue, Memory Changes, and Falls

The patient had been in her usual state of health until 3 weeks before the current presentation, when fatigue developed during a summer vacation in Maine. She had spent time outdoors near a lake but had had no known tick bites. One week before the current presentation, the patient had increasing fatigue while driving. She parked the car and called her husband, who took her to the emergency department of another hospital for evaluation.

In the emergency department, the patient reported fatigue and poor sleep. She had no dysuria, chest pain, or abdominal pain. A physical examination and an electrocardiogram were reportedly normal. The blood levels of electrolytes, troponin, thyrotropin, alanine aminotransferase, aspartate aminotransferase, bilirubin, and alkaline phosphatase were normal, as were the complete blood count with differential count and the results of tests of kidney function. Urinalysis showed trace ketones (reference value, negative) and 1+ leukocyte esterase (reference value, negative), and microscopic examination of the urine sediment revealed many squamous cells and 6 white cells per high-power field (reference value, <4). A test for Lyme disease was negative. The results of computed tomography (CT) of the head, performed without the administration of intravenous contrast material, were reportedly normal. The patient was discharged home with plans to follow up with her primary care physician.

Two days later, and 4 days before the current presentation, the patient began to have an unsteady gait, and her husband took her to the emergency department of a second hospital for evaluation. She reported feeling “off balance” while walking and having difficulty with concentrating on tasks. She had no headache or change in vision. Her performance on finger-to-nose testing was accurate but slow. She required multiple attempts to correctly touch her left thumb to her right ear and was unable to calculate the value of nine quarters; these findings differed from baseline findings. Her gait was cautious, but she was able to ambulate without support. The remainder of the examination was normal. Results of tests of coagulation were normal. The erythrocyte sedimentation rate was 7 mm per hour (reference range, 0 to 30), and the blood level of C-reactive protein was 1.2 mg per liter (reference range, 0.0 to 10.0). Nucleic acid amplification testing for ehrlichia and anaplasma DNA was negative.
Magnetic resonance imaging (MRI) of the head was recommended, but the patient elected to leave the emergency department. Her primary care physician arranged for the MRI to be performed on an outpatient basis.

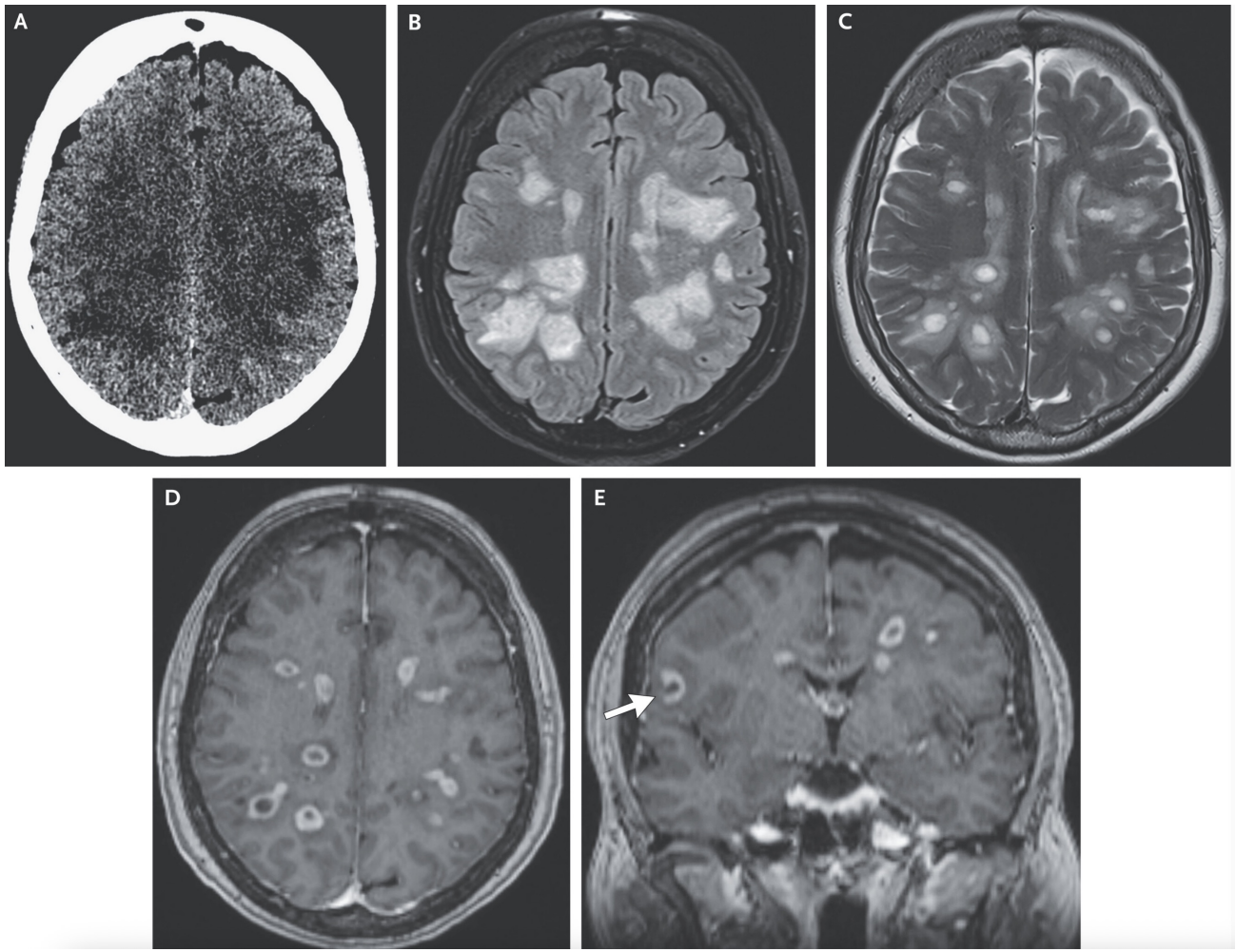

Initial Imaging Studies of the Head.

CT of the head was performed 4 days before the current presentation. An image obtained without the administration of contrast material (Panel A) shows scattered hypoattenuation in the cerebral white matter. MRI of the head was performed on the day of the current presentation at a magnetic field strength of 1.5 Tesla. A fluid-attenuated inversion recovery (FLAIR) image (Panel B) and a T2-weighted image (Panel C), both obtained without the administration of contrast material, show lesions within the supratentorial white matter with central signal hyperintensity, a T2-hypointense rim, and mild edema. Axial and coronal T1-weighted images (Panels D and E, respectively), obtained after the administration of contrast material, show central hypointensity with predominantly closed-ring enhancement. A subset of the lesions shows open-ring enhancement oriented toward the cortex (Panel E, arrow).

Medications included escitalopram, levothyroxine, and lisinopril–hydrochlorothiazide; lorazepam and ramelteon were used as needed for sleep, and she had recently completed a 5-day course of nitrofurantoin. She had no known adverse reactions to medications. She lived with her husband in Massachusetts and worked as an administrator in health care but had no contact with patients. She was a lifelong nonsmoker and drank alcohol occasionally; she did not use illicit drugs.

On examination, the temporal temperature was 36.9°C, the blood pressure 153/73 mm Hg, the heart rate 50 beats per minute, the respiratory rate 18 breaths per minute, and the oxygen saturation 98% while the patient was breathing ambient air. The body-mass index (the weight in kilograms divided by the square of the height in meters) was 28.1. The patient was awake, alert, and appropriately interactive and oriented. Slight inattention and slowness with stating the days of the week backward were noted. She was unable to subtract 7 from 100. Her speech was fluent without paraphasic errors. She was able to follow simple commands and to lift both arms against gravity, with slight orbiting of the left arm. Slight weakness was observed in the right leg, but she was able to walk without assistance. The remainder of the examination was normal.

Differential Diagnosis

This 64-year-old woman presented with a 1-week history of progressive neurologic symptoms and encephalopathy. MRI of the head showed numerous hyperintensities on FLAIR images. To develop a differential diagnosis to explain the patient's symptoms, I will start by combining neurologic localization with the time course of her disease progression.

Localization

The patient's prodromal symptoms of fatigue and poor sleep are nonlocalizing. Difficulty with concentration and with performing tasks indicates a cerebral process affecting attention.

Subacute Multifocal Cerebral Disease

Subacute multifocal cerebral disease can be caused by infection, cancer, rapid accrual of vascular thrombi, or immune-mediated disorders.

Infection

The patient is probably immunocompetent, given that she has no known history of human immunodeficiency virus infection, other immunosuppressive conditions, or opportunistic infections.

Cancer

Both primary cancer of the central nervous system (CNS) and metastatic disease involving the CNS can cause subacute confusion and imbalance.

Vascular Thrombosis

Thrombotic thrombocytopenic purpura, antiphospholipid syndrome, infective endocarditis, and vasculitis can all cause rapid accrual of small ischemic lesions, leading to subacute ischemic encephalopathy.

Immune-Mediated Disorder

Immune-mediated disorders that cause focal brain lesions can be grouped broadly into demyelinating disorders, systemic autoimmune diseases with neurologic involvement, and primary autoimmune encephalitides. Multiple sclerosis (MS) is the most common demyelinating disease, with an average age at diagnosis of 32 years. Over the past several decades, however, the number of persons older than 50 years of age in whom MS is diagnosed has increased, and this age group now accounts for approximately 10% of new diagnoses. Therefore, age alone does not rule out MS.

Two other important causes of demyelination are aquaporin-4 (AQP4) antibodies and myelin oligodendrocyte glycoprotein (MOG) antibodies, and testing for these should be performed.

This patient has no clinical history of systemic autoimmunity, but some rheumatologic disorders, especially sarcoidosis, may manifest as CNS disease initially. MRI findings in persons with neurosarcoidosis typically show leptomeningeal gadolinium enhancement, which was not seen on MRI in this patient.

Primary autoimmune encephalitides are typically characterized by inflammatory changes rather than the discrete, masslike enhancing lesions that were observed on MRI in this patient. In addition, the absence of blood products on MRI in this patient would be unusual for inflammation associated with cerebral amyloid angiopathy.

Lumbar puncture was performed, with an opening pressure of 21 cm of water. Analysis of the CSF showed mild lymphocytic pleocytosis, with 6 to 9 nucleated cells per microliter (reference range, 0 to 5), of which 95% were lymphocytes. The CSF glucose level was 62 mg per deciliter (3.4 mmol per liter; reference range, 50 to 75 mg per deciliter [2.8 to 4.2 mmol per liter]), and the total protein level was 57 mg per deciliter (reference range, 5 to 55). No organisms were seen on Gram's staining, and testing for toxoplasma IgM and IgG was negative. Cytologic evaluation of the CSF showed no malignant cells, and a nucleic acid amplification test for a *MYD88* mutation was negative. A CSF sample was sent for testing for the presence of oligoclonal bands and measurement of the level of free kappa light chain.

Whole-body positron-emission tomography (PET) did not show ^{18}F-fluorodeoxyglucose (FDG)–avid lesions, although an FDG-PET scan of the head showed multifocal uptake in the supratentorial white-matter abnormalities that had previously been noted on MRI. MRI of the cervical and thoracic spine did not show any spinal cord abnormalities. Blood tests for MOG and AQP4 antibodies were negative.

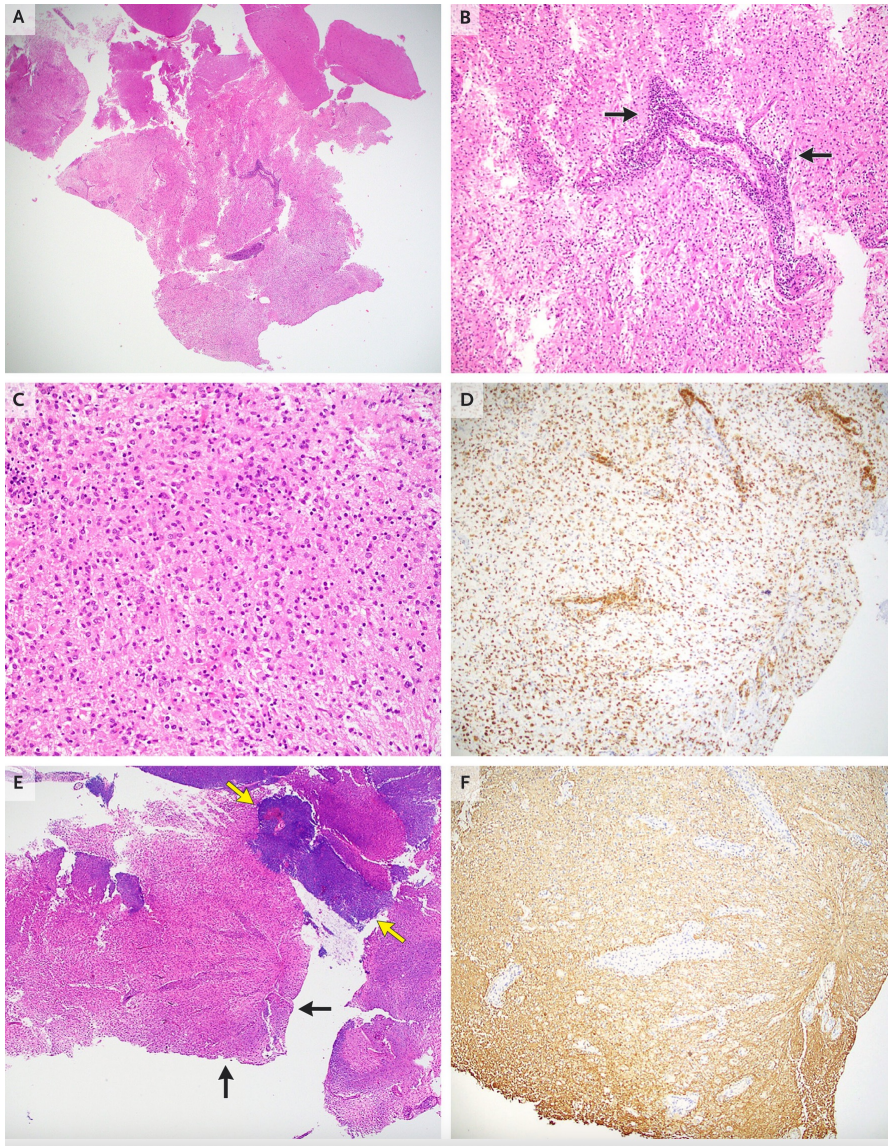

Biopsy Specimens of the Brain.

Hematoxylin and eosin staining of sections obtained from multiple lesions in the right frontal lobe show brain parenchyma involved by a cellular, mixed inflammatory lesion consisting of numerous plump, eosinophilic macrophages (Panels A, B, and C) and parenchymal and perivascular lymphocytes (best seen in Panel B, arrows). Immunohistochemical staining for CD68 (Panel D) shows sheets of macrophages within the lesion. Luxol fast blue–hematoxylin and eosin staining (Panel E) shows loss of myelin within the lesion, which appears pink (black arrows) in contrast to the adjacent blue, myelinated white matter (yellow arrows). Immunohistochemical staining for neurofilament (Panel F) shows relative preservation of axons within the white matter of the lesion. Macrophage-rich inflammatory lesions with loss of myelin and preservation of axons are consistent with acute demyelinating lesions. Additional testing for infectious sources (not shown) was negative.

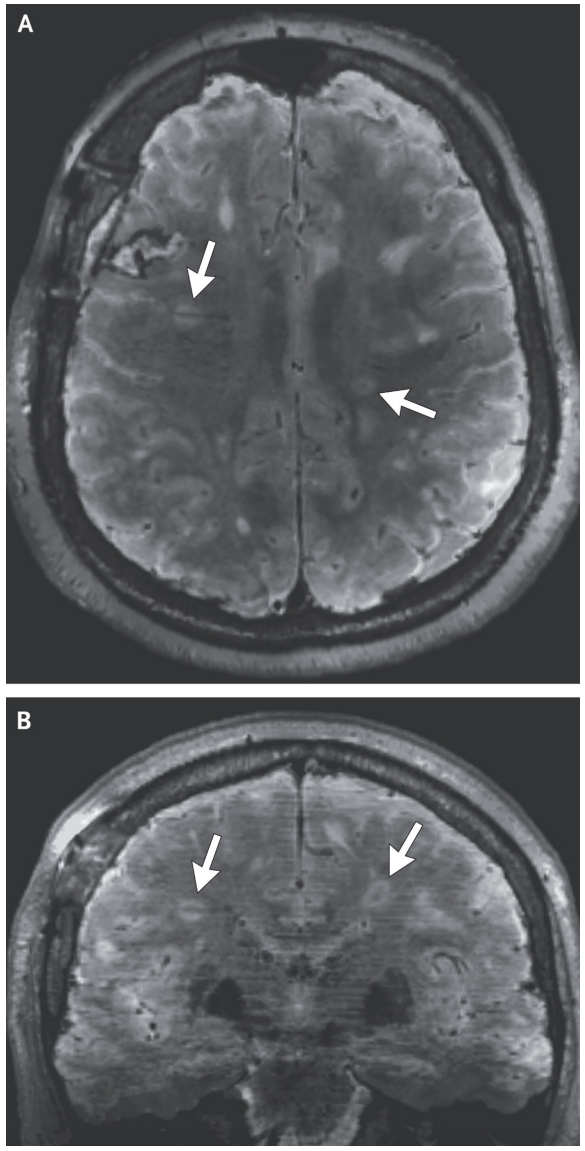

Follow-up MRI of the Head.

MRI of the head was performed approximately 7 weeks after the current presentation. Axial and coronal FLAIR–T2*-weighted fusion images (Panels A and B, respectively) show that the lesions have slightly contracted in size as compared with that observed on initial imaging, and a central vein is visible in a majority of the lesions in the deep and periventricular white matter (arrows). A rim of paramagnetic susceptibility was not observed.

Final Diagnosis
Multiple sclerosis.

Approximately 1% of MS cases are diagnosed in patients older than 60 years of age. Late-onset MS is more likely to occur in women than in men and is associated with more extensive motor involvement and a higher risk of progressive disease than MS with onset at an earlier age. Although the efficacy of disease-modifying therapy declines with age, subgroup analyses performed in clinical trials and observational studies have consistently shown a greater benefit with highly effective therapies than with agents with low or moderate efficacy, even among older adults.

Ocrelizumab ist ein verschreibungspflichtiger, humanisierter monoklonaler Antikörper. Es wird zur Behandlung von Multipler Sklerose (MS) eingesetzt. Als erste zugelassene Therapie für die primär progrediente MS (PPMS) sowie zur Behandlung der schubförmigen MS (RMS) wirkt es gezielt, indem es bestimmte fehlgeleitete B-Zellen (CD20-positiv) im Immunsystem zerstört.

Indikationen: Aktive schubförmige MS (RRMS) und frühe Formen der primär progredienten MS (PPMS).

•**Dosierung:** Die Standarddosis beträgt 920 mg alle 6 Monate.

•**Verabreichungsart:** Traditionell als intravenöse (IV) Infusion. Mittlerweile gibt es in vielen Regionen auch die Form der kürzeren subkutanen Injektion, die unter die Bauchhaut gespritzt wird und nur ca. 10 bis 15 Minuten dauert.

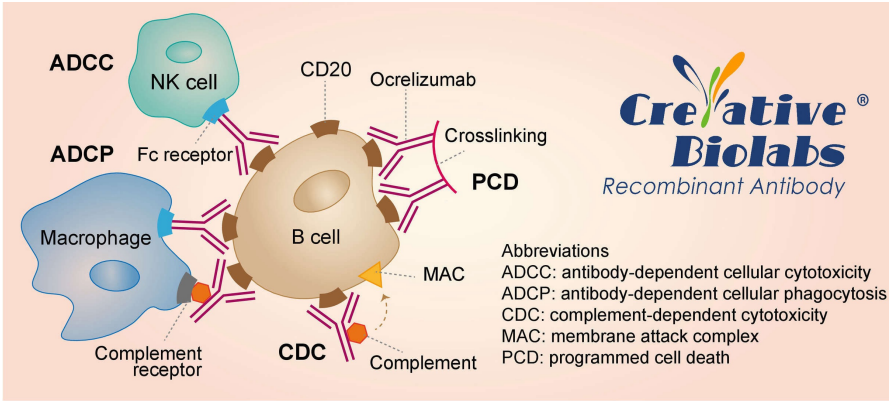

•**Wirkung**

•Der Wirkstoff bindet gezielt an das Protein CD20 auf der Oberfläche schädlicher B-Zellen.

•Dies führt zu deren rascher Zerstörung, wodurch Entzündungen im zentralen Nervensystem (Gehirn und Rückenmark) unterbunden oder signifikant reduziert werden.

Efficacy and safety of a bodyweight–adjusted higher dose of ocrelizumab in relapsing (MUSETTE) and primary progressive (GAVOTTE) multiple sclerosis: two multicentre, randomised, double-blind, parallel-group phase 3b trials

Summary

Background Ocrelizumab is a humanised anti-CD20 monoclonal antibody approved for people with relapsing (RMS) or primary progressive multiple sclerosis (PPMS). In a post-hoc analysis of phase 3 trials in RMS and PPMS using a 600 mg dose, higher exposure to ocrelizumab was associated with greater B-cell depletion and lower risk of confirmed disability progression. Here, we prospectively assessed the efficacy and safety of a high dose of ocrelizumab in patients with RMS or PPMS.

Methods Two multicentre, double-blind, phase 3 controlled trials were conducted to compare high-dose ocrelizumab with the approved 600 mg dose of the drug in patients with RMS (MUSETTE) and PPMS (GAVOTTE) aged 18–56 years. MUSETTE involved 122 centres in 21 countries and GAVOTTE involved 149 centres in 22 countries. Participants were randomly assigned 2:1, with a permuted-block randomisation method, to high-dose ocrelizumab (1200 mg or 1800 mg for baseline body weight <75 kg or ≥75 kg, respectively) or 600 mg ocrelizumab. Patients, investigators, and the sponsor were blinded to treatment allocation. Patients received ocrelizumab infusions every 24 weeks for a minimum 120 weeks and until a prespecified minimum number of confirmed disability events (MUSETTE, 205; GAVOTTE, 357) had occurred. In both trials, the primary endpoint was time to onset of 12-week composite confirmed disability progression (cCDP), assessed by prespecified increases in Expanded Disability Status Scale, Timed 25-Foot Walk Test, or 9-Hole Peg Test scores. Efficacy endpoints were evaluated in all randomised participants and safety endpoints were evaluated in participants who received at least one ocrelizumab infusion. These studies are registered with ClinicalTrials.gov: MUSETTE, NCT04544436; GAVOTTE, NCT04548999.

Findings Participants in MUSETTE were enrolled between Nov 26, 2020, and Aug 30, 2022; participants in GAVOTTE were enrolled between Dec 3, 2020, and May 15, 2023. In MUSETTE, 860 patients were randomly assigned (high-dose ocrelizumab, n=577; 600 mg ocrelizumab, n=283) and had median overall treatment duration of 184·4 weeks. In GAVOTTE, 753 patients were randomly assigned (high-dose ocrelizumab, n=500; 600 mg ocrelizumab, n=253) and had median overall treatment duration of 174·1 weeks. In MUSETTE, the percentage of patients with 12-week cCDP was 34% (198 of 577) with high-dose ocrelizumab versus 37% (104 of 283) with 600 mg ocrelizumab (hazard ratio [HR] 0·93 [95% CI 0·73–1·18]; p=0·53). In GAVOTTE, the percentage of patients with 12-week cCDP was 47% (235 of 500) with high-dose ocrelizumab versus 49% (124 of 253) with 600 mg ocrelizumab (HR 0·95 [95% CI 0·76–1·18]; p=0·64). Safety profiles were similar for the high-dose ocrelizumab and 600 mg ocrelizumab; in MUSETTE, rates of adverse events (552 [96%] of 577 and 267 [94%] of 283), serious adverse events (77 [13%] of 577 and 34 [12%] of 283), and fatalities (four [1%] of 577 and one [<1%] of 283) were comparable, as were rates of adverse events (447 [90%] of 499 and 230 [91%] of 254), serious adverse events (61 [12%] of 499 and 29 [11%] of 254), and fatalities (two [<1%] of 499 and three [1%] of 254) in GAVOTTE.

Interpretation In both studies, high-dose ocrelizumab did not further improve control of disability progression in either RMS or PPMS, and no new safety concerns were identified.

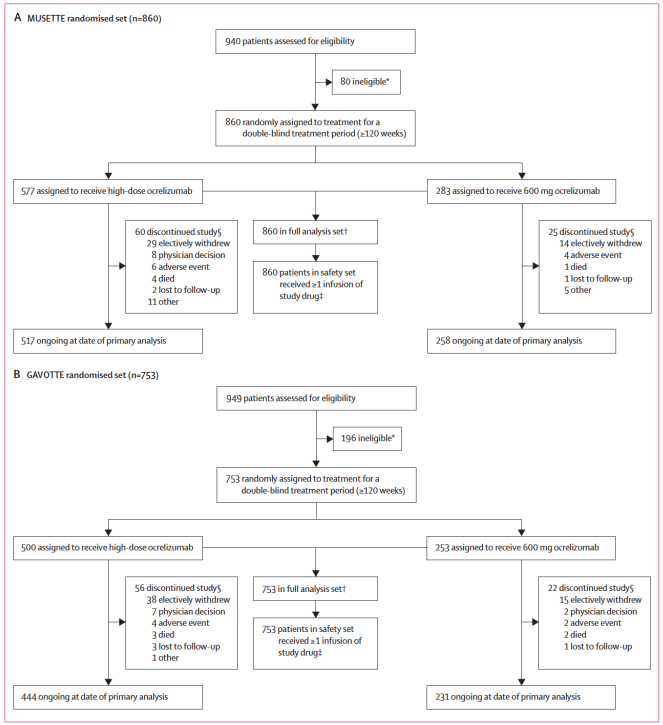

Figure 1: **Trial profile for patients in MUSETTE and GAVOTTE**
*A full list of reasons for ineligibility is provided in the appendix (pp 13-15, 25-26). †The full analysis set included all randomised participants. ‡The safety analysis set included all participants who received at least one infusion (partial or complete). §Patients who voluntarily discontinued from study treatment were asked to remain in the main double-blind study phase and were included in efficacy and safety analyses at minimum 120 weeks.

	MUSETTE			GAVOTTE		
	High-dose ocrelizumab (n=577)	600 mg ocrelizumab (n=283)	All patients (n=860)	High-dose ocrelizumab (n=500)	600 mg ocrelizumab (n=253)	All patients (n=753)
Age, years*	35 (18–55)	36 (18–54)	35 (18–55)	43 (18–56)	43 (18–56)	43 (18–56)
Sex						
Female	360 (62%)	180 (64%)	540 (63%)	266 (53%)	133 (53%)	399 (53%)
Male	217 (38%)	103 (36%)	320 (37%)	234 (47%)	120 (47%)	354 (47%)
Region						
USA	76 (13%)	31 (11%)	107 (12%)	32 (6%)	18 (7%)	50 (7%)
Rest of the world†	501 (87%)	252 (89%)	753 (88%)	468 (94%)	235 (93%)	703 (93%)
Race						
American Indian or Alaska Native	36 (6%)	19 (7%)	55 (6%)	24 (5%)	9 (4%)	33 (4%)
Asian	0	1 (<1%)	1 (<1%)	3 (1%)	1 (<1%)	4 (1%)
Black or African American	18 (3%)	5 (2%)	23 (3%)	10 (2%)	14 (6%)	24 (3%)
Native Hawaiian or other Pacific Islander	1 (<1%)	0	1 (<1%)	0	0	0
White	511 (89%)	249 (88%)	760 (88%)	444 (89%)	215 (85%)	659 (88%)
Multiple or unknown	11 (2%)	9 (3%)	20 (2%)	19 (4%)	14 (6%)	33 (4%)
Ethnicity‡						
Hispanic or Latino	101 (18%)	57 (20%)	158 (19%)	77 (16%)	34 (14%)	111 (15%)
Not Hispanic or not Latino	466 (81%)	221 (79%)	687 (80%)	404 (83%)	207 (85%)	611 (84%)
Not stated or unknown	6 (1%)	3 (1%)	9 (1%)	4 (1%)	3 (1%)	7 (1%)
BMI, kg/m²	24·2 (15·0–46·6)	24·4 (14·9–44·7)	24·2 (14·9–46·6)	24·7 (15·1–47·7)	24·0 (15·1–47·9)	24·3 (15·1–47·9)
Weight, kg	70·0 (40·5–151·0)	70·6 (43·1–148·5)	70·0 (40·5–151·0)	72·1 (39·4– 141·8)	72·0 (36·7–140·8)	72·0 (36·7–141·8)
Weight stratification category						
<75 kg	353 (61%)	175 (62%)	528 (61%)	284 (57%)	148 (58%)	432 (57%)
≥75 kg	224 (39%)	108 (38%)	332 (39%)	216 (43%)	105 (42%)	321 (43%)
EDSS score§	3·0 (0·0–6·0)	2·5 (0·0–5·5)	3·0 (0·0–6·0)	4·5 (1·0–7·0)	4·5 (3·0–6·5)	4·5 (1·0–7·0)
Duration since multiple sclerosis symptom onset, years	5·6 (0·2–32·3)	5·8 (0·2–31·2)	5·7 (0·2–32·3)	5·7 (1·1–17·8)	5·3 (1·0–19·4)	5·6 (1·0–19·4)
Previous disease-modifying therapy use	294 (51%)	140 (49%)	434 (50%)	79 (16%)	38 (15%)	117 (16%)
Patients with at least one T1 gadolinium-enhancing lesion present	225 (39%)	110 (39%; n=282)	335 (39%; n=859)	131 (26%)	66 (26%)	197 (26%)
Patients with new or enlarging T2 lesions	..	..	..	191 (39%; n=486)	92 (37%; n=247)	283 (39%; n=733)
Number of T2 lesions	46·0 (4·0–233·0)	43·0 (4·0–177·0)	45·0 (4·0–233·0)	55·0 (5·0–198·0)	57·0 (6·0–223·0)	57·0 (5·0–223·0)

Data are median (range) or n (%). EDSS=Expanded Disability Status Scale. *Inclusion was based on age at screening, but demographic characteristics were collected at baseline; some participants turned age 56 years between screening and baseline (up to 6 months). †A full list of patients in each country is provided in the appendix (p 24). ‡There were 573 participants in the high-dose arm and 281 in the 600 mg dose arm in MUSETTE and 485 in the high-dose arm and 244 in the GAVOTTE as ethnicity was not allowed to be reported at all sites per local regulations. §Protocol deviations in EDSS score were only noted retrospectively and patients remained in the study if there were no safety concerns. In MUSETTE, retrospective updates of EDSS scores were required due to noted inconsistencies and resulted in unqualified baseline scores. In GAVOTTE, one patient had an eligible EDSS score at screening but progressed before baseline, and in error, the site did not screen the failure at baseline.

Table 1: **Baseline demographics and disease characteristics**

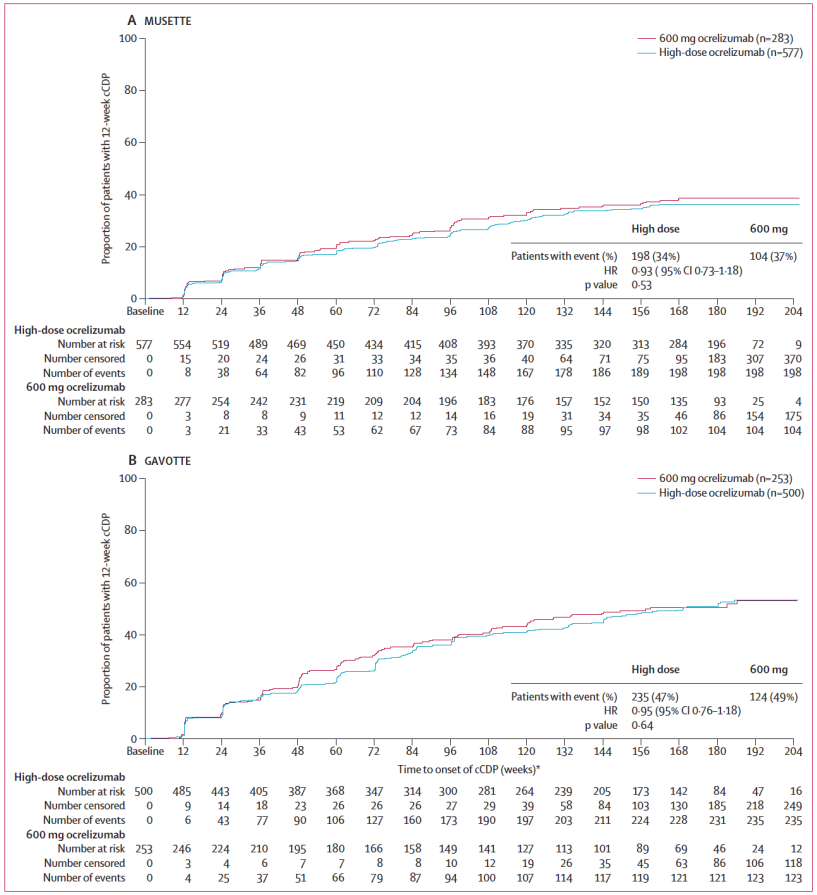

Figure 2: **Time to onset of 12-week cCDP in (A) MUSETTE and (B) GAVOTTE**
9HPT=9-Hole Peg Test. Baseline=week 0. cCDP=composite confirmed disability progression. EDSS=Expanded Disability Status Scale. HR=hazard ratio. T25FWT=Timed 25-Foot Walk Test. *cCDP requires at least one of the three: (1) an increase in EDSS score of at least 1·0 points from a baseline score of 5·5 points or less, or at least a 0·5-point increase from a baseline score of more than 5·5 points; (2) a 20% increase from baseline in time to complete the 9HPT; or (3) a 20% increase from baseline in the T25FWT.

	High-dose ocrelizumab	600 mg ocrelizumab	HR or difference between treatment arms (95% CI)	p value
MUSETTE				
Primary endpoint				
Time to onset of 12-week cCDP	198/577 (34%)	104/283 (37%)	0·93 (0·73 to 1·18)	0·53
Secondary endpoints*				
Time to onset of 24-week cCDP	155/577 (27%)	83/283 (29%)	0·92 (0·70 to 1·20)	0·53
Time to ≥20% increase in 12-week confirmed T25FWT score	139/567 (25%)	79/280 (28%)	0·86 (0·65 to 1·13)	0·27
Time to onset of 12-week cPIRA	173/577 (30%)	96/283 (34%)	0·87 (0·67 to 1·11)	0·26
Percentage change from baseline in NfL at week 48	−37 (−38 to −35; n=485) p<0·0001	−37 (−40 to −34; n=243) p<0·0001	..	..
Time to onset of 12-week CDP-EDSS	99/577 (17%)	45/283 (16%)	1·10 (0·77 to 1·57)	0·59
Time to onset of 48-week cCDP	100/577 (17%)	58/283 (20%)	0·86 (0·62 to 1·19)	0·37
Time to 12-week confirmed 4-point worsening in SDMT	81/568 (14%)	43/281 (15%)	0·88 (0·60 to 1·28)	0·49
Time to 24-week confirmed increase of 8 points in MSWS-12 score	123/491 (25%)	74/240 (31%)	0·80 (0·60 to 1·07)	0·13
Annual rate of percentage change from baseline in total brain volume	−0·402 (−0·463 to −0·340; n=559)	−0·397 (−0·463 to −0·331; n=276)	−0·005 (−0·063 to 0·053)	0·87
GAVOTTE				
Primary endpoint				
Time to onset of 12-week cCDP	235/500 (47%)	124/253 (49%)	0·95 (0·76 to 1·18)	0·64
Secondary endpoints*				
Time to onset of 24-week cCDP	202/500 (40%)	109/253 (43%)	0·91 (0·72 to 1·15)	0·41
Time to onset of 12-week cPIRA	229/500 (46%)	122/253 (48%)	0·94 (0·75 to 1·17)	0·58
Time to ≥20% increase in 12-week confirmed T25FWT	191/494 (39%)	105/251 (42%)	0·93 (0·73 to 1·18)	0·55
Time to onset of 12-week CDP-EDSS	130/500 (26%)	75/253 (30%)	0·86 (0·65 to 1·15)	0·32
Time to 12-week confirmed 4-point worsening in SDMT	85/487 (17%)	47/249 (19%)	0·92 (0·64 to 1·32)	0·65
Time to 24-week confirmed increase of 8 points in MSWS-12 score	176/382 (46%)	85/201 (42%)	1·22 (0·94 to 1·59)	0·13
Annual rate of percentage change from baseline in thalamic volume	−1·006 (−1·177 to −0·835; n=475)	−0·974 (−1·162 to −0·786; n=251)	−0·032 (−0·198 to 0·133)	0·70
Annual rate of percentage change from baseline in total brain volume	−0·548 (−0·634 to −0·463; n=476)	−0·480 (−0·574 to −0·385; n=251)	−0·069 (−0·145 to 0·008)	0·08
Percentage change from baseline in NfL at week 96	−18 (−21 to −15, n=382; p<0·0001)	−22 (−26 to −18, n=197; p<0·0001)	..	..
Change in NfL (ratio to baseline) at week 96	0·82 (0·79 to 0·85)	0·78 (0·74 to 0·82)	1·05 (0·99 to 1·12)	0·11

Data are the number of patients with an event (%) unless otherwise specified. cCDP=composite confirmed disability progression. CDP=confirmed disability progression. cPIRA=confirmed progression independent of relapse activity. EDSS=Expanded Disability Status Scale. HR=hazard ratio. MSWS-12=12-Item Multiple Sclerosis Walking Scale. NfL=neurofilament light chain. SDMT=Symbol Digit Modalities Test. T25FWT=Timed 25-Foot Walk Test. *Secondary endpoints are reported in the order of prespecified hierarchical analysis.

Table 2: **Summary of primary and secondary endpoints**

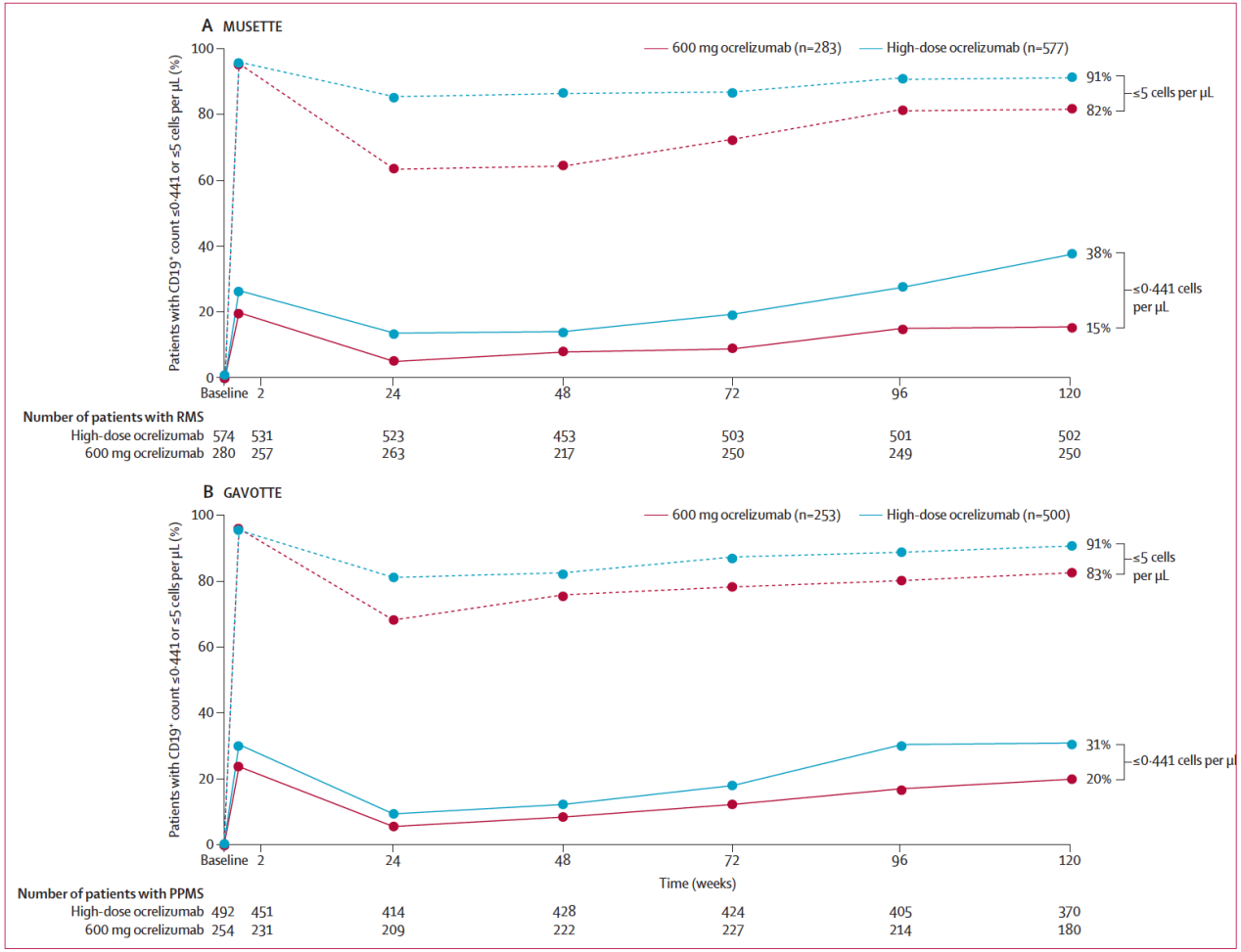

Figure 3: **Proportion of patients with CD19⁺ B-cell counts ≤5 cells per µL and ≤0·441 cells per µL in MUSETTE and GAVOTTE**
Baseline=week 0. PPMS=primary progressive multiple sclerosis. RMS=relapsing multiple sclerosis.

	MUSETTE		GAVOTTE	
	High-dose ocrelizumab (n=577)	600 mg ocrelizumab (n=283)	High-dose ocrelizumab (n=499)	600 mg ocrelizumab (n=254)
Patients with at least one adverse event	552 (96%)	267 (94%)	447 (90%)	230 (91%)
Total adverse events	4439	2103	3056	1381
Patients with at least one event				
Adverse event with fatal outcome*	4 (1%)	1 (<1%)	2 (<1%)	3 (1%)
Serious adverse event	77 (13%)	34 (12%)	61 (12%)	29 (11%)
Infections†				
Including COVID-19	451 (78%)	226 (80%)	321 (64%)	160 (63%)
Excluding COVID-19	408 (71%)	203 (72%)	301 (60%)	148 (58%)
Serious infections†				
Including COVID-19	35 (6%)	13 (5%)	22 (4%)	17 (7%)
Excluding COVID-19	18 (3%)	11 (4%)	18 (4%)	13 (5%)
Patients withdrawn from treatment due to an adverse event‡	20 (3%)	7 (2%)	11 (2%)	6 (2%)
Most frequent adverse events (>10% in any trial arm)				
Infusion-related reaction	198 (34%)	79 (28%)	120 (24%)	59 (23%)
COVID-19	217 (38%)	104 (37%)	82 (16%)	46 (18%)
Nasopharyngitis	133 (23%)	67 (24%)	84 (17%)	40 (16%)
Upper respiratory tract infection	107 (19%)	58 (20%)	77 (15%)	27 (11%)
Urinary tract infection	75 (13%)	30 (11%)	81 (16%)	27 (11%)
Headache	84 (15%)	46 (16%)	65 (13%)	36 (14%)
Infusion-related reactions				
Leading to withdrawal at first infusion	5 (1%)	0	0	1 (<1%)
Serious infusion-related reaction	0	1 (<1%)	2 (<1%)	0
Grade >3	6 (1%)	3 (1%)	9 (2%)	1 (<1%)
Medical concepts				
Malignancies§	4 (1%)	0	4 (1%)	4 (2%)

Data are the number of patients with an event (%) unless otherwise specified. MedDRA=Medical Dictionary for Regulatory Activities. *MUSETTE high dose, pneumonia (related) with concurrent neuroendocrine tumour of the lung (not related), COVID-19 in a patient not vaccinated against COVID-19 (related), pneumonia influenza (not related), liver metastases with primary malignancy unknown (not related); MUSETTE 600 mg, drowning (not related); GAVOTTE high dose, upper gastrointestinal haemorrhage (not related), subdural haematoma (not related); GAVOTTE 600 mg: carotid artery dissection (not related), pneumonia (not related), respiratory failure (not related). †Identified by MedDRA System Organ Class: Infections and Infestations. ‡Adverse events leading to treatment withdrawal are listed in the appendix (p 30). §Malignancies are identified using adverse events falling into the Standard MedDRA Query: malignant tumours (narrow).

***Table 3*: Adverse events in the safety population during the double-blind treatment phase**

Implications of all the available evidence

In both studies disease activity was almost completely controlled with ocrelizumab, and MUSETTE showed the lowest annualised relapse rate ever observed in a controlled phase 3 relapsing multiple sclerosis trial. The strong control of disease activity indicated that disability accumulation was almost entirely due to progression independent of relapse activity. However, high-dose ocrelizumab did not improve the control of disability progression. The absence of additional benefit despite greater peripheral B-cell depletion with a high dose of the drug indicates that further improvements might require targeting processes such as CNS-compartmentalised B cells or non-B-cell-mediated neurodegenerative mechanisms contributing to disease progression. The extent to which ocrelizumab modulates these processes remains unclear. Moreover, as greater peripheral B-cell depletion did not translate into improved outcomes, circulating B-cell concentrations alone might be an insufficient measure to guide treatment decisions in patients receiving ocrelizumab. Together, the evidence from these phase 3 trials confirms the favourable benefit–risk profile of 600 mg ocrelizumab for treating patients with either relapsing or primary progressive multiple sclerosis.

Efficacy and safety of ocrelizumab in primary progressive multiple sclerosis, including older patients and those with more advanced disease (ORATORIO-HAND): a multicentre, double-blind, randomised, placebo-controlled, phase 3b

Summary

Background The ORATORIO trial showed that ocrelizumab reduced the risk of disability progression versus placebo in patients with primary progressive multiple sclerosis (PPMS). We aimed to elucidate the effect of ocrelizumab in older and more disabled patients with PPMS, particularly regarding hand function preservation.

Methods ORATORIO-HAND was a multicentre, double-blind, randomised, placebo-controlled, phase 3b study with 138 sites across 22 countries. Patients with PPMS aged 18–65 years and Expanded Disability Status Scale (EDSS) score of 3·0–8·0 were randomly assigned 1:1 to intravenous ocrelizumab 600 mg or placebo every 6 months for 144 weeks or until a prespecified number of progression events occurred. Masking was achieved by use of a placebo solution administered in the same manner as ocrelizumab. Double-blinding across all periods was maintained through separation of investigators responsible for efficacy and safety assessments. MRI scans were evaluated by a masked central reader, and laboratory parameters that could reveal treatment allocation were masked to site personnel until the primary analysis. Two coprimary estimands were defined, with the endpoint of time to onset of 12-week composite confirmed disability progression (12W-cCDP) in 9-Hole Peg Test or EDSS evaluated in all randomly assigned patients, and the same endpoint evaluated in a subset of patients with MRI activity at baseline. This study is registered with ClinicalTrials.gov, NCT04035005 and is ongoing and not recruiting.

Findings Between Aug 12, 2019, and Dec 10, 2024, of 1360 patients assessed for eligibility, 1013 were randomly assigned (ocrelizumab [n=505]; placebo [n=508]). The proportion of patients with 12W-cCDP was 165 (33%) of 505 with ocrelizumab and 205 (40%) of 508 with placebo (hazard ratio, 95% CI 0·70 0·57–0·86; relative risk reduction=30%; p=0·0007). In the MRI-active subgroup, a significant risk reduction was also observed in 12W-cCDP (risk reduction=55%; p<0·0001). The overall safety profile was similar in both groups. More infections (245 [48%] of 506 *vs* 226 [45%] of 506) were observed with ocrelizumab, but not after COVID-19 was excluded (38% *vs* 37%). Rates of serious adverse events and serious infections were similar between groups.

Interpretation Ocrelizumab was superior to placebo in delaying disability progression, with stronger effect on hand function, in a broad PPMS population including older patients and those with more advanced disease, while maintaining a manageable safety profile.

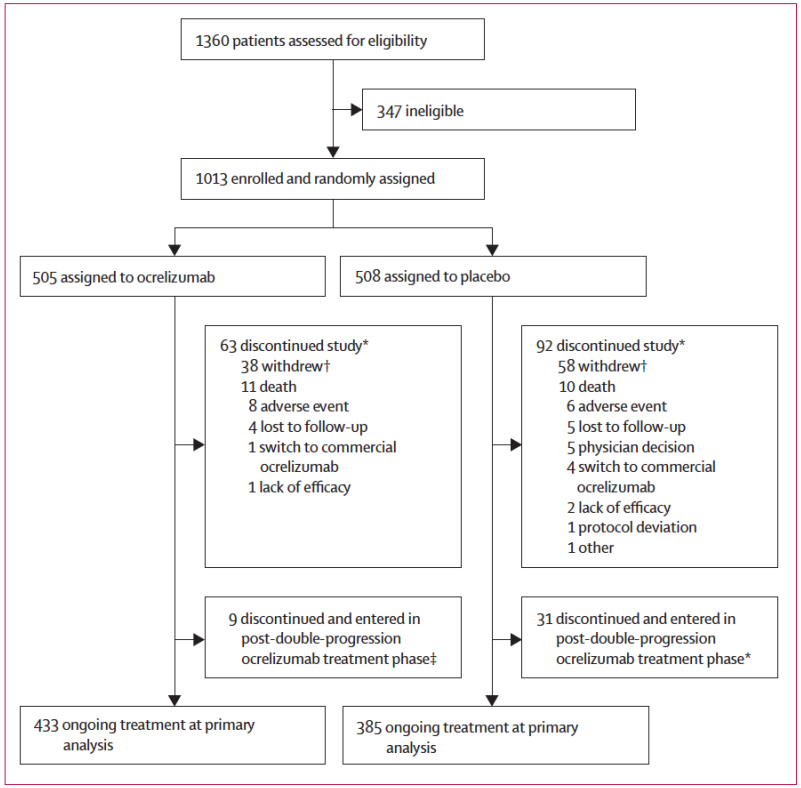

Figure 1: **Trial profile**

*Discontinued study during double-blind treatment or follow-up 1. †Categories for withdrawal by patient were retrieved from a manual review of individual patient narratives. Ocrelizumab: personal reasons (no further clarification received; n=20); perceived lack of efficacy (n=5); difficulties in following the schedule or visiting the site (n=3); Ukraine war (n=4); relocation (n=3). Placebo: personal reasons (no further clarification received; n=25); perceived lack of efficacy (n=13); difficulties in following the schedule or visiting the site (n=8); Ukraine war (n=4); perceived safety concern (n=2); other treatment or commercial ocrelizumab (n=3). ‡Patients who experienced a double-progression event (defined as a 20% increase in 9-Hole Peg Test time sustained for 24 weeks and an Expanded Disability Status Scale-confirmed-disability progression sustained for 12 weeks) were given the option to switch to treatment with ocrelizumab, but only once they had completed 120 weeks in the double-blind treatment. To maintain the masking in the treatment arm, the first dose of post-double-progression ocrelizumab treatment was administered as two infusions of 300 mg given 14 days apart for all patients. Patients who discontinued from the post-double progression ocrelizumab phase could continue to be followed up in the follow-up 2 phase.

	Ocrelizumab (n=505)	Placebo (n=508)
Age		
Years, mean (SD)	48 (11)	47 (11)
Years,* median range	48 (18–66)	47 (22–66)
≤55 years	366 (72%)	371 (73%)
>55 years	139 (28%)	137 (27%)
Female	290 (57%)	278 (55%)
Race		
American Indian or Alaska Native	18 (4%)	14 (3%)
Asian	0	2 (<1%)
Black or African American	2 (<1%)	1 (<1%)
Native Hawaiian or other Pacific Islander	2 (<1%)	0
White	464 (92%)	480 (94%)
Multiple or unknown	19 (4%)	11 (2%)
Ethnicity		
Hispanic or Latinx	31 (6%)	22 (4%)
Not Hispanic or Latinx	457 (90)	476 (94%)
Not stated or unknown	17 (3%)	10 (2%)
Expanded Disability Status Scale score	6·0 (3·0–8·0)	6·0 (2·5–8·0)
>6·5	77 (15%)	84 (17%)
9-Hole Peg Test, s	34·2 (25·1–216·9)	33·8 (24·5–221·8)
Patients with MRI activity	183 (36%)	185 (36)
T1 Gd+ lesions	121 (24%)	113 (22%)
New or enlarging T2 lesions†	181 (36%)	185 (36)
Duration since symptom onset, years‡	9·4 (0·7–27·6)	9·0 (0·7–37·4)
Duration since diagnosis, years	3·6 (0·1–26·4)	3·7 (0·1–24·4)
Previous disease-modifying treatment	42 (8%)	31 (6%)
Total volume of lesions on T2-weighted images, cm^3	16·6 (0·3–102·7)	17·5 (0·0–118·9)
Normalised brain volume, cm^3	1478·6 (1101·9–1787·3)	1485·0 (1175·8–1806·0)

Data are mean (SD), median range, or n (%). Gd+=gadolinium-enhancing. *All participants were younger than 66 years at the time of signing informed consent; however, one participant in each group of the intention-to-treat population was 66 years at the time of random assignment. †New or enlarging T2 lesions detected between two scans acquired during screening or baseline. ‡n=12 patients with disease duration above 20 years at random assignment (eight in the ocrelizumab group and four in the placebo group) were enrolled in the study.

Table 1: **Baseline demographics and disease characteristics in all patients**

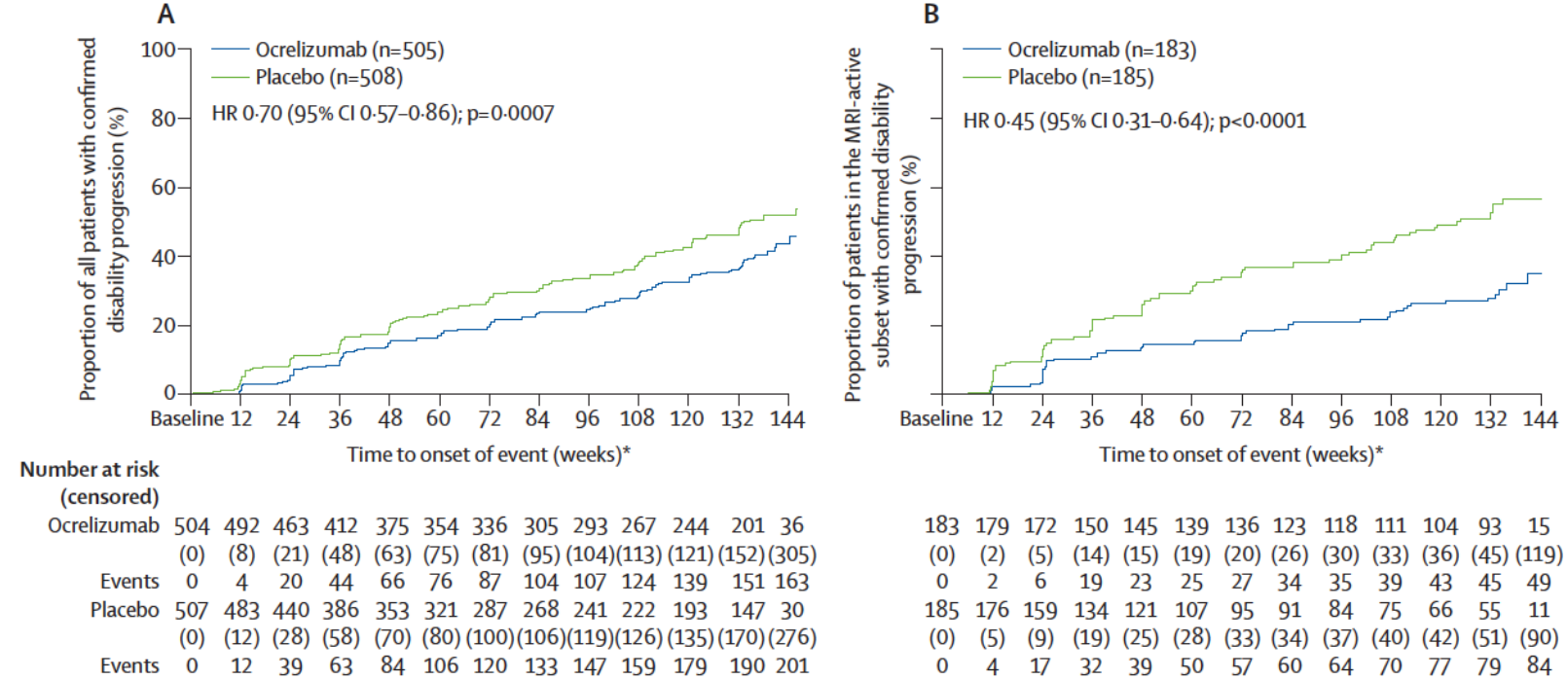

Number at risk (censored)													
Ocrelizumab	504	492	463	412	375	354	336	305	293	267	244	201	36
	(0)	(8)	(21)	(48)	(63)	(75)	(81)	(95)	(104)	(113)	(121)	(152)	(305)
Events	0	4	20	44	66	76	87	104	107	124	139	151	163
Placebo	507	483	440	386	353	321	287	268	241	222	193	147	30
	(0)	(12)	(28)	(58)	(70)	(80)	(100)	(106)	(119)	(126)	(135)	(170)	(276)
Events	0	12	39	63	84	106	120	133	147	159	179	190	201

	183	179	172	150	145	139	136	123	118	111	104	93	15
	(0)	(2)	(5)	(14)	(15)	(19)	(20)	(26)	(30)	(33)	(36)	(45)	(119)
	0	2	6	19	23	25	27	34	35	39	43	45	49
	185	176	159	134	121	107	95	91	84	75	66	55	11
	(0)	(5)	(9)	(19)	(25)	(28)	(33)	(34)	(37)	(40)	(42)	(51)	(90)
	0	4	17	32	39	50	57	60	64	70	77	79	84

Figure 2: **Time to onset of 12-week composite confirmed disability progression in all patients (A) and the MRI-active subset (B)†**

EDSS=Expanded Disability Status Scale. HR=hazard ratio. Clinical cutoff date Jan 15, 2025. *Data from weeks 156 and 168 are not shown here owing to low n values. †Defined as patients with T1 Gd-enhancing lesion(s) at baseline or new or enlarging T2 lesion(s) as detected in two separate scans during screening or at baseline. Data from weeks 156 and 168 are not shown here owing to low n values. For the full analysis set, HRs were estimated by Cox regression. HRs and log-rank test p value were stratified by MRI activity (yes *vs* no), age (≤55 years *vs* >55 years), EDSS score (≤6·5 *vs* >6·5), region (EU, the UK, and Canada *vs* other). MRI-active subset: HRs were estimated by Cox regression. HR and log-rank test p value were stratified by age (≤55 years *vs* >55 years), EDSS score (≤6·5 *vs* >6·5), region (EU, the UK, and Canada *vs* other).

	Ocrelizumab (n=505)	Placebo (n=508)	p value
Coprimary endpoint: time to onset of 12-week cCDP			
All patients			
Number of patients evaluated	504	507	..
Patients with event	165 (33%)	205 (40%)	..
HR	0·70 (0·57 to 0·86)	..	0·0007
MRI-active patients			
Number of patients evaluated	183	185	..
Patients with event	49/183 (27%)	85/185 (46%)	..
HR	0·45 (0·31 to 0·64)	..	<0·0001
Key secondary and exploratory endpoints in intention-to-treat population			
Time to 12-week CDP in 9HPT			
Number of patients evaluated	504	507	..
Patients with event	84/504 (17%)	126/507 (25%)	..
HR	0·59 (0·44 to 0·78)	..	0·0002
Time to 12-week CDP in EDSS			
Number of patients evaluated	504	507	..
Patients with event	116 (23%)	156 (31%)	..
HR	0·67 (0·53 to 0·86)	..	0·0013
Time to 24-week CDP in 9HPT			
Number of patients evaluated	504	507	..
Patients with event	67/504 (13%)	111 (22%)	..
HR	0·52 (0·38 to 0·71)	..	<0·0001
Time to 24-week CDP in EDSS			
Number of patients evaluated	504	507	..
Patients with event	105 (21%)	144 (28%)	..
HR	0·67 (0·52 to 0·86)	..	0·0018
Time to 24-week cCDP*			
Number of patients evaluated	504	507	..
Patients with event	140 (28%)	189 (37%)	..
HR	0·65 (0·52–0·81)	..	0·0001
Change from baseline in total volume of T2 lesions (annual rate, cm per year†)			
Number of patients evaluated	484	478	..
Annual rate of change	−0·016 (−0·021 to −0·010)	0·021 (0·013 to 0·029)	..
Difference in annual rate of change	−0·037 (−0·046 to −0·028)	..	<0·0001
Percent change in total brain volume from week 24 (annual rate, %)‡			
Number of patients evaluated	382	378	..
Rate of change	−0·566 (−0·654 to −0·477)	−0·564 (−0·660 to −0·468)	..
Difference in rate of change	−0·002 (−0·091 to 0·087)	..	0·97

Data are n (%) and HR (95% CI). 9HPT=9-Hole Peg Test. CDP=confirmed disability progression. cCDP=composite confirmed disability progression. EDSS=Expanded Disability Status Scale. HR=hazard ratio. *Time to 24-week cCDP is an exploratory endpoint but is included here for data completeness. †Lesional volumes were converted from cm^3 per year to cm per year through a cubic root transformation. ‡Analysis included patients with a week 24 MRI assessment and at least one additional MRI assessment post-week 24.

Table 2: **Summary of coprimary and secondary endpoints**

	All patients n=1011		Definition 1 (presence or absence of T1 Gd+ lesions or new or enlarging T2 lesions)*				Definition 2 (presence or absence of T1 Gd+ lesions)*			
			MRI-active, n=368		MRI-inactive, n=643		MRI-active, n=234		MRI-inactive, n=777	
	Ocrelizumab versus placebo with event, %; NNT	HR (95% CI)	Ocrelizumab versus placebo with event, %; NNT	HR (95% CI)	Ocrelizumab versus placebo with event, %; NNT	HR (95% CI)	Ocrelizumab versus placebo with event, %; NNT	HR (95% CI)	Ocrelizumab versus placebo with event, %; NNT	HR (95% CI)
Composite confirmed disability progression										
12-week	33% *vs* 40%; 13	0·70 (0·57–0·86)	27% *vs* 46%; 5	0·45 (0·31–0·64)	36% *vs* 37%; 88	0·89 (0·69–1·16)	29% *vs* 42%; 8	0·55 (0·35–0·86)	34% *vs* 40%; 16	0·76 (0·60–0·97)
24-week	28% *vs* 37%; 11	0·65 (0·52–0·81)	23% *vs* 44%; 5	0·40 (0·28–0·59)	30% *vs* 33%; 33	0·85 (0·65–1·13)	26% *vs*41%; 7	0·49 (0·30–0·78)	29% *vs* 36%; 13	0·72 (0·56–0·93)
48-week	24% *vs* 33%; 11	0·64 (0·50–0·81)	20% *vs* 39%; 5	0·40 (0·27–0·60)	26% *vs* 29%; 33	0·83 (0·62–1·12)	22% *vs* 36%; 7	0·50 (0·31–0·82)	24% *vs* 32%; 14	0·70 (0·53–0·92)
Expanded Disability Status Scale										
12-week	23% *vs* 31%; 13	0·67 (0·53–0·86)	18% *vs* 36%; 5	0·41 (0·27–0·62)	26% *vs* 28%; 56	0·89 (0·66–1·20)	21% *vs*34%; 8	0·52 (0·31–0·87)	24% *vs* 30%; 16	0·75 (0·57–0·99)
24-week	21% *vs* 28%; 13	0·67 (0·52–0·86)	18% *vs* 34%; 6	0·43 (0·28–0·65)	23% *vs* 25%; 41	0·88 (0·64–1·21)	21% *vs* 33%; 8	0·54 (0·32–0·91)	21% *vs* 27%; 16	0·75 (0·56–1·00)
48-week	18% *vs* 24%; 16	0·68 (0·52–0·89)	16% *vs* 30%; 7	0·45 (0·29–0·70)	19% versus 21%; 55	0·88 (0·62–1·24)	18% *vs* 27%; 11	0·58 (0·31–1·00)	18% *vs* 23%; 19	0·74 (0·54–1·01)
9-Hole Peg Test										
12-week	17 *vs* 25; 12	0·59 (0·44–0·78)	14 *vs* 31; 6	0·38 (0·23–0·61)	18 *vs* 21; 30	0·77 (0·54–1·10)	15 *vs* 30; 7	0·37 (0·20–0·67)	17 *vs* 23; 16	0·68 (0·49–0·94)
24-week	13 *vs* 22; 12	0·52 (0·38–0·71)	11*vs* 28; 6	0·32 (0·19–0·56)	15 *vs* 19; 25	0·69 (0·47–1·02)	12 *vs* 26; 7	0·32 (0·16–0·63)	14 *vs* 21; 14	0·60 (0·42–0·85)
48-week	10 *vs* 19; 12	0·50 (0·35–0·70)	7 *vs* 22; 7	0·25 (0·13–0·49)	12 *vs* 17; 23	0·68 (0·45–1·03)	7 *vs* 20; 8	0·29 (0·13–0·66)	11 *vs* 18; 15	0·58 (0·39–0·85)

Gd+=gadolinium-enhancing. HR=hazard ratio. NNT=number needed to treat (absolute risk reduction, calculated using proportions with disability events rounded to one decimal place). *In the ORATORIO-HAND protocol, MRI activity was defined as presence of T1 Gd+ lesions at baseline and/or new or enlarging T2 lesions detected in two separate scans during screening and/or baseline (definition 1); in the ORATORIO study, MRI activity was defined as presence of T1 Gd+ lesions at baseline (definition 2).

Table 3: **Subgroup analyses of composite confirmed disability progression and component endpoints based on baseline MRI activity defined using two different definitions**

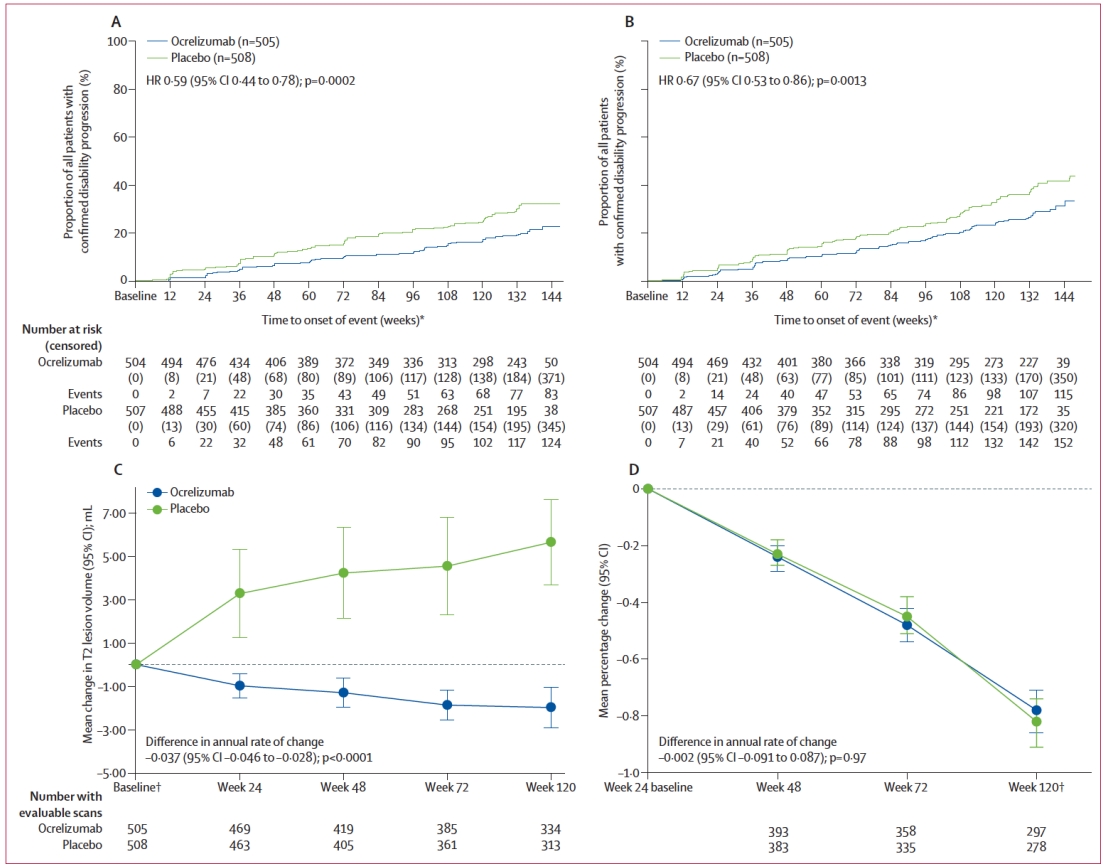

Figure 3: **Key secondary endpoints**

(A) Time to onset of 12-week 9-Hole Peg Test-confirmed disability progression. (B) Time to onset of 12-week EDSS-CDP in all patients. (C) Mean change from baseline to week 120 in total volume of T2 lesions. (D) Percentage change from week 24 to week 120 in total brain volume. EDSS=Expanded Disability Status Scale. EDSS-CDP= Expanded Disability Status Scale-confirmed disability progression. HR=hazard ratio. *Data from weeks 156 and 168 are not shown here owing to low n values. †Owing to poor availability, data are presented up to week 120 only. For parts A and B all patients' HRs were estimated by Cox regression; HRs and log-rank test p value were stratified by MRI activity (yes *vs* no), age (≤55 years *vs* >55 years), EDSS score (≤6·5 *vs* >6·5), region (EU, the UK, and Canada *vs* other). For part C estimates of annual rates of change are taken from a random coefficient regression model; the significance of the estimated mean difference is calculated using the Wald test. For part D estimates of annual rates of change are taken from a random coefficient regression model; the statistical significance of the estimated mean difference is calculated using the Wald test.

	n (%)		Rate per 100 patient-years (95%CI)*	
	Ocrelizumab (n=506)†	Placebo (n=506)	Ocrelizumab (n=506)†	Placebo (n=506)
All adverse events	379 (75%)	360 (71%)	143·5 (136·7–150·6)	127·8 (121·2–134·7)
Adverse events leading to study treatment discontinuation	15 (3%)	12 (2%)	1·3 (0·7–2·1)	1·2 (0·6–2·0)
Serious adverse events	65 (13%)	67 (13%)	8·5 (6·9–10·4)	8·2 (6·6–10·1)
Infusion-related reactions	105 (21%)	22 (4%)	13·9 (11·9–16·3)	3·4 (2·4–4·6)
Infections	245 (48%)	226 (45%)	41·3 (37·7–45·2)	39·9 (36·3–43·8)
Lower respiratory (including COVID-19)	141 (28%)	111 (22%)	14·6 (12·5–17·0)	11·4 (9·5–13·5)
COVID-19	97 (19%)	70 (14%)	9·1 (7·5–11·0)	6·6 (5·2–8·3)
Upper respiratory	82 (16%)	77 (15%)	9·3 (7·6–11·2)	9·7 (8·0–11·8)
Urinary tract	63 (12%)	76 (15%)	12·0 (10·1–14·1)	11·9 (10·0–14·1)
Serious infections				
Including COVID-19	32 (6%)	27 (5%)	3·4 (2·4–4·6)	2·8 (1·9–4·0)
Excluding COVID-19	12 (2%)	19 (4%)	1·5 (0·9–2·3)	2·0 (1·3–3·0)
Malignancies‡	5 (1%)	3 (<1%)	0·4 (0·1–1·0)	0·3 (0·1–0·8)
Deaths§	11 (2%)	10 (2%)	0·9 (0·5–1·7)	0·9 (0·4–1·7)

Data are n (%) unless stated otherwise. *Rates per 100 patient-years account for time on treatment, as the trial had variable duration and discontinuation rates were different between the two groups. †One patient randomly assigned to the placebo group mistakenly received ocrelizumab at the week 2 visit in the double-blind period; this patient was included in the ocrelizumab group for safety analyses. ‡Malignancies are identified using adverse events falling into the Standardised Medical Dictionary for Regulatory Activities queries "Malignant tumours (SMQ)". Ocrelizumab group—breast cancer (n=1), malignant melanoma (n=1), pancreatic carcinoma (n=1), metastatic pancreatic carcinoma (n=1), and stage IV prostate cancer (n=1); placebo group—acute myeloid leukaemia (n=1), colorectal cancer (n=1), and endometrial adenocarcinoma (n=1). §For reported deaths during the study, please see appendix (p 26).

Table 4: **Adverse events in the safety population during the double-blind treatment and follow-up 1 phase**

Implications of all the available evidence

The demonstration of ocrelizumab's efficacy in a second large randomised controlled trial solidifies the therapeutic rationale for treating PPMS, extending the window of opportunity to patients with advanced disease. These clinical findings are consistent with the hypothesised pathophysiological model of progressive multiple sclerosis as a length-dependent central axonopathy. This provides a compelling argument for shifting the focus of clinical assessment and treatment evaluation in advanced disease towards measures of upper-limb function. The validation of a composite endpoint incorporating upper-limb dexterity establishes a new standard for trial design in progressive multiple sclerosis. The adoption of similar endpoints in ongoing and future studies is essential for the robust evaluation of novel therapeutic agents. Collectively, this evidence counters the long-held notion of an intractable disease stage, offering a clear basis for intervention and highlighting the need to assess functional outcomes that reflect the underlying disease process while capturing aspects of the disease that are relevant to patients with multiple sclerosis.

Prasinezumab ist ein experimenteller, humanisierter monoklonaler Antikörper, der gezielt für die krankheitsmodifizierende Behandlung der **Parkinson-Krankheit** im Frühstadium entwickelt wird. Das Medikament wird von den Pharmaunternehmen Roche und Prothena erforscht.

Wirkmechanismus

•**Zielstruktur**: Der Antikörper bindet gezielt an aggregiertes **Alpha-Synuclein**.

•**Pathologie**: Fehlgefaltete Alpha-Synuclein-Proteine bilden im Gehirn toxische Klumpen (Lewy-Körperchen), die Nervenzellen zerstören.

•**Ansatz**: Prasinezumab soll diese Aggregate blockieren oder für den Abbau markieren, um das Fortschreiten der Erkrankung kausal zu verlangsamen.

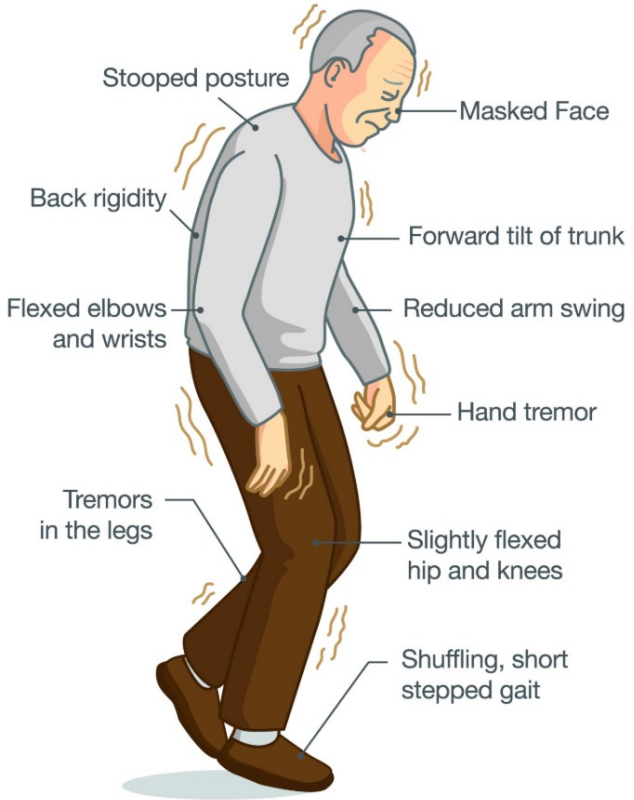

Efficacy and safety of intravenous prasinezumab in individuals with early-stage Parkinson's disease on stable symptomatic monotherapy (PADOVA): a phase 2b, multicentre, randomised, double-blind, placebo-controlled study

Summary

Background Prasinezumab has previously shown potential for reducing the progression of motor signs (Movement Disorder Society-sponsored Revision of the Unified Parkinson's Disease Rating Scale [MDS-UPDRS] Part III) in patients with early-stage Parkinson's disease who were treatment-naive or receiving monoamine oxidase type B (MAO-B) inhibitors. The aim of the PADOVA trial was to evaluate the efficacy and safety of prasinezumab in a broader population of patients receiving stable symptomatic medication.

Methods This phase 2b, multicentre, double-blind, parallel-group, placebo-controlled, randomised, superiority trial recruited participants with early-stage Parkinson's disease (age 50–85 years, 3 months to 3 years from diagnosis, Hoehn and Yahr stage 1 or 2) on stable symptomatic medication from 110 centres in nine countries in Europe and North America. Participants were individually randomly assigned (1:1) via permuted blocks (stratified by symptomatic medication [levodopa or MAO-B inhibitor]) to intravenous prasinezumab (1500 mg) or placebo every 4 weeks for at least 76 weeks and until the target number of motor progression events was reached. Participants, investigators, and clinical assessors were masked to group assignment. The primary endpoint was time to a confirmed motor progression event (≥5-point increase in MDS-UPDRS Part III off-medication score), assessed in the full analysis set (all randomly assigned participants according to the treatment to which they were assigned). Safety and tolerability were assessed in all randomly assigned participants who received at least one dose of study drug, with participants grouped according to treatment received. The trial is registered with ClinicalTrials.gov (NCT04777331) and EudraCT (2020-004997-23), and is active, not recruiting.

Findings Between May 5, 2021, and March 22, 2023, 787 individuals were screened. 586 were enrolled and randomly assigned (n=293 per group; mean age 64·2 years [SD 7·3]; 214 [37%] female and 372 [63%] male); 550 completed double-blind treatment (prasinezumab, n=277; placebo, n=273). The primary endpoint was not met; the primary analysis showed a non-significant delay in motor progression with prasinezumab versus placebo (hazard ratio 0·84 [95% CI 0·69–1·01]; p=0·066); median time to confirmed motor progression in the prasinezumab group was 61·1 weeks (95% CI 52·3–71·9), compared with 49·7 weeks (40·1–58·1) in the placebo group. The incidence of one or more serious adverse events was similar between groups (prasinezumab, 34 [12%] of 292; placebo, 34 [12%] of 290) and three recorded deaths were unrelated to the study drug (prasinezumab, n=1 [<1%]; placebo, n=2 [1%]).

Interpretation Although PADOVA did not meet the primary endpoint, prespecified exploratory evidence suggests clinical activity of prasinezumab in early-stage Parkinson's disease, supporting continued investigation in the ongoing phase 3 PARAISO trial (NCT07174310).

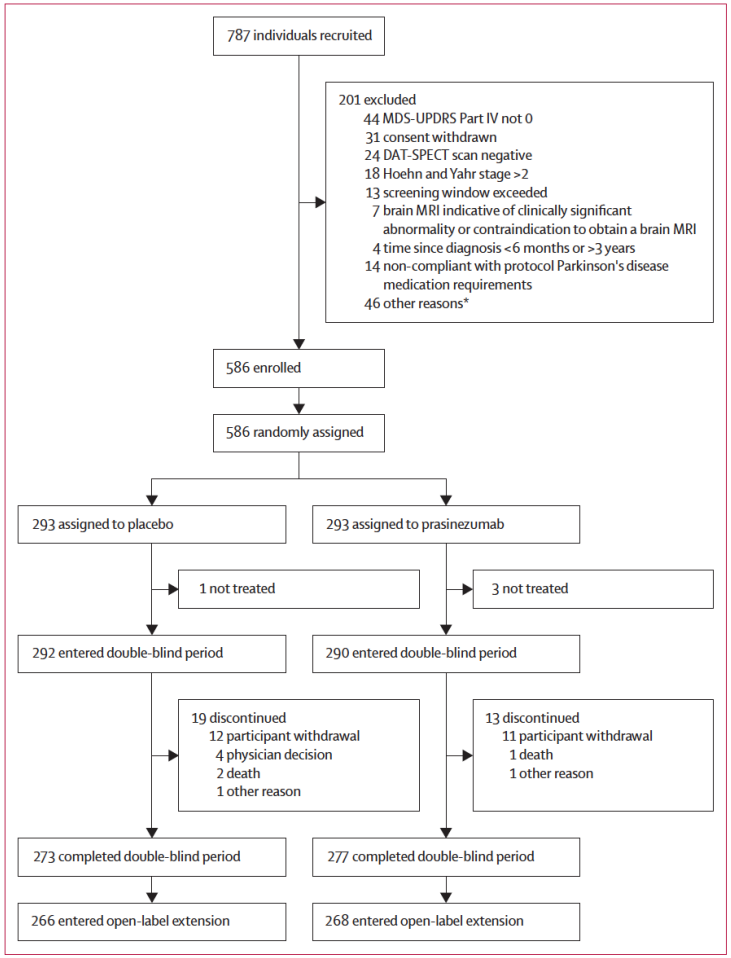

Figure 1: **Trial profile**
21 (4%) of 586 randomly assigned participants (prasinezumab, n=10; placebo, n=11) had a baseline MDS-UPDRS Part IV score of 1 or higher, which was an exclusion criterion (in addition to 44 individuals who were excluded at screening for this reason). DAT-SPECT=dopamine transporter single photon emission CT. MDS-UPDRS=Movement Disorder Society-sponsored Revision of the Unified Parkinson's Disease Rating Scale. *Other reasons include inability to comply with protocol procedures, concomitant disease or unstable medical condition, use of prohibited medication, exclusionary bodyweight or BMI, drug misuse, or poor venous access.

	Placebo group (n=293)	Prasinezumab group (n=293)	Total (n=586)
Age, years	64·4 (7·5)	64·0 (7·2)	64·2 (7·3)
Age group, years			
<60	87 (30%)	84 (29%)	171 (29%)
≥60	206 (70%)	209 (71%)	415 (71%)
Sex, n (%)			
Female	104 (35%)	110 (38%)	214 (37%)
Male	189 (65%)	183 (62%)	372 (63%)
Weight, kg	76·7 (13·6)	75·8 (14·2)	76·3 (13·9)
Race			
Asian	2 (1%)	4 (1%)	6 (1%)
Black or African American	2 (1%)	0	2 (<1%)
White	278 (95%)	275 (94%)	553 (94%)
Unknown	11 (4%)	14 (5%)	25 (4%)
Ethnicity			
Hispanic or Latino	31 (11%)	33 (11%)	64 (11%)
Not Hispanic or Latino	246 (84%)	241 (82%)	487 (83%)
Not stated	15 (5%)	19 (6%)	34 (6%)
Unknown	1 (<1%)	0	1 (<1%)
Height, cm	171·4 (9·3)	171·2 (10·0)	171·3 (9·6)
BMI, kg/m²	25·8 (3·6)	25·7 (3·7)	25·8 (3·6)
Time since diagnosis, months			
Mean (SD)	18·4 (9·0)	18·8 (9·5)	18·6 (9·2)
Median (IQR)	16·0 (10·9–24·9)	17·1 (10·1–26·6)	16·3 (10·6–25·4)
<12	90 (31%)	103 (35%)	193 (33%)
12–24	124 (42%)	106 (36%)	230 (39%)
>24	79 (27%)	84 (29%)	163 (28%)
MDS-UPDRS			
Part II total score	5·1 (4·1)	4·9 (3·5)	5·0 (3·8)
Part III total score (off-medication)	24·6 (10·8)	24·3 (9·9)	24·5 (10·4)
Part III total score (on)	19·5 (9·8)	19·0 (8·9)	19·2 (9·4)
Part IV total score category			
0	283 (97%)	282 (96%)	565 (96%)
≥1	10 (3%)	11 (4%)	21 (4%)
SE-ADL Current Level of Disability category*			
Completely independent†	288 (98%)	285 (97%)	573 (98%)
Not completely independent‡	3 (1%)	2 (1%)	5 (1%)
Missing	2 (1%)	6 (2%)	8 (1%)
Hoehn and Yahr stage			
1	40 (14%)	38 (13%)	78 (13%)
2	250 (85%)	251 (86%)	501 (86%)
3	3 (1%)	4 (1%)	7 (1%)
REM Sleep Behaviour Disorder Score category*			
Negative (<5)	185 (63%)	179 (61%)	364 (62%)
Positive (≥5)	106 (36%)	112 (38%)	218 (37%)
Missing	2 (1%)	2 (1%)	4 (1%)
Striatal binding ratio (putamen-ipsilateral§)	0·87 (0·28)	0·88 (0·31)	0·87 (0·30)
Stratification factor			
Levodopa	217 (74%)	218 (74%)	435 (74%)
MAO-B inhibitor	76 (26%)	75 (26%)	151 (26%)

Data are mean (SD), n (%), or median (IQR). MDS-UPDRS, Movement Disorder Society-sponsored Revision of the Unified Parkinson's Disease Rating Scale. SE-ADL=Schwab and England Activities of Daily Living scale. REM, rapid eye movement. MAO-B=monoamine oxidase type B. *Baseline data were not available for all participants. †Score of >70% to 100%. ‡Score of ≤70%. §Ipsilateral to the more affected side of the body.

Table 1: **Baseline demographic and clinical characteristics (full analysis set)**

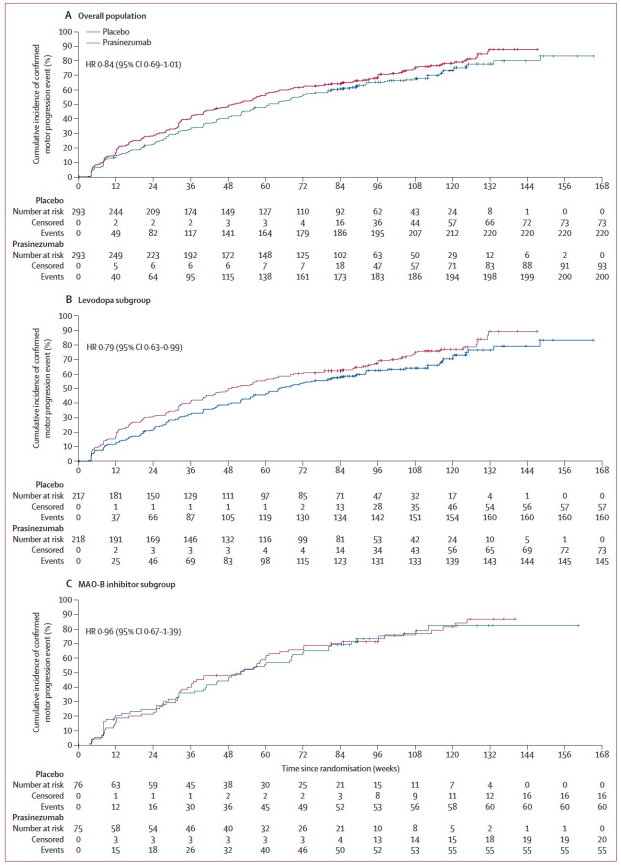

Figure 2: Cumulative probability of confirmed motor progression event in the full analysis set
A motor progression event was defined as at least a 5-point increase from baseline in MDS-UPDRS Part III off-medication score. (A) Overall population (primary endpoint). (B) Levodopa subgroup. (C) MAO-B inhibitor subgroup. HR=hazard ratio. MAO-B=monoamine oxidase type B. MDS-UPDRS=Movement Disorder Society-sponsored Revision of the Unified Parkinson's Disease Rating Scale.

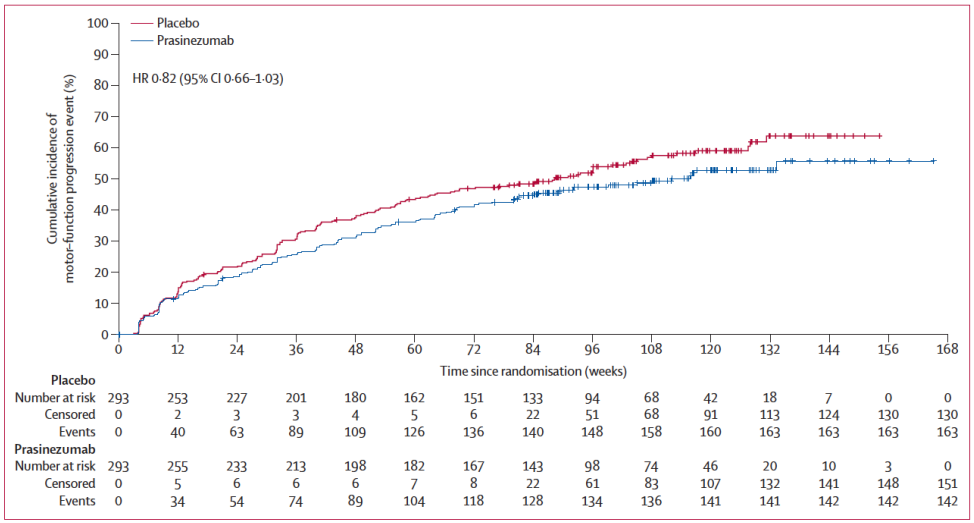

Placebo															
Number at risk	293	253	227	201	180	162	151	133	94	68	42	18	7	0	0
Censored	0	2	3	3	4	5	6	22	51	68	91	113	124	130	130
Events	0	40	63	89	109	126	136	140	148	158	160	163	163	163	163
Prasinezumab															
Number at risk	293	255	233	213	198	182	167	143	98	74	46	20	10	3	0
Censored	0	5	6	6	6	7	8	22	61	83	107	132	141	148	151
Events	0	34	54	74	89	104	118	128	134	136	141	141	142	142	142

***Figure 3*: Cumulative probability of a motor-function progression event in the full analysis set**
A motor-function progression event was defined as confirmed motor progression concurrent with or followed by meaningful worsening in patient-reported functioning. HR=hazard ratio.

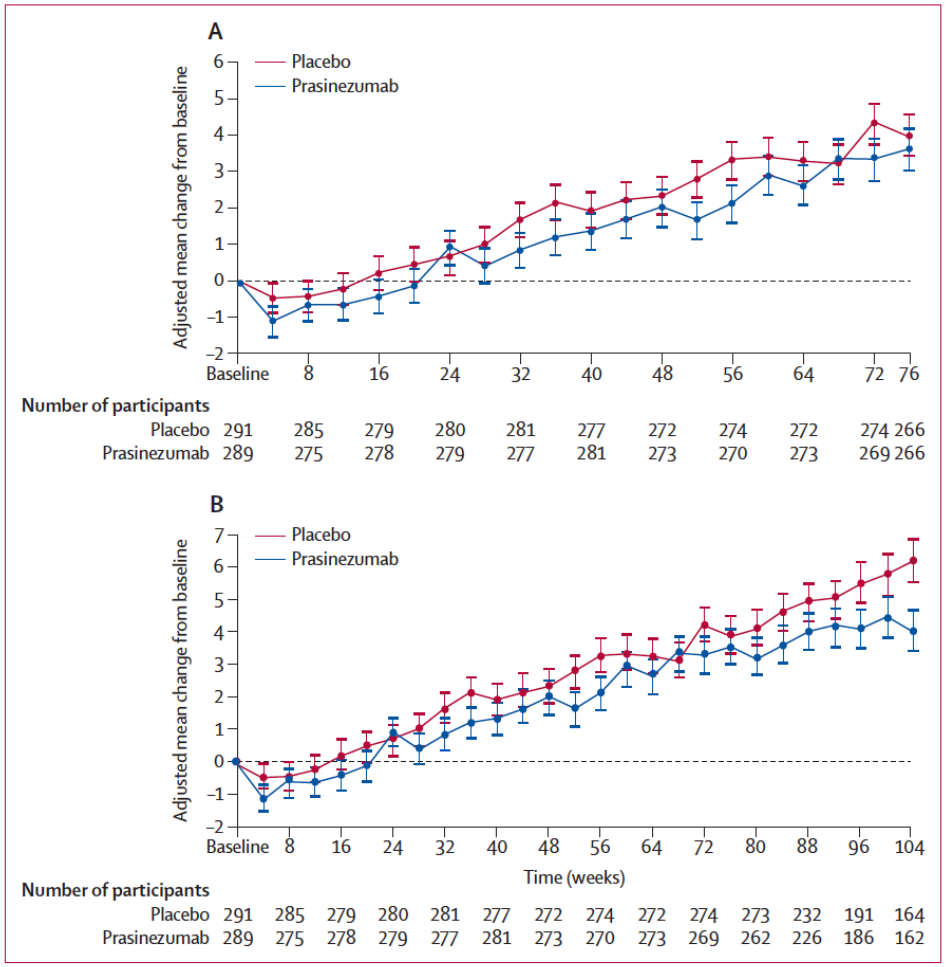

Figure 4: **Change from baseline in MDS-UPDRS Part III off-medication score**
Change in MDS-UPDRS Part III off-medication score is shown at (A) 76 weeks (secondary endpoint) and (B) 104 weeks (exploratory endpoint). Error bars indicate standard error. MDS-UPDRS=Movement Disorder Society-sponsored Revision of the Unified Parkinson's Disease Rating Scale.

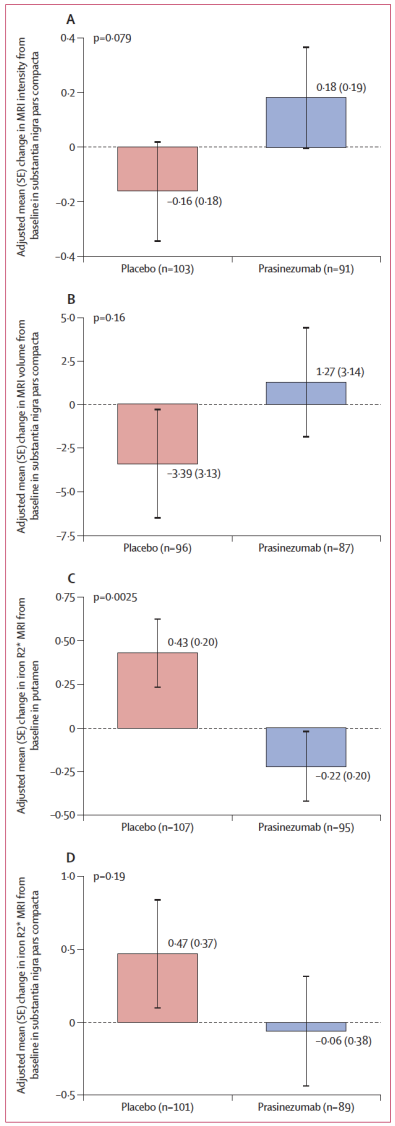

Figure 5: **MRI biomarker endpoints**
Change from baseline at 76 weeks in (A) neuromelanin MRI intensity in substantia nigra pars compacta, (B) neuromelanin MRI volume in substantia nigra pars compacta, (C) iron R2* MRI in putamen (average), and (D) iron R2* MRI in substantia nigra pars compacta (average).

	Placebo group (n=290)	Prasinezumab group (n=292)	Total (n=582)
Participants with at least one adverse event	260 (90%)	267 (91%)	527 (91%)
Leading to treatment withdrawal	3 (1%)	2 (1%)	5 (1%)
Leading to dose modification or interruption	12 (4%)	13 (4%)	25 (4%)
At least one grade 3–5 adverse event	41 (14%)	37 (13%)	78 (13%)
Withdrawn from trial due to an adverse event	0	0	0
Total number of adverse events	1632	1704	3336
Most frequently reported adverse events*			
COVID-19	68 (23%)	84 (29%)	152 (26%)
Back pain	41 (14%)	46 (16%)	87 (15%)
Infusion-related reaction	37 (13%)	31 (11%)	68 (12%)
Nasopharyngitis	31 (11%)	36 (12%)	67 (12%)
Fall	30 (10%)	36 (12%)	66 (11%)
Urinary tract infection	32 (11%)	26 (9%)	58 (10%)
Arthralgia	25 (9%)	26 (9%)	51 (9%)
Headache	18 (6%)	27 (9%)	45 (8%)
Upper respiratory tract infection	19 (7%)	21 (7%)	40 (7%)
Pain in extremity	18 (6%)	20 (7%)	38 (7%)
Influenza	16 (6%)	21 (7%)	37 (6%)
Constipation	15 (5%)	19 (7%)	34 (6%)
Anxiety	18 (6%)	17 (6%)	35 (6%)
Hypertension	20 (7%)	14 (5%)	34 (6%)
Insomnia	16 (6%)	17 (6%)	33 (6%)
Fatigue	11 (4%)	21 (7%)	32 (5%)
Dizziness	18 (6%)	13 (4%)	31 (5%)
Diarrhoea	13 (4%)	15 (5%)	28 (5%)
Participants with at least one related adverse event†	59 (20%)	51 (17%)	110 (19%)
Leading to treatment withdrawal	0	1 (<1%)	1 (<1%)
Leading to dose modification or interruption	0	2 (1%)	2 (<1%)
Participants with at least one serious adverse event	34 (12%)	34 (12%)	68 (12%)
Leading to treatment withdrawal	0	2 (1%)	2 (<1%)
Leading to dose modification or interruption	5 (2%)	4 (1%)	9 (2%)
Serious adverse events by System Organ Class			
Infections and infestations	4 (1%)	7 (2%)	11 (2%)
Injury, poisoning and procedural complications	4 (1%)	6 (2%)	10 (2%)
Neoplasms, benign, malignant, and unspecified (including cysts and polyps)	5 (2%)	5 (2%)	10 (2%)
Cardiac disorders	3 (1%)	6 (2%)	9 (2%)
Gastrointestinal disorders	6 (2%)	3 (1%)	9 (2%)
Nervous system disorders	5 (2%)	4 (1%)	9 (2%)
Musculoskeletal and connective tissue disorders	5 (2%)	2 (1%)	7 (1%)
Renal and urinary disorders	2 (1%)	2 (1%)	4 (1%)
Respiratory, thoracic and mediastinal disorders	3 (1%)	1 (<1%)	4 (1%)
Vascular disorders	2 (1%)	2 (1%)	4 (1%)
General disorders and administration site conditions	3 (1%)	0	3 (1%)
Hepatobiliary disorders	2 (1%)	1 (<1%)	3 (1%)
Psychiatric disorders	1 (<1%)	1 (<1%)	2 (<1%)
Blood and lymphatic system disorders	1 (<1%)	0	1 (<1%)
Eye disorders	1 (<1%)	0	1 (<1%)
Surgical and medical procedures	0	1 (<1%)	1 (<1%)

(Table 2 continues on next page)

(Continued from previous page)

	Placebo group (n=290)	Prasinezumab group (n=292)	Total (n=582)
Most frequently reported serious adverse events‡			
Acute myocardial infarction	1 (<1%)	4 (1%)	5 (1%)
Inguinal hernia	3 (1%)	2 (1%)	5 (1%)
Urinary tract infection	0	3 (1%)	3 (1%)
Femur fracture	1 (<1%)	2 (1%)	3 (1%)
Prostate cancer	2 (1%)	1 (<1%)	3 (1%)
Back pain	2 (1%)	0	2 (<1%)
Osteoarthritis	2 (1%)	0	2 (<1%)
Dyspnoea	2 (1%)	0	2 (<1%)
Participants with at least one related serious adverse event†	2 (1%)	1 (<1%)	3 (1%)
Types of related serious adverse event†			
Infusion-related reaction	2 (1%)	0	2 (<1%)
Endocarditis	0	1 (<1%)	1 (<1%)
Participants with adverse events with fatal outcome	2 (1%)	1 (<1%)	3 (1%)
Types of adverse events with fatal outcome			
Metastatic malignant melanoma	1 (<1%)	0	1 (<1%)
Urosepsis	1 (<1%)	0	1 (<1%)
Intracranial haemorrhage	0	1 (<1%)	1 (<1%)
Participants with at least one adverse event of special interest	0	0	0
Participants with at least one infusion-related reaction	37 (13%)	32 (11%)	69 (12%)
Non-serious adverse events leading to treatment discontinuation	3 (1%)	0	3 (1%)
Increased amylase	1 (<1%)	0	1 (<1%)
Prostate neoplasm	1 (<1%)	0	1 (<1%)
Abnormal liver function test	1 (<1%)	0	1 (<1%)

Data are n or n (%) unless otherwise indicated. *Adverse events occurring in ≥5% of participants in either treatment group. †Refers to causality with either prasinezumab or dopamine transporter single photon emission CT tracer. ‡Serious adverse events in more than one participant in either treatment group.

Table 2: **Summary of adverse events (safety analysis set)**

Research in context

Evidence before this study

We searched PubMed for English-language reports on immunotherapies with α-synuclein-specific monoclonal antibodies for Parkinson's disease, published from database inception up to Jan 21, 2026, using the search terms "Parkinson's disease" AND "synuclein" AND "immunotherapy" OR "antibody". α-synuclein aggregation is hypothesised to drive neurodegeneration, making it a key target for slowing disease progression. The search identified several phase 1 studies of immunotherapies targeting α-synuclein (exidavnemab, cinpanemab, Lu AF82422, and MEDI1341) and two phase 2 studies (cinpanemab and prasinezumab) but, among this previous evidence, prasinezumab was the only antibody to show a signal of potentially slowing motor progression in early-stage Parkinson's disease. In the phase 2 PASADENA study (NCT03100149), although the primary endpoint was not met, a signal favouring prasinezumab was observed on the Movement Disorder Society-sponsored Revision of the Unified Parkinson's Disease Rating Scale Part III; this slowing was sustained over a 4-year period when compared with a matched cohort from the Parkinson's Progression Markers Initiative study.

Added value of this study

Before PADOVA, disease-modification trials recruited mostly treatment-naive participants to avoid the confounding effects of symptomatic medication. By contrast, to ensure real-world relevance, PADOVA recruited a population receiving standard-of-care treatment. We demonstrate that a time-to-event approach, with a primary endpoint defined by a confirmed, meaningful motor progression threshold, can assess Parkinson's disease progression delay. At present, PADOVA is the largest (n=586) and longest-running trial of α-synuclein immunotherapy in early-stage Parkinson's disease (double-blind period of 76–168 weeks of treatment). Furthermore, PADOVA provides the first exploratory biomarker evidence of an effect of an α-synuclein-targeting therapy on the underlying pathobiology of Parkinson's disease (reduced neurodegeneration in the substantia nigra and mitigated iron accumulation in the basal ganglia, both revealed using MRI).

Implications of all the available evidence

Although the primary endpoint was not met, evidence from PADOVA suggests that prasinezumab, when given alongside effective symptomatic medication, might delay progression in patients with early-stage Parkinson's disease. The study findings provide supportive exploratory signals that align with previous observations from PASADENA, which, combined with the effect on MRI biomarkers, support the potential of prasinezumab to modify the disease course. Prasinezumab demonstrated a favourable safety and tolerability profile across both studies, with high retention rates confirming the feasibility of long-term treatment. Taken together, our data indicate that targeting the C-terminus of aggregated α-synuclein is a promising disease-modifying strategy, and continued investigation of prasinezumab in a phase 3 study (PARAISO; NCT07174310) is justified.

Alzheimer's disease neuropathology plasma biomarkers and cognition in midlife: a community-based cohort study

Summary

Background Alzheimer's disease neuropathology, characterised by amyloid β (Aβ) and phosphorylated-tau (p-tau) protein accumulation, has primarily been assessed with biomarkers in clinical samples of older adults. Less is known about plasma biomarkers of Alzheimer's disease neuropathology and their associations with cognitive outcomes in midlife in diverse community-based samples. Our goal was to address these gaps.

Methods In this cohort study, we analysed participants who were retained in the US Coronary Artery Risk Development in Young Adults (CARDIA) Study with available plasma biomarkers at year 35 (2020–22). We excluded participants without cognitive measures and individuals with probable dementia. Cognition in five domains was measured with standardised tests at years 30 and 35; accelerated cognitive decline in each domain was defined as a 5-year decline at least 1·5 SD greater than the cohort mean change. Plasma Aβ42, Aβ40, and p-tau217 concentrations were assayed with the use of the Fujirebio Lumipulse G1200 analyser and used to calculate the p-tau217-to-Aβ42 ratio (p-tau217/Aβ42) and Aβ42-to-Aβ40 ratio (Aβ42/40). Alzheimer's disease neuropathology status (ie, negative, intermediate, or positive) was defined based on amyloid PET-validated cutpoints for each biomarker (p-tau217/Aβ42, p-tau217, and Aβ42/40). Associations of Alzheimer's disease neuropathology with cognition (Z scores) and accelerated decline were evaluated with the use of multivariable linear and logistic regression.

Findings From the 2248 CARDIA participants who completed the year 35 visit, we randomly selected 1500 participants for plasma biomarker measurement. We excluded three participants with poor biomarker assay quality, 143 without cognitive measures, and four with probable dementia resulting in a final cohort of 1350. The mean participant age was 61 years (SD 3·6, range 53·0–69·0); 779 (58%) participants were women, 571 (42%) were men, 613 (45%) were Black, and 737 (55%) were White. Alzheimer's disease neuropathology positivity was present in 86 (6%) participants based on p-tau217/Aβ42, 196 (15%) based on Aβ42/40, and 48 (4%) based on p-tau217, and was associated with worse performance on processing speed (standardised cognitive difference comparing Alzheimer's disease neuropathology positive to negative for Aβ42/40, p-tau217, and p-tau217/Aβ42 –0·54 to –0·25; p values 0·0001 to 0·0048) and executive function (–0·42 to –0·19; p values 0·0070 to 0·049). Alzheimer's disease neuropathology positivity was also associated with increased odds of accelerated decline on verbal memory (Aβ42/40: odds ratio 4·31, 95% CI 1·71–10·9, p-tau217/Aβ42: 2·44, 1·16–5·13) and processing speed (p-tau217: 3·98, 1·71–9·3; p-tau217/Aβ42: 3·35, 1·77–6·35) compared with Alzheimer's disease neuropathology negativity. There was no association for global cognition or fluency. Although not consistent, some effect modification was observed, with stronger associations among women and Black participants and individuals with *APOE ε4*.

Interpretation Alzheimer's disease neuropathology is relatively uncommon in midlife but associated with worse cognitive performance and accelerated decline and might have stronger association among some groups. Early Alzheimer's disease neuropathology detection with the use of plasma biomarkers might enable timely prevention and intervention in midlife adults including risk reduction and pharmacological therapies.

AB4

PTau

AB4/PTau

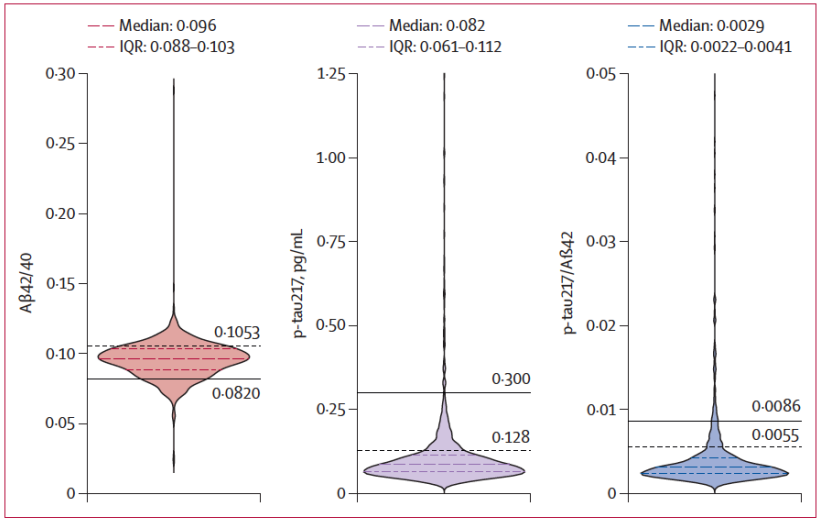

Figure 1: **Violin plots for plasma biomarkers in middle-aged adults**
With a two-cutoff approach, horizontal dashed grey lines indicate the cutoffs between negative and intermediate Alzheimer's disease neuropathology and solid grey lines indicate the cutoffs between intermediate and positive Alzheimer's disease neuropathology. Aβ=amyloid β. Aβ42/40=Aβ42-to-Aβ40 ratio. p-tau217=phosphorylated tau217. p-tau217/Aβ42=p-tau217-to-Aβ42 ratio.

	Aβ42/40			p-tau217			p-tau217/Aβ42		
	Negative (n=234; 17%)	Intermediate (n=920; 68%)	Positive (n=196; 15%)	Negative (n=1104; 82%)	Intermediate (n=198; 15%)	Positive (n=48; 4%)	Negative (n=1160; 86%)	Intermediate (n=104; 8%)	Positive (n=86; 6%)
Age, years (n=1350)	60·9 (3·5)	61·2(3·6)	62·1 (3·5)*	61·1(3·6)	62·4 (3·3)*	61·6(3·9)	61·1 (3·6)	62·9 (3·2)*	61·8 (3·6)
Sex (n=1350)									
Female	152 (65%)	529 (58%)*	98 (50%)*	650 (59%)	103 (52%)	26 (54%)	682 (59%)	51 (49%)	46 (53%)
Male	82 (35%)	391 (42%)	98 (50%)	454 (41%)	95 (48%)	22 (46%)	478 (41%)	53 (51%)	40 (47%)
Race (n=1350)									
Black	112 (48%)	417 (45%)	84 (43%)	508 (46%)	82 (41%)	23 (48%)	534 (46%)	41 (39%)	38 (44%)
White	122 (52%)	503 (55%)	112 (57%)	596 (54%)	116 (59%)	25 (52%)	626 (54%)	63 (61%)	48 (56%)
Time in education, years (n=1343)	15 (2·6)	15 (2·6)	15 (2·5)	15 (2·6)	15 (2·6)	15 (2·6)	15 (2·6)	15 (2·6)	15 (2·6)
APOE ε4 carrier (n=1228)	37 (17%)	255 (30%)*	91 (52%)*	281 (28%)	81 (46%)*	21 (50%)*	294 (28%)	47 (49%)*	42 (55%)*
Physically active (n=1337)	132 (57%)	448 (49%)*	91 (46%)*	557 (51%)	91 (46%)	23 (49%)	574 (50%)	52 (50%)	45 (53%)
Current smoker (n=1308)	12 (5%)	76 (9%)	24 (13%)*	93 (9%)	12 (6%)	7 (15%)	93 (8%)	7 (7%)	12 (14%)
Depression (n=1062)	36 (19%)	116 (16%)	25 (17%)	142 (16%)	26 (16%)	9 (26%)	153 (17%)	14 (16%)	10 (16%)
Hypertension (n=1350)	128 (55%)	529 (58%)	124 (63%)	634 (57%)	117 (59%)	30 (63%)	664 (57%)	61 (59%)	56 (65%)
Diabetes (n=1347)	23 (10%)	171 (19%)*	49 (25%)*	189 (17%)	49 (25%)*	5 (10%)	215 (19%)	20 (19%)	8 (9%)
Dyslipidaemia (n=1349)	30 (13%)	238 (26%)*	60 (31%)*	274 (25%)	47 (24%)	7 (15%)	287 (25%)	23 (22%)	18 (21%)
BMI, kg/m² (n=1339)	28·7 (7·0)	31 (7·3)*	30·7 (7·3)*	30·6 (7·3)	30·5 (7·2)	28·8 (6·4)	30·7 (7·4)	30·5 (7·1)	28·6 (5·7)*
Cardiovascular disease (n=1350)	10 (4%)	43 (5%)	22 (11%)*	56 (5%)	13 (7%)	6 (13%)	60 (5%)	8 (8%)	7 (8%)
eGFR, mL/min per 1·73 m² (n=1346)	81 (16)	84 (15)	83 (18)	84 (14)	79 (17)*	72 (25)*	84 (15)	80 (16)	79 (22)

Data are mean (SD) or n (%). Aβ=amyloid β. Aβ42/40=Aβ42 to Aβ40 ratio. eGFR=estimated glomerular filtration rate. p-tau217=phosphorylated tau217. p-tau217/Aβ42=p-tau217-to-Aβ42 ratio. *p<0·05 based on post-hoc comparisons with the group negative for Alzheimer's disease neuropathology, with the use of Bonferroni-corrected tests for continuous variables and unadjusted logistic regression for dichotomous variables

Table 1: **Participant characteristics by negative, intermediate, and positive Alzheimer's disease neuropathology based on plasma biomarkers**

	Aβ42/40			p-tau217			p-tau217/Aβ42		
	Negative (n=234; 17%)	Intermediate (n=920; 68%)	Positive (n=196; 15%)	Negative (n=1104; 82%)	Intermediate (n=198; 15%)	Positive (n=48; 4%)	Negative (n=1160; 86%)	Intermediate (n=104; 8%)	Positive (n=86; 6%)
Processing speed	67·3 (16·6)	65·5 (16·5)	60·7 (17·5)*	66 (16·5)	61·7 (16·6)*	58·2 (20·2)*	65·7 (16·6)	62·7 (16·9)	60·5 (17·9)*
Executive function	−22·8 (12·4)	−23·8 (12·1)	−26 (13·5)*	−23·6 (12·2)	−24·9 (12·6)	−28·4 (15·6)*	−23·7 (12·3)	−24·3 (11·1)	−26·8 (15)
Global cognition	24·6 (4·0)	24·2 (3·9)	24·3 (3·8)	24·3 (3·9)	24·4 (3·7)	24 (4·0)	24·3 (3·9)	24·6 (3·7)	24·1 (4·0)
Verbal memory	9 (3·6)	8·5 (3·5)	8·2 (3·8)	8·6 (3·5)	8·2 (3·8)	8·3 (4·1)	8·5 (3·5)	8·7 (3·9)	8·3 (3·9)
Verbal fluency	31·2 (9·5)	30·2 (8·3)	29·8 (8·6)	30·5 (8·7)	29·6 (8·2)	29·4 (8·3)	30·3 (8·6)	30·2 (8·7)	30·3 (7·9)

Data are mean (SD). Aβ=amyloid β. Aβ42/40=Aβ42 to Aβ40 ratio. p-tau217=phosphorylated tau217. p-tau217/Aβ42=p-tau217-to-Aβ42 ratio. *p<0·05 based on post-hoc comparisons with the group negative for Alzheimer's disease neuropathology, with the use of Bonferroni-corrected tests

Table 2: **Cognitive scores at year 35 by negative, intermediate, and positive Alzheimer's disease neuropathology based on plasma biomarkers**

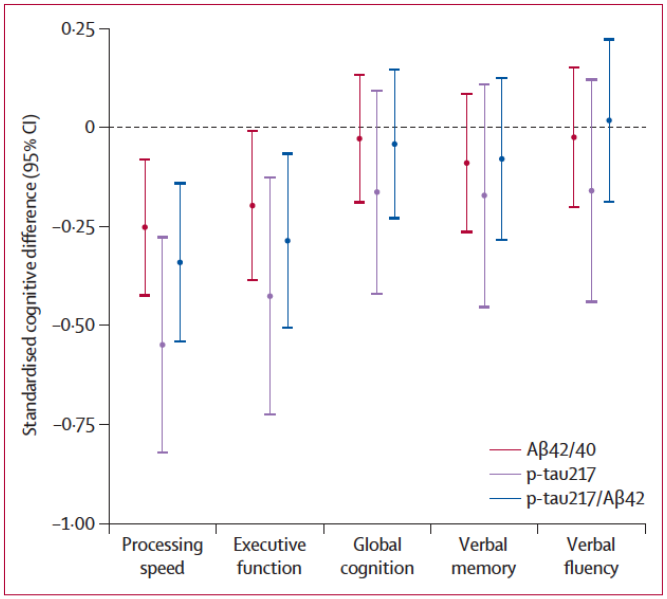

Figure 2: **Multivariable associations between Alzheimer's disease neuropathology and cognition in midlife**
Standardised differences in cognitive performance for participants positive for Alzheimer's disease neuropathology compared with individuals negative for Alzheimer's disease neuropathology. Models were adjusted for age, sex, race, education, BMI, and estimated glomerular filtration rate. Aβ=amyloid β. Aβ42/40=Aβ42 to Aβ40 ratio. p-tau217=phosphorylated tau217. p-tau217/Aβ42=p-tau217-to-Aβ42 ratio.

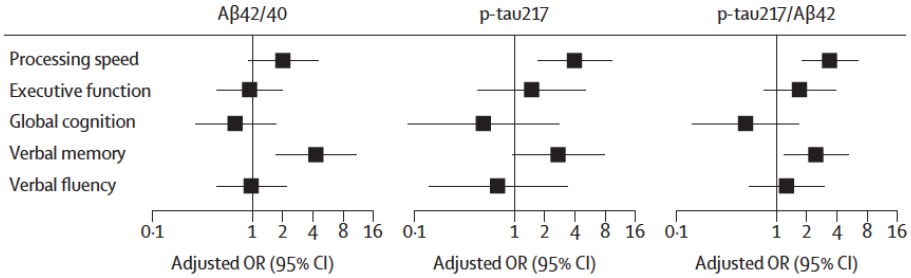

Figure 3: **Multivariable associations between Alzheimer's disease neuropathology and accelerated midlife cognitive decline**

Adjusted ORs with 95% CIs for accelerated decline in each cognitive domain, comparing individuals positive for Alzheimer's disease neuropathology with people negative for Alzheimer's disease neuropathology. Models were adjusted for age, sex, race, education, BMI, and estimated glomerular filtration rate. Aβ=amyloid β. OR=odds ratio. p-tau217=phosphorylated tau217.Aβ=amyloid β. Aβ42/40=Aβ42 to Aβ40 ratio. p-tau217/Aβ42=p-tau217-to-Aβ42 ratio.

	Adjusted for age, sex, race, and education		Additionally adjusted for BMI and eGFR	
	β (95% CI)	p value	β (95% CI)	p value
Aβ42/40 (decrease)				
Processing speed	−0·1 (−0·15 to −0·05)	<0·0001	−0·09 (−0·14 to −0·04)	0·0003
Executive function	−0·08 (−0·14 to −0·03)	0·0031	−0·08 (−0·13 to −0·02)	0·0075
Global cognition	0·0 (−0·05 to 0·04)	0·87	−0·01 (−0·06 to 0·04)	0·76
Verbal memory	−0·01 (−0·06 to 0·04)	0·70	−0·01 (−0·06 to 0·04)	0·68
Verbal fluency	−0·02 (−0·07 to 0·03)	0·46	−0·01 (−0·06 to 0·04)	0·69
p-tau217				
Processing speed	−0·08 (−0·13 to −0·03)	0·0016	−0·1 (−0·15 to −0·05)	0·0002
Executive function	−0·07 (−0·13 to −0·02)	0·0086	−0·07 (−0·13 to −0·02)	0·013
Global cognition	0·0 (−0·04 to 0·05)	0·90	0·0 (−0·05 to 0·05)	0·99
Verbal memory	0·0 (−0·05 to 0·04)	0·84	−0·01 (−0·06 to 0·04)	0·72
Verbal fluency	−0·02 (−0·07 to 0·03)	0·52	−0·02 (−0·07 to 0·04)	0·52
p-tau217/Aβ42				
Processing speed	−0·07 (−0·12 to −0·02)	0·0072	−0·07 (−0·12 to −0·02)	0·0036
Executive function	−0·06 (−0·12 to −0·01)	0·0206	−0·06 (−0·12 to 0)	0·0338
Global cognition	0·01 (−0·04 to 0·06)	0·72	0·01 (−0·04 to 0·06)	0·70
Verbal memory	0·0 (−0·05 to 0·05)	0·97	0·0 (−0·05 to 0·05)	0·89
Verbal fluency	0·0(−0·05 to 0·05)	0·99	0·0 (−0·05 to 0·06)	0·94

Cognition was modelled with the use of Z scores. Biomarkers were analysed as continuous variables on the natural log scale; β estimates represent associations per 1-IQR increase (or decrease for Aβ42/40) in linear regression models. The IQRs were 0·156 for Aβ42/40, 0·608 for p-tau217, and 0·612 for p-tau217/Aβ42 on the natural log scale. Aβ=amyloid β.Aβ42/40=Aβ42 to Aβ40 ratio. eGFR=estimated glomerular filtration rate. p-tau217=phosphorylated tau217. p-tau217/Aβ42=p-tau217-to-Aβ42 ratio.

Table 3: **Associations between plasma biomarkers (continuous, per 1-IQR) and cognitive performance in midlife**

Research in context

Evidence before this study

We searched PubMed for articles published up to Oct 31, 2025, with the terms "plasma" OR "blood" AND "biomarker" AND "Alzheimer's disease" OR "amyloid" OR "tau" AND "cognition" OR "cognitive decline" OR "cognitive outcome". We screened papers by title and abstract and reviewed citation lists to identify full-text articles relevant to our study. We focused on studies that analysed plasma biomarkers among midlife adults and assessed associations between cognition and biomarkers of Alzheimer's disease, including amyloid β (Aβ) and phosphorylated tau (p-tau) isoforms. Previous research suggests that midlife plasma biomarkers, including p-tau181, p-tau217, and Aβ42-to-Aβ40 ratio, are associated with increased risk of late-life mild cognitive impairment and dementia; however, studies examining plasma Alzheimer's disease biomarkers and cognition focused primarily on midlife are insufficient, and rarely conducted in diverse community-based cohorts.

Added value of this study

We conducted one of the first community-based investigations of plasma Alzheimer's disease neuropathology biomarkers and cognition in midlife individuals. Among many Black and White participants in an ongoing cohort study, we assessed plasma Alzheimer's disease neuropathology biomarkers with the use of state-of-the-art assays and validated cutoffs for Alzheimer's disease neuropathology status. We show that Alzheimer's disease neuropathology positivity, defined by amyloid PET-validated p-tau217-to-Aβ42 ratio cutoffs and related markers, is already detectable in midlife, although uncommon, and is associated with worse cognitive outcomes across multiple domains independent of demographics, BMI, renal function, and *APOE* genotype. In a novel investigation, we show that these associations vary by race, *APOE*, and sex, with stronger associations observed in Black individuals, *APOE ε4* carriers, and women, but not on all comparisons.

Implications of all the available evidence

Our results extend previous work on Alzheimer's disease biomarkers in older adults by showing that evidence of Alzheimer's disease neuropathology is present in midlife, although infrequent, and is already linked to measurable cognitive differences. These findings support the concept that Alzheimer's disease begins decades before clinical symptoms emerge and highlight the potential value of plasma biomarkers for early detection in the general population. Identifying individuals with early Alzheimer's disease neuropathology through accessible, blood-based assays could help target preventive strategies and clinical trials aimed at delaying or preventing the onset of dementia, with implications for both clinical practice and public health policy.

Comparison of [18F]flortaucipir and [18F]MK6240 for the detection of tau pathology in Alzheimer's disease (HEAD): a multicentre, prospective, cross-sectional, within-participant study

Summary

Background Tau PET imaging has emerged as a critical biomarker for Alzheimer's disease, informing diagnosis, staging, and therapeutic selection. We investigated whether PET tracer selection alters tau detection.

Methods We conducted a prospective, multicentre, non-randomised, within-participant comparison of [18F]flortaucipir (Tauvid), currently used in clinical settings in the USA and Europe, and [18F]MK6240, an investigational tau PET tracer. Participants were recruited from eight north American sites and underwent tau PET, amyloid-β (Aβ) PET, and detailed cognitive assessments. Tau PET with both agents was acquired within a 45-day window. Coprimary outcomes were the discriminative accuracy for Alzheimer's disease-related cognitive impairment and the frequency of tau positivity in early medial temporal lobe (MTL) and late neocortical regions. The study is registered with ClinicalTrials.gov, NCT05361382.

Findings Between March 2, 2022, and Aug 27, 2025, 775 individuals were enrolled, with 682 completing all procedures (373 [55%] female, 309 [45%] male; 38 [6%] aged 19–27 years, 214 [31%] aged 50–65 years, and 430 [63%] aged 65–89 years). 32 (5%) participants identified as Hispanic or Latino. 637 (93%) identified as White, 24 (4%) as Black or African American, 16 (2%) as Asian, and five (1%) as other. In addition, 49 (7%) individuals were identified as being from a rural area. [18F]MK6240 showed greater accuracy than [18F]flortaucipir in distinguishing Alzheimer's disease from non-Alzheimer's disease impairment (area under the curve 0·93, 95% CI 0·89–0·95 *vs* 0·86, 0·75–0·91; p<0·0001). Among the older adults, tau positivity status was concordant in 560 (87%) for MTL and 603 (94%) for neocortical regions. In cognitively unimpaired participants, [18F]MK6240 identified twice as many MTL-positive cases as [18F]flortaucipir (n=54 [15%] *vs* n=23 [6%]). Prevalence ratio in Aβ-positive was 2·43 (95% CI 1·50–3·94; p=0·0003), identifying 23 additional cases per 100. Among discordant cases, 75 (89%) were [18F]MK6240-positive only and had higher Aβ burden (p<0·0001), APOEε4 frequency (p<0·0001), and cognitive impairment (p=0·0043) than those negative on both tracers. Neocortical tau positivity was more frequent with [18F]MK6240 than with [18F]flortaucipir in cognitively impaired individuals (80 [28%] *vs* 46 [16%]). Prevalence ratio in Aβ-positive was 1·74 (95% CI 1·32–2·29; p<0·0001), identifying 15 additional mild cognitive impairment and 21 dementia cases per 100.

Interpretation Tau PET tracer selection influences the frequency of detection of tau pathology across the ageing and Alzheimer's disease spectrum. Compared with [18F]flortaucipir, [18F]MK6240 identified more individuals with tau pathology in cognitively unimpaired and cognitively impaired individuals, with direct implications for patient stratification in clinical trials and more precise guidance for therapeutic decision-making.

	Young adults (n=38)	Older cognitively unimpaired adults (n=362)	Mild cognitive impairment (n=183)	Dementia (n=99)
Age	23 (2·0)	67 (8·3)	71 (7·4)	72 (8·9)
Sex				
Female	23 (61%)	220 (61%)	82 (45%)	48 (48%)
Male	15 (39%)	142 (39%)	101 (55%)	51 (52%)
*APOE*ε4 carrier	11 (29%)	109 (30%)	94 (51%)	59 (60%)
Education, years	16 (2·0)	16 (2·5)	16 (2·9)	15 (3·3)
MMSE score	29 (1·0)	29 (1·5)	28 (2·0)	21 (4·9)
CDR sum of boxes	0·0 (0·0)	0·02 (0·1)	1·7 (1·2)	4·7 (2·5)
Aβ positivity	0·0 (0·0%)	77 (21%)	108 (59%)	87 (88%)
MTL [^{18}F]flortaucipir SUVR	1·0 (0·1)	1·1 (0·11)	1·3 (0·27)	1·5 (0·33)
MTL [^{18}F]MK6240 SUVR	0·76 (0·1)	0·92 (0·24)	1·4 (0·70)	2·0 (0·82)
Neocortex [^{18}F]flortaucipir SUVR	1·1 (0·09)	1·1 (0·08)	1·1 (0·14)	1·3 (0·35)
Neocortex [^{18}F]MK6240 SUVR	0·89 (0·10)	0·91 (0·11)	1·0 (0·33)	1·6 (0·92)

Data are mean (SD) or n (%). Missing: five APOEε4 status, six education years, five MMSE score, and one CDR sum of boxes. Aβ=amyloid-β. CDR=Clinical Dementia Rating. MMSE=Mini-Mental State Examination. MTL=medial temporal lobe. SUVR=standardised uptake value ratio.

Table: **Participant characteristics**

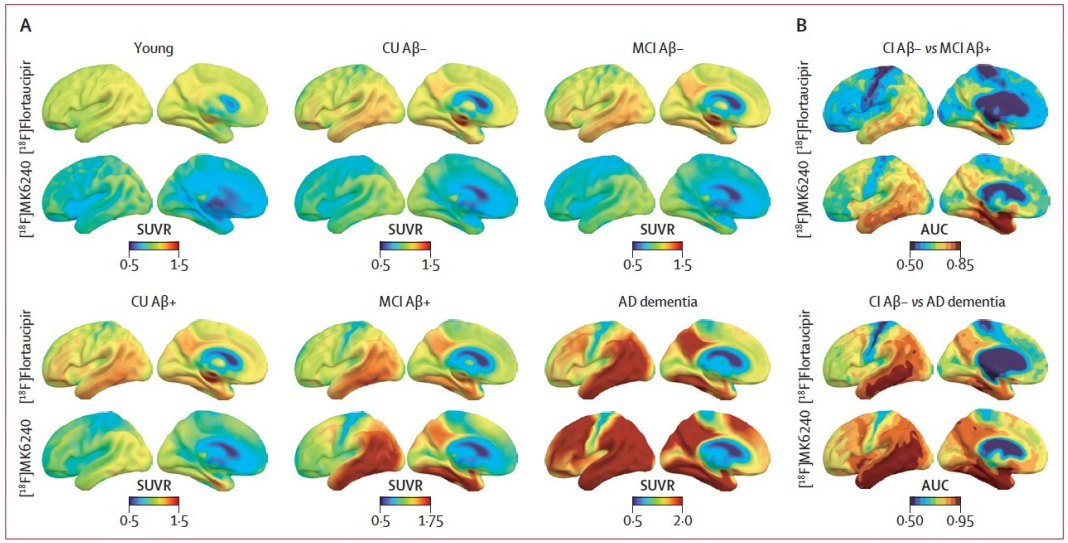

Figure 1: **Discriminative accuracy of [^{18}F]flortaucipir and [^{18}F]MK6240 tau PET for distinguishing clinical groups**
(A) Voxelwise mean SUVRs for [^{18}F]flortaucipir and [^{18}F]MK6240 across different diagnostic and Aβ status groups. (B) Voxelwise AUC values for distinguishing MCI due to AD (top) or AD dementia from non-AD cognitive impairment disorders (bottom) using [^{18}F]flortaucipir and [^{18}F]MK6240. Participants with Alzheimer's disease dementia were, by definition, Aβ-positive. Aβ−=amyloid-β negative. Aβ+=amyloid-β positive. AD=Alzheimer's disease. AUC=area under the curve. CI=cognitively impaired. CU=cognitively unimpaired. MCI=mild cognitive impairment. SUVR=standardised uptake value ratio.

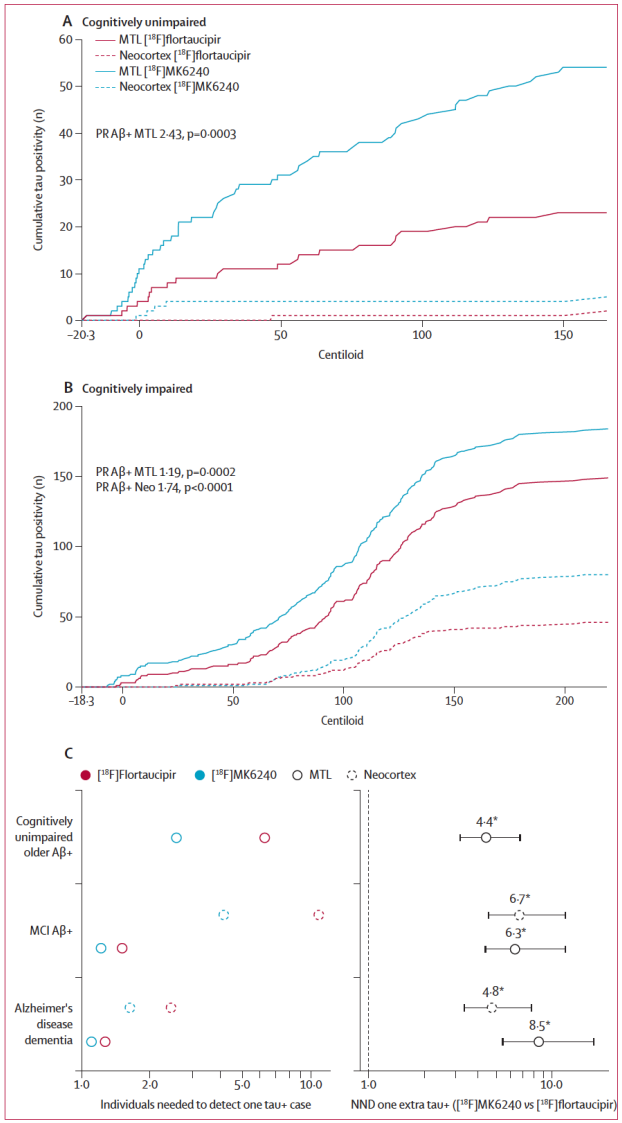

***Figure 2*: Frequency of [^{18}F]flortaucipir and [^{18}F]MK6240 tau positivity across cognitive status**

Cumulative tau MTL and neocortical positivity of [^{18}F]flortaucipir and [^{18}F]MK6240 as a function of Aβ burden (Centiloid) in cognitively unimpaired (A) and cognitively impaired (B) participants. (C) The number of individuals required to detect one tau-positive case and NND one extra tau positive case stratified by diagnostic and Aβ status. Neocortical region is composed of Braak V and VI regions. p values indicate whether detection of tau positivity differs between [^{18}F]MK6240 and [^{18}F]flortaucipir. Error bars indicate 95% CI. Asterisks indicate NND estimates for which the 95% CI of the paired absolute risk difference did not include zero. Participants with Alzheimer's disease dementia were, by definition, Aβ-positive. Analysis accounted for Centiloid, age, sex, and study site. Aβ+=amyloid-β positive. PR=prevalence ratio. MCI=mild cognitive impairment. MTL=medial temporal lobe. Neo=neocortex. NND=number needed to detect. tau+=tau positive.

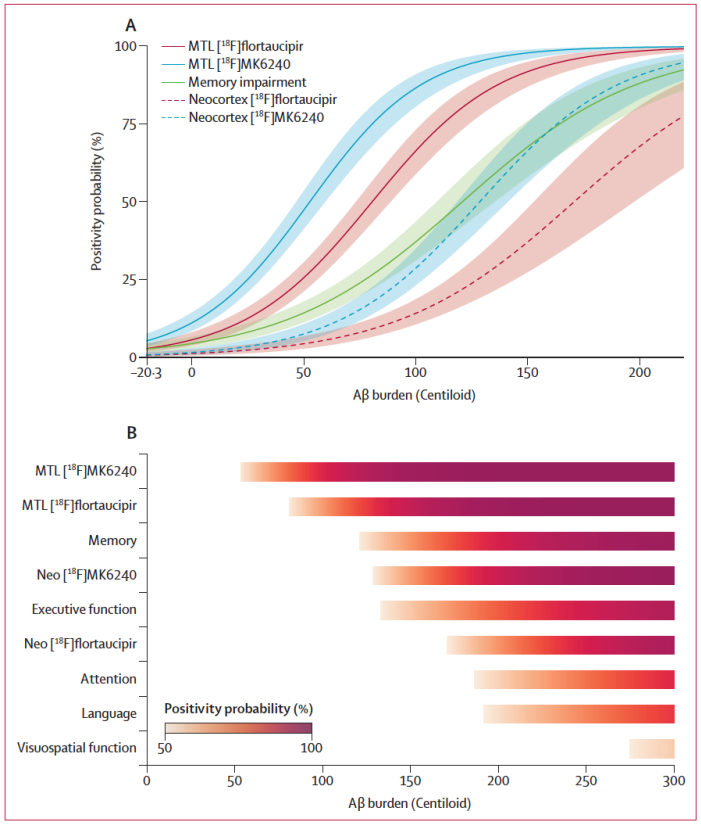

Figure 3: **[18F]Flortaucipir and [18F]MK6240 tau positivity as a function of amyloid-β burden**
(A) Probability of tau positivity in the MTL and neocortex for [18F]flortaucipir and [18F]MK6240, and probability of memory impairment, as a function of Aβ burden (Centiloid). (B) Centiloid thresholds for 50% probability of tau positivity with each tracer and for 50% probability of decline in memory, executive function, attention, language, and visuospatial function. Shaded areas represent 95% CI. Aβ=amyloid-β. MTL=medial temporal lobe. Neo=neocortex.

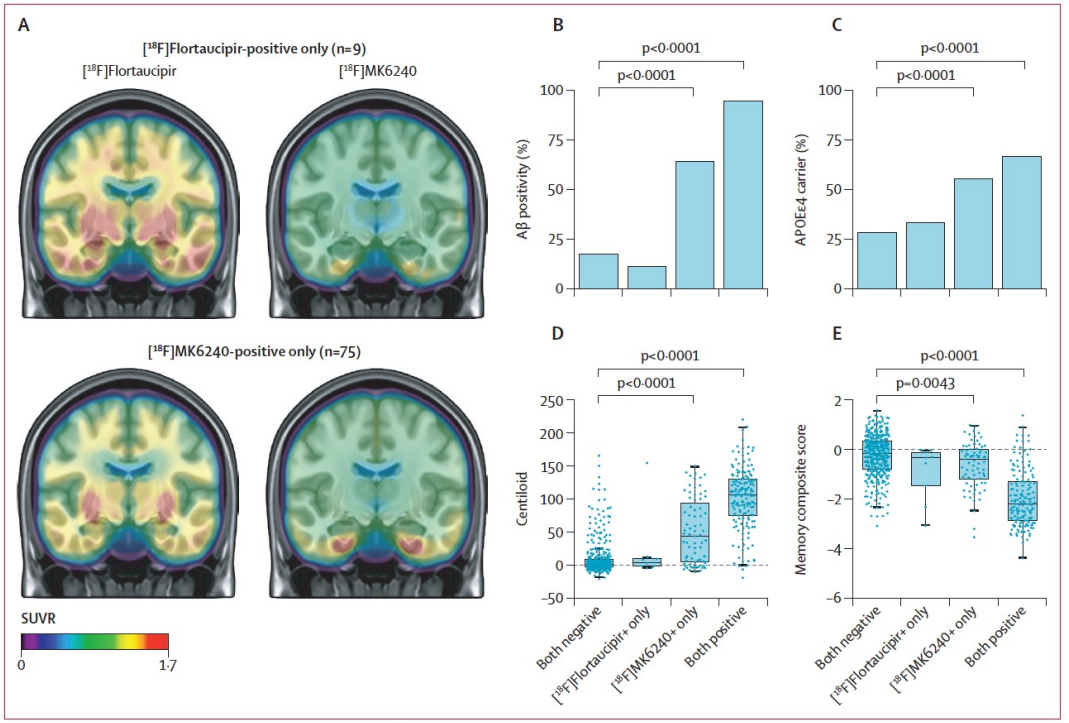

Figure 4: **Discordant classifications of tau positivity with [18F]flortaucipir and [18F]MK6240**
(A) Average SUVR maps of individuals positive only for [18F]flortaucipir (top) and only for [18F]MK6240 (bottom). Distribution of Aβ positivity (B), APOEε4 carriership (C), Centiloid levels (D), and memory composite score (E) according to [18F]flortaucipir and [18F]MK6240 status. Data are represented as median (IQR). Aβ=amyloid-β. Both negative=individuals negative on [18F]flortaucipir and [18F]MK6240. Both positive=individuals positive on [18F]flortaucipir and [18F]MK6240. SUVR=standardised uptake value ratio.

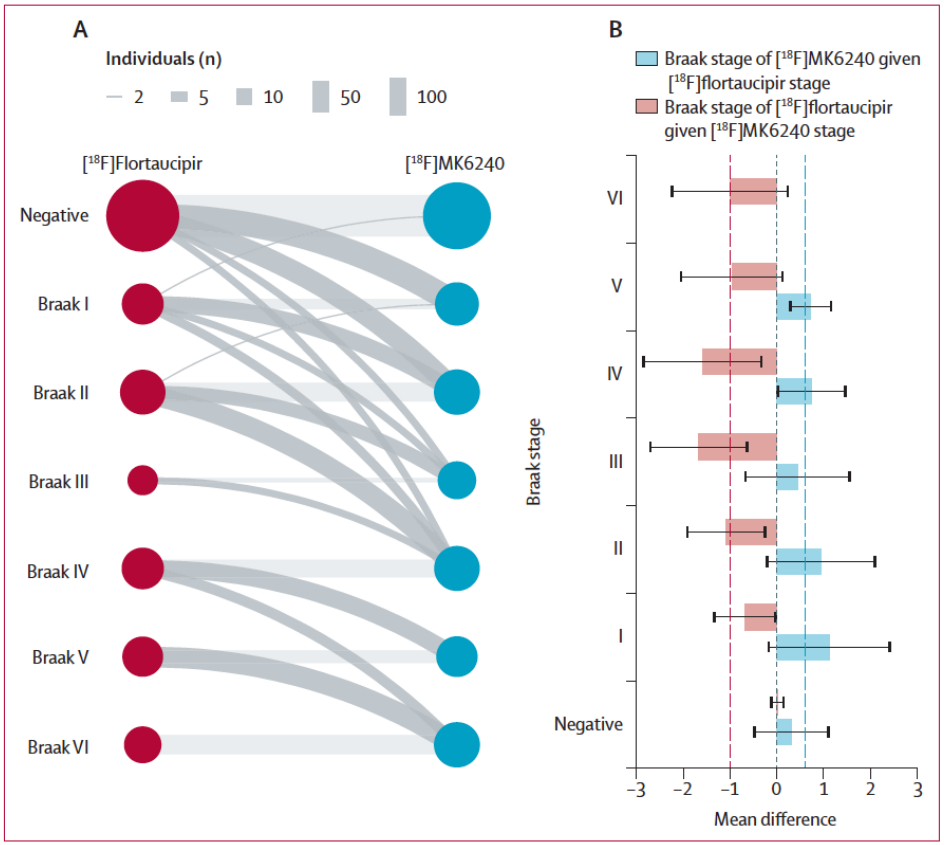

Figure 5: **PET-based Braak staging using [^{18}F]flortaucipir and [^{18}F]MK6240**
(A) Individual concordance in Braak stage classification between [^{18}F]flortaucipir and [^{18}F]MK6240. Node size reflects number of individuals per stage; links represent cross-classification between tracers. Links with only one individual were omitted. (B) Quantification of average Braak staging differences. The error bars represent 95% CI. The vertical dashed lines indicate the mean difference in Braak stage between tracers for each comparison direction. Individuals who did not follow Braak staging are not represented.

Research in context

Evidence before this study

We searched PubMed, Scopus, and Embase for studies published from database inception to Oct 20, 2025, using the terms "tau PET", "T807", "flortaucipir", "Tauvid", "MK6240", "Alzheimer's disease", and "head-to-head tau PET" without language restrictions. Tau PET imaging has emerged as a critical biomarker for Alzheimer's disease, informing diagnosis, staging, and therapeutic selection. [^{18}F]Flortaucipir, the first introduced tau PET tracer, reliably detects advanced neocortical tau pathology, but has limited sensitivity for early tau deposition in medial temporal regions. [^{18}F]MK6240, developed subsequently, potentially exhibits higher sensitivity for neurofibrillary tangles and superior signal-to-noise ratio. However, no previous large-scale study has compared these tracers within the same individuals across the Alzheimer's disease spectrum, nor evaluated their relative performance for early detection, staging concordance, or diagnostic accuracy.

Added value of this study

This multicentre, prospective, within-participant study represents, to the best of our knowledge, the largest head-to-head comparison of [^{18}F]flortaucipir and [^{18}F]MK6240 to date. Using harmonised acquisition protocols, standardised processing pipelines, and quantitative thresholds derived from young, healthy controls, we directly assessed the impact of tracer selection on tau detection, staging, and diagnostic discrimination. Compared with [^{18}F]flortaucipir, [^{18}F]MK6240 identified twice as many cognitively unimpaired Aβ-positive individuals with early medial temporal tau accumulation and more cognitively impaired Aβ-positive participants with neocortical tau involvement. [^{18}F]MK6240 reached positivity at lower Aβ burden, detected tau pathology earlier in the disease continuum, and staged individuals on average one Braak stage higher. These findings show that tracer selection influences disease classification, staging, and eligibility for early intervention trials. They also prompt a re-evaluation of the natural history of tau PET positivity in vivo, which might have been underestimated due to limitations in tracer sensitivity.

Implications of all the available evidence

Alzheimer's disease affects over 55 million people worldwide, with rising prevalence and profound societal, economic, and health-care burden. Tau PET imaging, more closely aligned with symptom onset and disease progression than Aβ PET, is increasingly used to guide diagnosis, prognosis, and therapeutic enrolment. Our findings show that [^{18}F]MK6240 enables earlier detection of tau pathology than [^{18}F]flortaucipir, with direct implications for clinical trial design, biomarker qualification, and health system preparedness for early intervention strategies. These results suggest that current estimates of tau PET positivity might be substantially underestimated, potentially delaying recognition of tau pathology and limiting access to disease-modifying therapies informed by tau PET. Tracer selection should be considered a critical determinant in Alzheimer's disease care pathways, regulatory frameworks, and global efforts to advance early detection, equitable access, and precision medicine in neurodegenerative disease.

Efficacy and safety of oral semaglutide 14 mg (flexible dose) in early-stage symptomatic Alzheimer's disease (evoke and evoke+): two phase 3, randomised, placebo-controlled trials

Summary

Background Evidence, including animal, clinical, and real-world studies in individuals with type 2 diabetes and/or obesity, suggests reduced risk of dementia and Alzheimer's disease after GLP-1 receptor agonist exposure. The evoke and evoke+ trials aimed to investigate the efficacy and safety of oral semaglutide in individuals with early Alzheimer's disease.

Methods evoke and evoke+ were multicentre, randomised, double-blind, placebo-controlled phase 3 trials conducted across 566 sites in 40 countries. The trials assessed the efficacy and safety of oral semaglutide up to 14 mg once daily in participants with amyloid-confirmed Alzheimer's disease, aged 55–85 years, with mild cognitive impairment or mild dementia due to Alzheimer's disease. In evoke+, participants with significant small vessel pathology were included. Participants were randomly assigned (1:1) to once-daily semaglutide 14 mg (flexible dose) or placebo for up to 156 weeks. The primary endpoint was change in Clinical Dementia Rating—Sum of Boxes (CDR-SB) score from baseline to week 104, assessed in all randomised participants. Safety was assessed in all randomised participants and reported for those receiving at least one dose of study drug. These trials were registered at ClinicalTrials.gov (NCT04777396 and NCT04777409); both trials have been discontinued due to negative clinical outcome.

Findings Between May 18, 2021, and Sept 8, 2023, 9981 participants were screened, of whom 3808 were randomly assigned; 1855 in evoke (semaglutide, n=928; placebo, n=927) and 1953 in evoke+ (semaglutide, n=976; placebo, n=977). Mean age was 72·2 years (SD 7·1), and mean CDR-SB score was 3·7 (SD 1·6) at baseline. In evoke+, 54 (2·8%) participants had small vessel pathology. In evoke and evoke+, mean changes in CDR-SB score from baseline to week 104 were 2·3 (SE 0·1) and 2·2 (0·1) with semaglutide, compared with 2·3 (0·1) and 2·1 (0·1) with placebo (estimated difference –0·08 [95% CI –0·35 to 0·20], p=0·57 in evoke and 0·10 [–0·17 to 0·38], p=0·46 in evoke+). Treatment-emergent adverse events were reported in 1729 (91·2%) of 1896 participants receiving semaglutide versus 1613 (84·8%) of 1902 receiving placebo. There were five fatalities considered treatment-related by the investigators (one in the semaglutide group and four in the placebo group).

Interpretation Oral semaglutide was not efficacious in slowing clinical progression in participants with early Alzheimer's disease. Safety and tolerability of semaglutide in early Alzheimer's disease is consistent with studies in other indications.

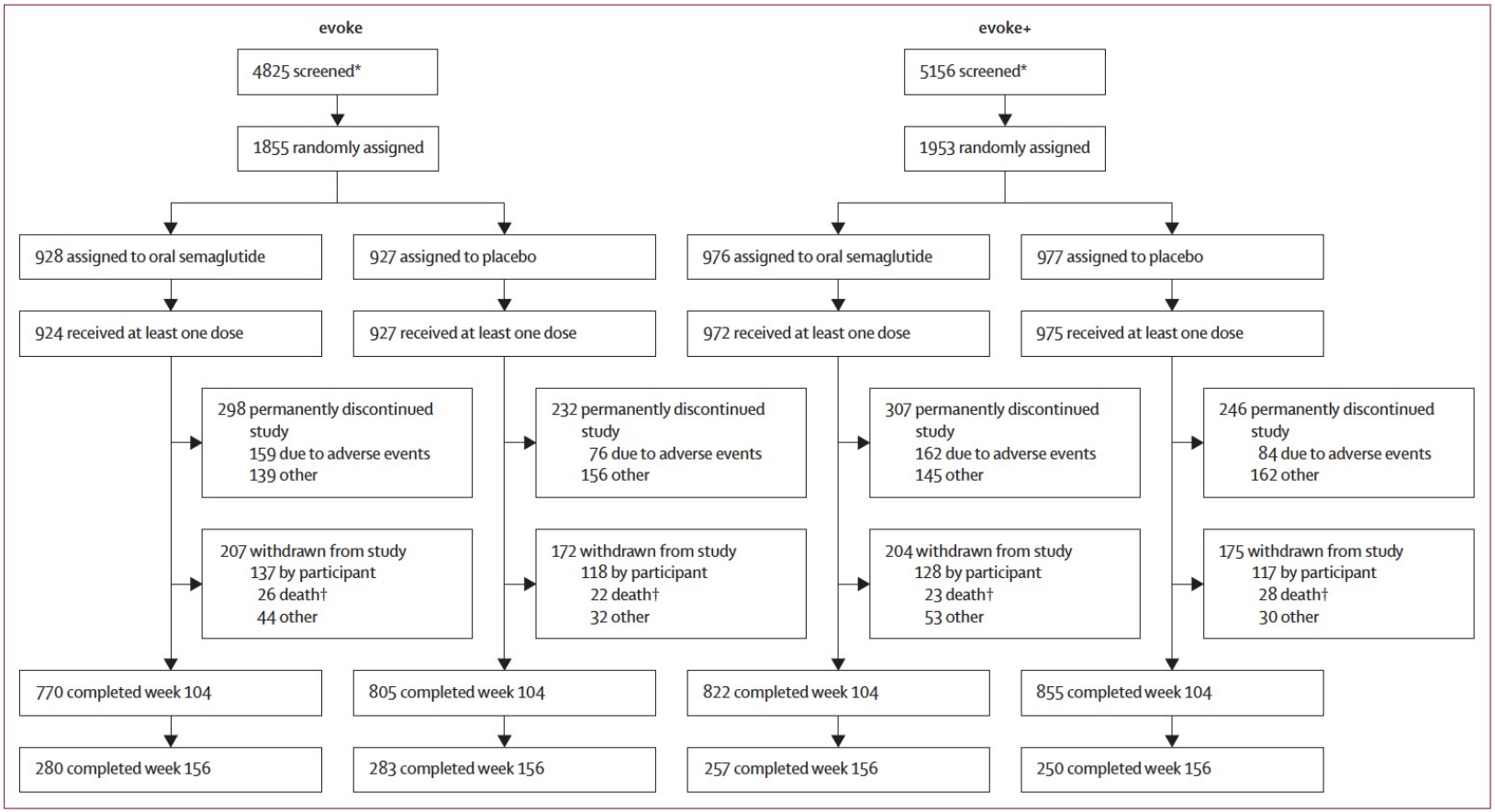

Figure 1: **Trial profiles**

*See the appendix (pp 46–47) for details on screening failures. †Includes fatalities reported for participants during trial participation.

	evoke		evoke+		Pooled evoke(+)
	Semaglutide 14 mg (n=928)	Placebo (n=927)	Semaglutide 14 mg (n=976)	Placebo (n=977)	Total (N=3808)
Age, years; mean (SD)	71·9 (7·0)	71·7 (7·1)	72·6 (7·0)	72·5 (7·2)	72·2 (7·1)
Sex					
Female	489 (52·7%)	496 (53·5%)	515 (52·8%)	498 (51·0%)	1998 (52·5%)
Male	439 (47·3%)	431 (46·5%)	461 (47·2%)	479 (49·0%)	1810 (47·5%)
Ethnicity*					
Hispanic or Latino	114 (12·3%)	130 (14·0%)	117 (12·0%)	85 (8·7%)	446 (11·7%)
Race*					
American Indian or Alaska Native	3 (0·3%)	1 (0·1%)	1 (0·1%)	0	5 (0·1%)
Asian	117 (12·6%)	102 (11·0%)	202 (20·7%)	205 (21·0%)	626 (16·4%)
Black or African American	13 (1·4%)	10 (1·1%)	9 (0·9%)	10 (1·0%)	42 (1·1%)
Native Hawaiian or Other Pacific Islander	1 (0·1%)	1 (0·1%)	3 (0·3%)	0	5 (0·1%)
White	735 (79·2%)	765 (82·5%)	725 (74·3%)	726 (74·3%)	2951 (77·5%)
Other	24 (2·6%)	25 (2·7%)	4 (0·4%)	2 (0·2%)	55 (1·4%)
BMI, kg/m²					
<18·5	28 (3·0%)	18 (1·9%)	22 (2·3%)	28 (2·9%)	96 (2·5%)
18·5 to <25	421 (45·4%)	432 (46·6%)	463 (47·4%)	465 (47·6%)	1781 (46·8%)
25 to <30	337 (36·3%)	333 (35·9%)	334 (34·2%)	329 (33·7%)	1333 (35·0%)
≥30	142 (15·3%)	139 (15·0%)	156 (16·0%)	154 (15·8%)	591 (15·5%)
Missing	0	5 (0·5%)	1 (0·1%)	1 (0·1%)	7 (0·2%)
Type 2 diabetes	99 (10·7%)	116 (12·5%)	155 (15·9%)	148 (15·1%)	518 (13·6%)
Concurrent significant small vessel pathology	NA	NA	26 (2·7%)	28 (2·9%)	54 (1·4%)
hsCRP, mg/L; geometric mean (CV)†	0·8 (160·2)	0·9 (174·5)	0·9 (178·1)	0·8 (167·9)	0·8 (170·3)
APOE-ε4 gene carrier status					
APOE-ε4 carrier (heterozygote)	451 (48·6%)	448 (48·3%)	443 (45·4%)	437 (44·7%)	1779 (46·7%)
APOE-ε4 carrier (homozygote)	117 (12·6%)	120 (12·9%)	111 (11·4%)	122 (12·5%)	470 (12·3%)
Any concomitant Alzheimer's disease medications ongoing at randomisation	559 (60·2%)	527 (56·9%)	546 (55·9%)	525 (53·7%)	2157 (56·6%)
Symptomatic treatments					
Donepezil	362 (39·0%)	330 (35·6%)	346 (35·5%)	345 (35·3%)	1383 (36·3%)
Rivastigmine	101 (10·9%)	101 (10·9%)	103 (10·6%)	90 (9·2%)	395 (10·4%)
Galantamine	31 (3·3%)	38 (4·1%)	31 (3·2%)	35 (3·6%)	135 (3·5%)
Huperzine A	1 (0·1%)	0	1 (0·1%)	1 (0·1%)	3 (0·1%)
Memantine	142 (15·3%)	118 (12·7%)	144 (14·8%)	125 (12·8%)	529 (13·9%)
Monoclonal antibodies					
Aducanumab	0	0	1 (0·1%)	0	1 (0·0%)
CDR-SB‡					
Mean (SD)	3·8 (1·6)	3·7 (1·5)	3·7 (1·5)	3·7 (1·7)	3·7 (1·6)
Range	0·5–11·0	1·0–11·0	0·5–10·0	0·5–12·0	0·5–12·0
CDR-G					
0·5	670 (72·2%)	680 (73·4%)	699 (71·6%)	697 (71·3%)	2746 (72·1%)
1	252 (27·2%)	240 (25·9%)	273 (28·0%)	269 (27·5%)	1034 (27·2%)
ADCS-ADL-MCI‡					
Mean (SD)	39·2 (7·3)	39·7 (7·4)	38·7 (7·5)	39·2 (7·5)	39·2 (7·4)
Range	12·0–53·0	10·0–53·0	12·0–53·0	10·0–52·0	10·0–53·0
MMSE‡					
Mean (SD)	24·1 (2·9)	24·0 (3·1)	24·0 (3·1)	24·1 (3·1)	24·0 (3·0)
Range	15·0–30·0	15·0–30·0	13·0–30·0	13·0–30·0	13·0–30·0

Data are n (%) unless otherwise stated. ADCS-ADL-MCI=Alzheimer's Disease Cooperative Study Activities of Daily Living Scale for mild cognitive impairment. *APOE*-ε4=apolipoprotein E ε4 variant. CDR-G=Clinical Dementia Rating—Global. CDR-SB=Clinical Dementia Rating—Sum of Boxes. CV=coefficient of variation in %. hsCRP=high-sensitivity C-reactive protein. MMSE=Mini-Mental State Examination. NA=not applicable. *In France, the law prohibits collection of data on race and ethnicity. †In evoke, oral semaglutide, n=911; placebo, n=916; in evoke+, oral semaglutide, n=964; placebo, n=967. ‡In evoke, oral semaglutide, n=927; placebo, n=927.

Table 1: **Demographic and clinical characteristics of the participants at baseline for evoke(+)**

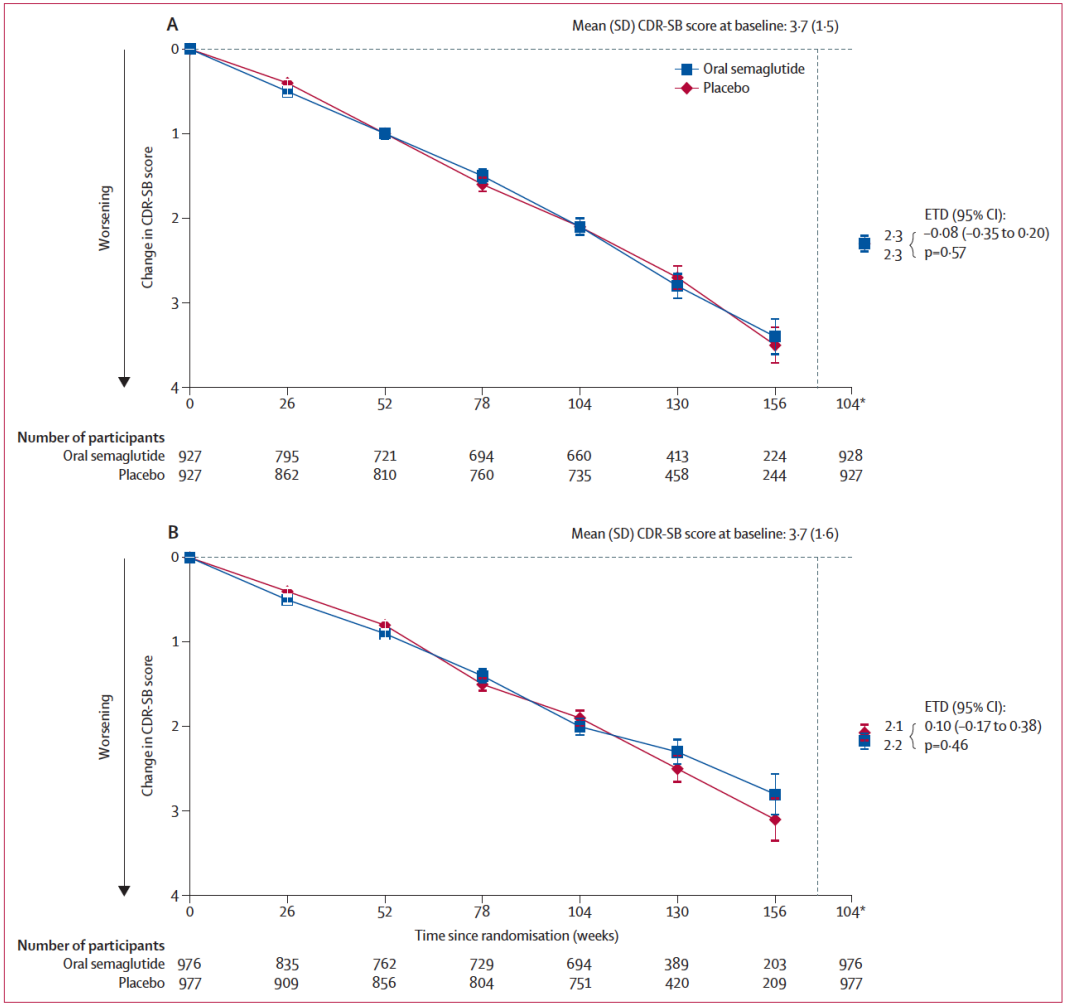

Figure 2: **Change in CDR-SB score from baseline up to week 104 for evoke (A) and evoke+ (B)**
Observed data from the on-treatment dataset. One participant in the oral semaglutide group had a missing baseline value and did not contribute to observed mean at week 0; however, they did contribute to the analyses for estimated mean as participants were assessed post randomisation. Error bars show mean (SE). CDR-SB=Clinical Dementia Rating—Square of Boxes. ETD=estimated treatment difference. HTC=hypothetical–treatment policy–composite. *Estimated mean and corresponding SE at week 104 based on the on-treatment dataset, using the hybrid-HTC estimand.

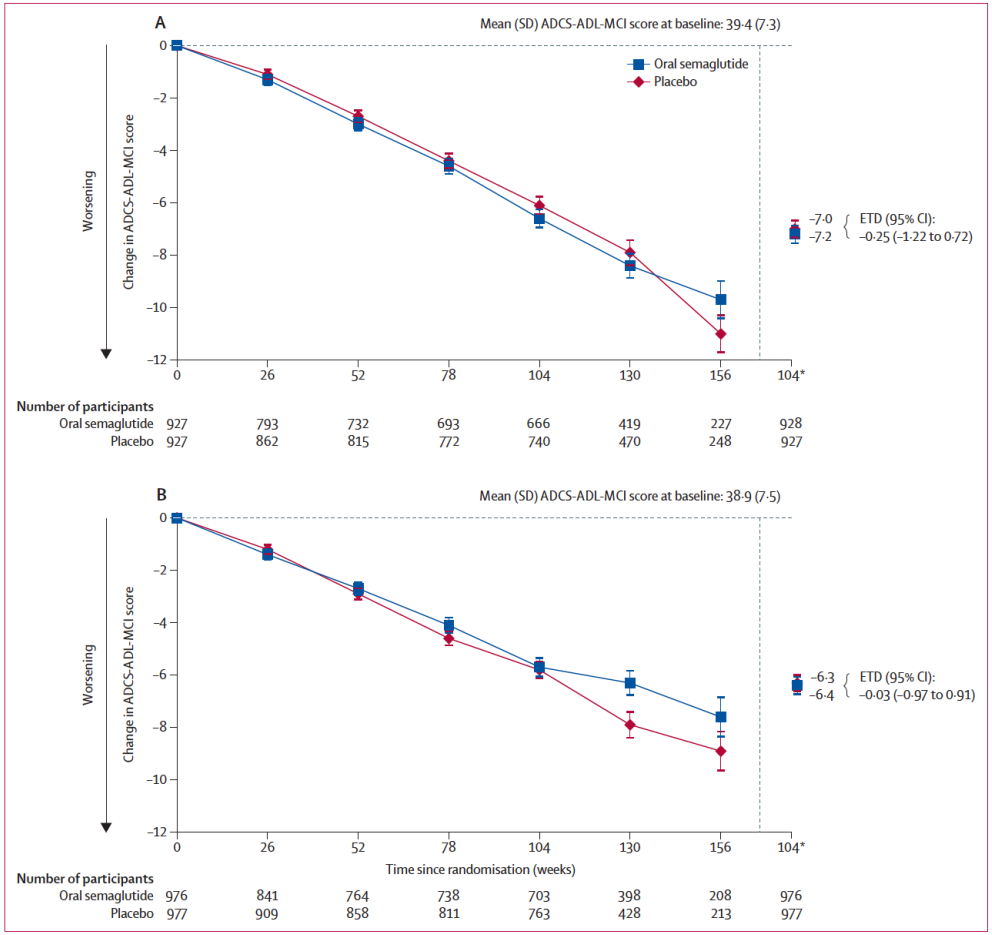

Figure 3: **Change in ADCS-ADL-MCI score from baseline up to week 104 for evoke (A) and evoke+ (B)**
Observed data from the on-treatment dataset. One participant in the oral semaglutide group had a missing baseline value and did not contribute to observed mean at week 0; however, they did contribute to the analyses for estimated mean as participants were assessed post randomisation. Error bars show mean (SE). ADCS-ADL-MCI=Alzheimer's Disease Cooperative Study Activities of Daily Living Scale for mild cognitive impairment. ETD=estimated treatment difference. HTC=hypothetical–treatment policy–composite. *Estimated mean and corresponding SE at week 104 based on the on-treatment dataset, using the hybrid-HTC estimand.

	evoke						evoke+					
	Semaglutide 14 mg (n=924)			Placebo (n=927)			Semaglutide 14 mg (n=972)			Placebo (n=975)		
	Participants	Events	Events per 100 patient-years	Participants	Events	Events per 100 patient-years	Participants	Events	Events per 100 patient-years	Participants	Events	Events per 100 patient-years
Any TEAE	837 (90·6%)	4895	246·2	793 (85·5%)	4248	195·6	892 (91·8%)	5770	278·9	820 (84·1%)	4667	209·2
SAEs	176 (19·0%)	267	13·4	232 (25·0%)	403	18·6	210 (21·6%)	186	17·3	221 (22·7%)	353	15·8
AEs leading to permanent trial product discontinuation	159 (17·2%)	159	8·0	75 (8·1%)	75	3·5	162 (16·7%)	162	7·8	84 (8·6%)	84	3·8
Fatal events*	28 (3·0%)	31	1·4	23 (2·5%)	28	1·2	23 (2·4%)	29	1·3	28 (2·9%)	30	1·3
AEs occurring in ≥10% of participants												
Weight decreased	335 (36·3%)	403	20·3	60 (6·5%)	72	3·3	357 (36·7%)	427	20·6	81 (8·3%)	87	3·9
Decreased appetite	293 (31·7%)	351	17·7	53 (5·7%)	58	2·7	334 (34·4%)	406	19·6	61 (6·3%)	76	3·4
Nausea	233 (25·2%)	344	17·3	64 (6·9%)	77	3·6	227 (23·4%)	323	15·6	66 (6·8%)	81	3·6
Diarrhoea	136 (14·7%)	183	9·2	104 (11·2%)	143	6·6	139 (14·3%)	210	10·2	81 (8·3%)	103	4·6
Vomiting	114 (12·3%)	180	9·1	38 (4·1%)	55	2·5	120 (12·3%)	189	9·1	31 (3·2%)	35	1·6
COVID-19	97 (10·5%)	103	5·2	103 (11·1%)	109	5·0	109 (11·2%)	116	5·6	111 (11·4%)	122	5·5

Data are n (%) or n. Data from baseline up to week 156 for all participants randomly assigned to study drug and who took at least one dose of study drug were included. AE=adverse event. SAE=serious adverse event. TEAE=treatment-emergent adverse event. *Data are for the in-study period and include fatalities reported for participants who withdrew from the trials. Participants could have several ongoing AEs that the investigator reported as having a fatal outcome.

Table 2: **Adverse events for evoke and evoke+**

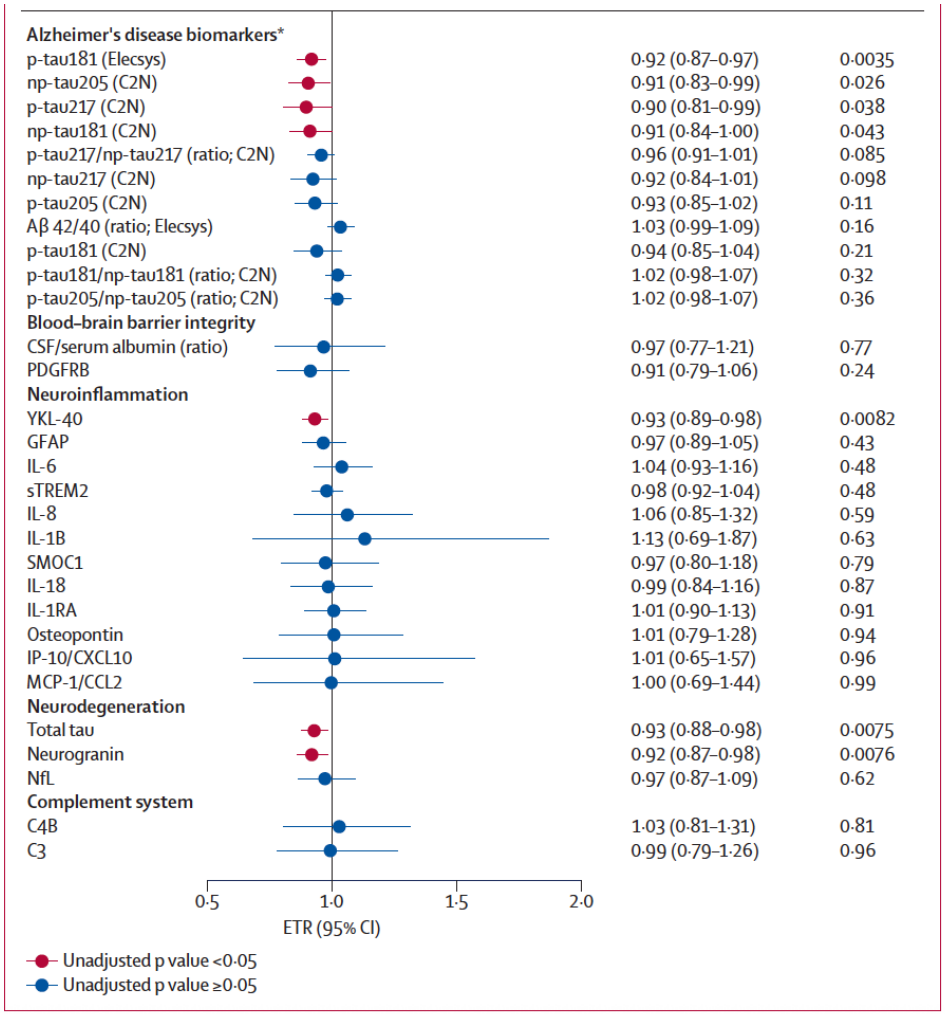

Figure 4: **Changes in plasma biomarkers in evoke and evoke+ (A), and changes in CSF biomarkers in the CSF substudy (B)**
CSF biomarker data are not adjusted for multiplicity. Aβ=amyloid β. CCL2=C-C motif chemokine ligand 2. CSF=cerebrospinal fluid. CXCL10=C-X-C motif chemokine ligand 10. ETR=estimated treatment ratio. GFAP=glial fibrillary acidic protein. IL=interleukin. IL-1RA=interleukin 1 receptor antagonist. IP=interferon gamma-induced protein. MCP-1=monocyte chemoattractant protein-1. NfL=neurofilament light chain. np-tau=non-phosphorylated tau. PDGFRB=platelet-derived growth factor receptor beta. p-tau=phosphorylated tau. SMOC1=SPARC-related modular calcium-binding protein 1. sTREM2=soluble triggering receptor expressed on myeloid cells 2. *Different assays were used by different diagnostics companies (Elecsys and C2N) to measure the Alzheimer's disease biomarkers.

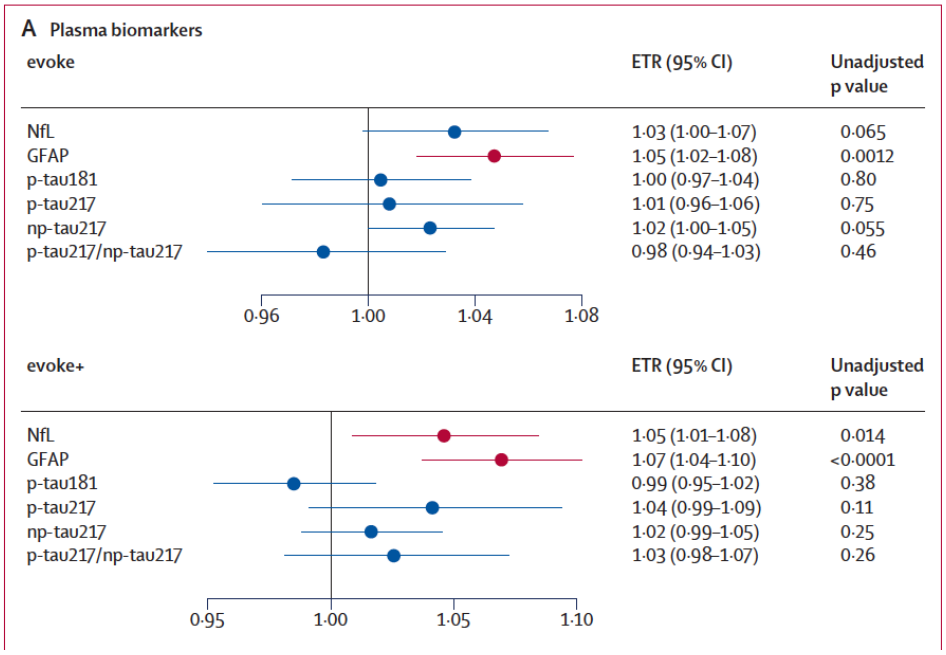

Research in context

Evidence before this study

We searched PubMed on May 15, 2025, with no date or language restrictions, using the search terms "glucagon-like peptide-1 receptor agonist", "GLP-1RA", "Alzheimer's disease", "MCI", "AD", "small vessel pathology", and "cognitive function". In observational, longitudinal cohort studies in patients with type 2 diabetes and/or obesity, a reduced risk of dementia and clinical diagnosis of Alzheimer's disease was reported after GLP-1 receptor agonist exposure. Animal studies demonstrate that GLP-1 receptor agonist exposure reduces systemic and CNS inflammation, improves memory function, and preserves blood–brain barrier integrity. In humans, two small investigator-sponsored studies suggested GLP-1 receptor agonist treatment might prevent cognitive decline or slow disease progression in Alzheimer's disease. These studies provided the basis for the mechanistic hypotheses of the current study relating to anti-inflammatory, neuroprotective, vascular, and blood–brain barrier effects in Alzheimer's disease. The evoke(+) trials were initiated to assess the safety and efficacy of a GLP-1 receptor agonist (once-daily semaglutide up to 14 mg) on top of standard of care for slowing disease progression in individuals with early Alzheimer's disease.

Added value of this study

The evoke(+) trials were the first large-scale, multi-country, randomised clinical trials investigating the clinical efficacy and safety of semaglutide in early-stage Alzheimer's disease. Neither trial demonstrated superiority of oral semaglutide 14 mg to placebo in slowing cognitive or global decline in people with early-stage Alzheimer's disease from baseline to week 104. Prespecified pooled trial analyses did not demonstrate a delay in time to progression to dementia in participants with mild cognitive impairment (MCI) due to Alzheimer's disease from baseline up to week 156. In the cerebrospinal fluid (CSF) substudy, semaglutide led to significant reductions of up to 10% in CSF-based core biomarkers associated with Alzheimer's disease (phosphorylated-tau181 [p-tau181], p-tau217, non-phosphorylated-tau181 [np-tau181], and np-tau205) and CSF biomarkers of neuroinflammation, neurodegeneration, and synaptic function (YKL-40, total tau, and neurogranin). Semaglutide treatment was also associated with significantly reduced plasma high-sensitivity C-reactive protein concentrations.

Implications of all the available evidence

The results of the large evoke(+) trials do not support the efficacy of 14 mg/day of semaglutide given for up to 156 weeks in participants with biomarker-confirmed Alzheimer's disease in the MCI or mild dementia stage.

Alzheimer's disease

Alzheimer's disease is the leading cause of dementia and among the top ten leading causes of death in high-income countries. Exponential advances in epidemiology, genetics, diagnostic imaging and fluid biomarkers, treatment, and prevention in the last decade reinforce the notion that we are entering a new era in the clinical management of Alzheimer's disease. However, far from triumphalism, this momentum should be accelerated to achieve the goals of preventing Alzheimer's disease and arresting its progression. In this Seminar, we summarise this progress and highlight unmet needs and areas of research priority.

Panel 1: Pathophysiology of Alzheimer's disease

The key players in Alzheimer's disease pathophysiology are shown in figure 1 and elaborated in this panel.

Aβ accumulation

In autosomal dominant Alzheimer's disease caused by *APP*, *PSEN1*, or *PSEN2* mutations, Aβ accrual results from a shift towards longer, aggregation-prone Aβ species due to increased amyloidogenic processing of Aβ precursor protein (AβPP) by the γ-secretase complex.[20] In Down syndrome (21 trisomy), the three *APP* copies cause an overexpression of AβPP and overproduction of Aβ.[21] In late-onset Alzheimer's disease, impaired age-related Aβ clearance predominates and is exacerbated in *APOE*ε4 homozygotes, contributing to earlier onset.[22] Aβ monomers aggregate into soluble oligomers and, by a process of seeding-nucleation-polymerisation, these aggregate into insoluble amyloid fibrils, which deposit into Aβ plaques. These are not inert but rather act as reservoirs of synaptotoxic and neurotoxic oligomeric Aβ species as well as inflammatory cytokines and reactive oxygen species released by reactive microglia and astrocytes, all of which cause neuritic dystrophic changes in axons and dendrites (ie, neuritic plaques), as well as loss of synapses.[23,24]

Tau accumulation

Tau, an axonal microtubule-associated protein, which becomes hyperphosphorylated and misfolded through poorly understood mechanisms, detaches from microtubules, and relocates to the neuronal somato-dendritic compartment, disrupting axonal transport. Like Aβ, misfolded hyperphosphorylated tau aggregates into soluble oligomers and these into paired helical filaments that form neurofibrillary tangles. The molecular mechanisms linking extracellular Aβ accumulation with intraneuronal tau hyperphosphorylation, misfolding, and aggregation are not well understood. Tau accumulates preferentially in excitatory pyramidal neurons and spreads along neural networks following a stereotyped spatiotemporal pattern defined by the Braak neurofibrillary tangle staging,[25] which likely reflects selective vulnerability of these neurons and brain regions combined with prion-like trans-synaptic neuron-to-neuron propagation of tau seeds.[26]

Synaptic loss and neuronal death

Synaptic loss is the strongest correlate of the severity of cognitive decline.[24] Both Aβ and tau oligomers disrupt synaptic function and tag synapses for elimination by reactive microglia and astrocytes. Neuronal death is predominantly apoptotic, although alternative mechanisms such as necroptosis have been proposed. Some neurofibrillary tangle-bearing neurons end up dying leaving an extracellular ghost or tombstone neurofibrillary tangle but the number of neurons missing in the Alzheimer's disease brain is an order of magnitude greater than the sum of observable intraneuronal and extracellular neurofibrillary tangles, suggesting that many neurons die through a neurofibrillary tangle-independent mechanism or that extracellular neurofibrillary tangles are rapidly removed or degraded.[25]

Reactive glia

Aβ plaques, tau neurofibrillary tangles, and their soluble oligomers trigger microglia and astrocyte responses, collectively termed reactive gliosis. Reactive gliosis is a dynamic and complex phenomenon that involves gains and losses of functions.[27,28] Reactive glia might initially be protective but is thought to become chronically maladaptive, with gain of toxic functions and loss of homeostatic properties that accelerate synaptic and neuronal dysfunction and neurodegeneration. These responses are amplified in *APOE*ε4 carriers, particularly within microglia.[22,29,30]

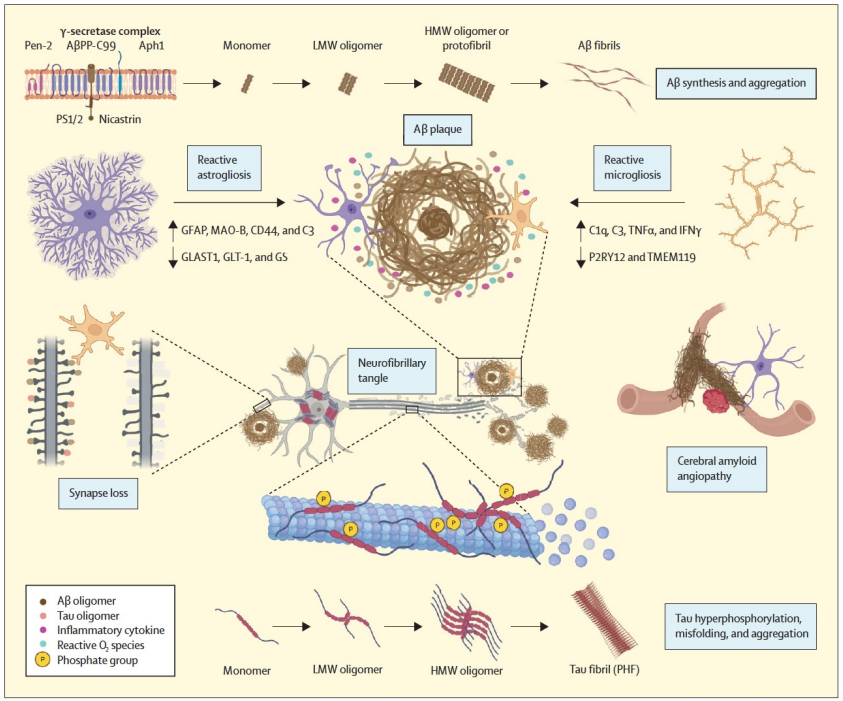

Figure 1: **Pathophysiology of Alzheimer's disease**
Aβ is released upon the cleavage of Aβ precursor protein (AβPP) C-terminal 99 amino acid fragment by the proteolytic activity of presenilin within the γ-secretase complex. Aβ monomers aggregate into LMW oligomers, these into HMW oligomers and protofibrils, which polymerise into Aβ fibrils. Aβ fibrils deposit in the parenchyma as plaques and in the wall of small and medium-sized parenchymal and leptomeningeal arteries as well as parenchymal capillaries as cerebral amyloid angiopathy. Severe cerebral amyloid angiopathy leads to lobar cerebral microbleeds, which can be the precursor of a major intracerebral haemorrhage. Aβ plaques trigger morphological, molecular, and functional changes in astrocytes and microglia, collectively termed reactive gliosis. Aβ plaques are not inert but act as reservoirs of Aβ oligomers, inflammatory cytokines, and reactive oxygen species, which are toxic to synapses and neurons. Tau stabilises microtubules within neuronal axons but becomes abnormally hyperphosphorylated and detaches from microtubules. Microtubule destabilisation impairs the neuron axonal transport. Hyperphosphorylated tau misfolds and aggregates into oligomers and these aggregate into tau fibrils. Synapses tagged by Aβ and tau oligomers are opsonised by complement factors (C1q and C3) and phagocytosed by reactive microglia and astrocytes. C1q=complement 1q factor. C3=complement 3 factor. GFAP=glial fibrillary acidic protein. HMW=high molecular weight. LMW=low molecular weight. MAO-B=monoamine oxidase-B. P2RY12=P2Y purinergic receptor 12. PHF=paired helical filament. TMEM119=transmembrane protein 119. TNF=tumour necrosis factor. Figure created in BioRender.

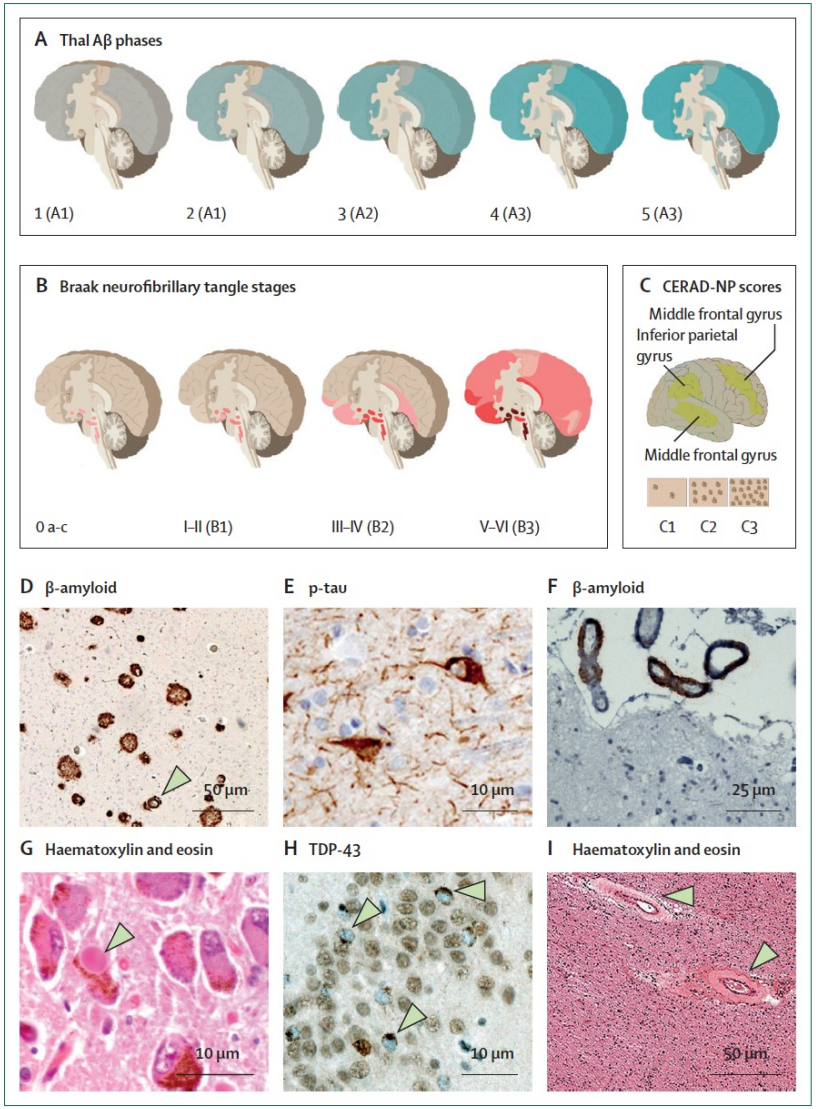

Figure 2: **Neuropathological characteristics and stages of Alzheimer's disease**

Panels A–C depict the stereotypical spread of Alzheimer's disease neuropathologic change across three staging schemes integrated in the National Institute on Aging–Alzheimer's Association ABC score. (A) Thal Aβ phases (A0 [none] to A3) reflect the stereotypical spreading of Aβ deposits from neocortex to hippocampus (A1), subcortical regions (A2), and brainstem and cerebellum (A3). (B) Braak neurofibrillary tangle stages (B0–B3) reflect the stereotypical progression of neurofibrillary tangles from the neuromodulatory subcortical system (B0 a–c) to transentorhinal cortex and hippocampus (B1), limbic areas (B2), and then widespread in neocortical regions (B3). (C) CERAD-NP scores (C0–C3) indicate the density of neuritic plaques from none (C0) to sparse (C1), moderate (C2), and frequent (C3) in any of three neocortical regions (middle frontal, middle and superior temporal, or inferior parietal). The combined ABC score provides an overall estimate of Alzheimer's disease neuropathologic change (not, low, intermediate, or high). Panels D–I depict microscopic photographs of histological preparations illustrating common neuropathological changes associated with cognitive decline. (D) Neuritic plaques, composed of Aβ deposits (brown). The arrow highlights an example of parenchymal cerebral amyloid angiopathy. (E) Neurofibrillary tangles of hyperphosphorylated tau with associated neuropil threads. (F) Leptomeningeal cerebral amyloid angiopathy (ie, amyloid-β deposition in the wall of leptomeningeal arteries). (G) Lewy body (arrow) within a substantia nigra neuron, typical of Lewy body disease. (H) TDP-43 pathology with cytoplasmic inclusions in dentate gyrus granule neurons (arrows). This section was immunostained for TDP-43; under normal conditions, neuronal nuclei are TDP-43-positive (brown), whereas in pathological conditions neurons lose nuclear TDP-43 (hence, appearing blue due to haematoxylin counterstain) and abnormal TDP-43 inclusions accumulate in the cytoplasm. (I) Arteriolosclerosis, characterised by thickened small vessel walls (arrows), a common age-related vascular pathology. Scale bars are as indicated. CERAD-NP=Consortium to Establish a Registry for Alzheimer's Disease neuritic plaque.

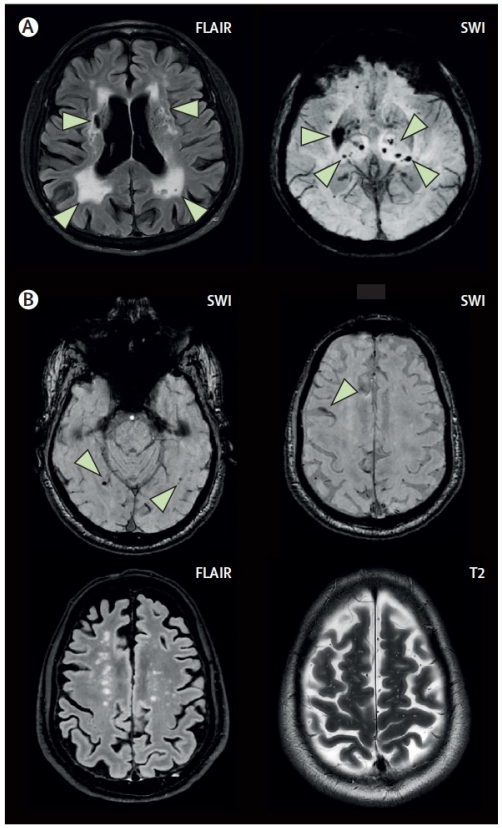

Figure 3: **Use of MRI in the diagnosis of Alzheimer's disease**
(A) MRI features of small vessel disease in an 86-year-old man with poorly controlled chronic hypertension. FLAIR shows severe periventricular white matter hyperintensities and lacunar strokes in basal ganglia (arrows). SWI shows multiple microbleeds in basal ganglia typical of hypertensive microangiopathy (arrows). (B) MRI features of cerebral amyloid angiopathy in a 71-year-old man with mild cognitive impairment and a positive [^{18}F]-florbetaben amyloid PET. SWI revealed up to 12 microbleeds and three areas of focal cortical superficial siderosis (arrows), one in the right frontal lobe. FLAIR showed the typical multispot pattern of white matter hyperintensities in centri semiovale. T2 showed enlarged perivascular spaces in centri semiovale. FLAIR=fluid-attenuated inversion recovery. SWI=susceptibility weighted imaging.

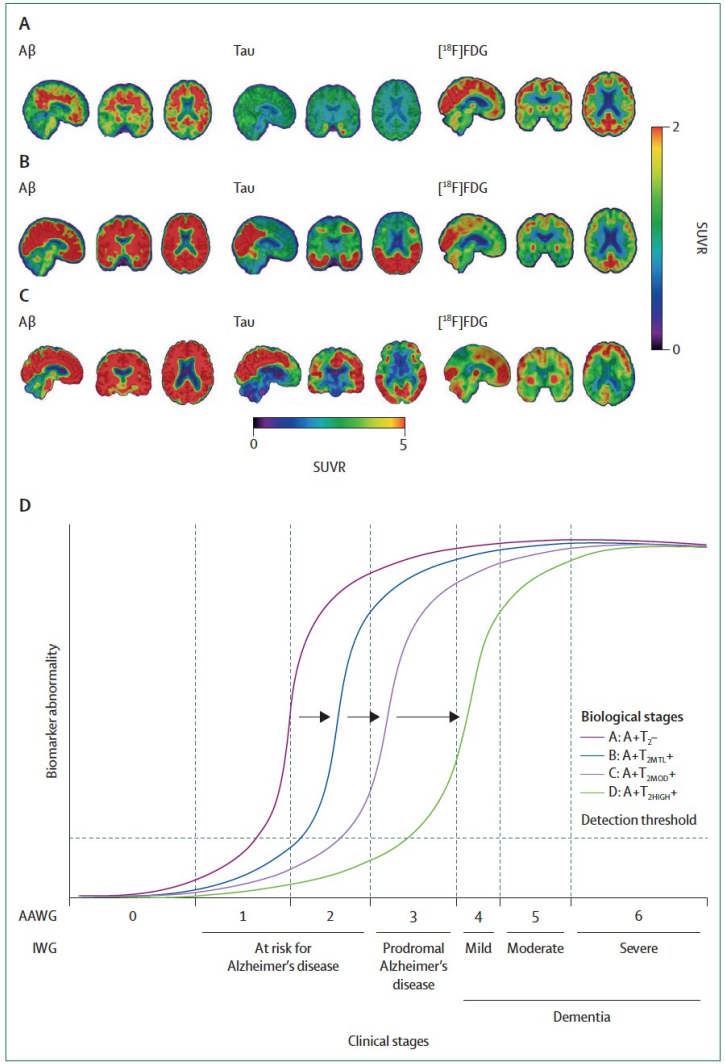

Figure 4: **Use of PET imaging biomarkers in the diagnosis and staging of Alzheimer's disease**
(A) A 66-year-old non-Hispanic white woman with *APOE*ε3/ε4 genotype and a clinical diagnosis of amnestic mild cognitive impairment (CDR global=0·5, CDR-SB=0·5) due to Alzheimer's disease based on a positive Aβ PET ([^{18}F]NAV4694) and a tau PET ([^{18}F]MK-6240) showing tau accumulation restricted to the medial temporal region. The [^{18}F]FDG-PET still revealed normal cerebral glucose metabolism. (B) A 70-year-old non-Hispanic white man with *APOE*ε3/ε4 genotype and a clinical diagnosis of mild dementia (CDR global=1·0, CDR-SB=4·5) due to Alzheimer's disease supported by a positive Aβ PET ([^{18}F]NAV4694) and a tau PET ([^{18}F]-MK-6240) showing extensive tau deposition in temporal and occipital cortices, posterior cingulate gyrus, and praecuneus. The [^{18}F]FDG-PET showed the typical Alzheimer's disease pattern of symmetric hypometabolism in the temporoparietal regions and posterior cingulate cortex. (C) A 62-year-old non-Hispanic white woman with *APOE*ε3/ε4 genotype and a clinical diagnosis of posterior cortical atrophy (CDR global=1·0, CDR-SB=8·0) due to Alzheimer's disease supported by a positive Aβ PET ([^{18}F]NAV4694) and a tau PET ([^{18}F]MK-6240) showing tau deposition predominantly in the occipital cortex, already extending to frontal regions. The [^{18}F]FDG-PET showed severe glucose hypometabolism in occipital cortex extending into parietal and temporal areas, and reduced metabolism in posterior cingulate gyri and praecuneus. (D) Biological and clinical stages of Alzheimer's disease proposed by the AAWG based on Aβ and tau PET. Biological stages advance from A to D, where stage A (initial) is defined by positive Aβ PET or cerebrospinal fluid Alzheimer's disease biomarkers or an accurate blood-based biomarker, but negative tau PET (ie, A+T$_{2-}$); stage B (early) requires positive Aβ PET or cerebrospinal fluid Alzheimer's disease biomarkers or an accurate blood-based biomarker plus tau PET uptake restricted to the medial temporal lobe (ie, A+T$_{2MTL}$+); stage C (intermediate) is characterised by moderate neocortical tau PET uptake (ie, A+T$_{2MOD}$+); and stage D (advanced) implies high neocortical tau PET uptake (ie, A+T$_{2HIGH}$+). Clinical stages advance from 0 to 6 where stage 0 represents pre-symptomatic genetically determined Alzheimer's disease (ie, asymptomatic individuals with a deterministic gene (eg, autosomal dominant Alzheimer's disease or Down syndrome-associated Alzheimer's disease) as per the AAWG staging, or with pre-symptomatic Alzheimer's disease as per the IWG); stage 1 is preclinical Alzheimer's disease (ie, asymptomatic with biomarker evidence only as per the AAWG staging, or individuals at risk for Alzheimer's disease based on the IWG staging, including those with pre-symptomatic Alzheimer's disease based on a specific biomarker profile correlated with very high risk of progression to clinical disease); stage 2 roughly corresponds to subjective cognitive decline (transitional decline, mild detectable change but minimal impact on daily function as per AAWG staging, and still at risk for Alzheimer's disease in the IWG staging); stage 3 roughly corresponds to mild cognitive impairment (cognitive impairment with early functional impact in the AAWG staging or prodromal Alzheimer's disease in the IWG staging); and stages 4–6 roughly represent mild (stage 4), moderate (stage 5), and severe dementia (stage 6). The vertical dashed lines separating the clinical stages are placed along the x-axis based on an archetypical individual. Figure created in BioRender. [^{18}F]FDG=[^{18}F]Fluorodeoxyglucose. AAWG=Alzheimer's Association Workgroup. CDR=clinical dementia rating. IWG=International Working Group. SB=sum of boxes. SUVR=standardised uptake value ratio.

	Mechanism of action	Route of administration	Indication	Adverse side-effects	Evidence source
Cognitive impairment					
Acetyl-cholinesterase inhibitors (eg, donepezil, rivastigmine, and galantamine)	Inhibition of acetyl-cholinesterase	Orally or transdermally	Mild, moderate, and severe dementia	Nausea, vomiting, diarrhoea, leg cramps, and REMSBD	RCT
Memantine	NMDA receptor antagonist	Orally	Moderate and severe dementia	Nausea, insomnia, and headaches	RCT
Neuropsychiatric symptoms					
SSRIs (eg, citalopram, escitalopram, and sertraline)	Inhibition of serotonin reuptake	Orally	Depression and anxiety	Long QTc, serotonin syndrome, REMSBD, and tremor	Empirical
SNRIs (eg, venlafaxine and duloxetine)	Inhibition of serotonin and norepinephrine reuptake	Orally	Depression and anxiety	Long QTc, serotonin syndrome, hypertension, and REMSBD	Empirical
Bupropion	Inhibition of dopamine and norepinephrine reuptake	Orally	Depression and anxiety	Hypertension, seizures, insomnia, and tremor	Empirical
Buspirone	5-HT1A receptor partial agonist	Orally	Anxiety	Serotonin syndrome and REMSBD	Empirical
Atypical neuroleptic drugs (eg, quetiapine, olanzapine, risperidone, and ziprasidone)	D2 dopamine receptor blockage	Orally, intramuscularly, or intravenously	Psychosis	Metabolic syndrome, parkinsonism, long QTc, NMS, and black box warning	RCT
Pimavanserine	5-HTA2A receptor inverse agonist and antagonist, lesser activity at 5-HT2C receptor	Orally	Psychosis	Long QTc and serotonin syndrome	RCT
Brexpiprazole	α1B and α2C noradrenergic and 5-HT2A serotonergic receptor antagonist, 5-HT1A serotoninergic, and D2 dopaminergic receptor partial agonist	Orally	Agitation	Akathisia, dystonia, EDS, weight gain, and insomnia	RCT
Methylphenidate	Increased release of dopamine and noradrenaline	Orally	Apathy	Hypertension, tachycardia, anxiety, and insomnia	RCT
Dextromethorphan and quinidine	NMDA receptor antagonist and sigma-1 receptor agonist (dextromethorphan); Na^+ channel blocker (quinidine)	Orally	Pseudobulbar affect (pathological crying or laughing)	Diarrhoea, dizziness, long QTc, thrombocytopenia, and elevated liver function test	RCT
Melatonin	Melatonin replacement	Orally	Insomnia and REMSBD	EDS	Empirical
Trazodone	Serotonin antagonist and reuptake inhibitor	Orally	Insomnia and agitation	EDS, long QTc, and REMSBD	RCT
DORAs (eg, suvorexant and lemborexant)	Dual orexin receptor antagonists	Orally	Insomnia	EDS	RCT
Clonazepam	Benzodiazepine	Orally	REMSBD	EDS	RCT
Anorexia or weight loss					
Mirtazapine	α2 adrenergic, 5-HT2 and 5-HT3 serotonergic and H1 histaminic receptor antagonist	Orally	Anorexia and weight loss	EDS, long QTc, and increased appetite or weight gain	Empirical
Megestrol	Progesterone receptor agonist	Orally	Anorexia and weight loss	Increased appetite or weight gain, hypogonadism, and glucocorticoid effects	Empirical
Seizures					
Anti-epileptic drugs (eg, levetiracetam and lamotrigine)	Various mechanisms	Orally	Epilepsy	Drug-specific adverse effects	Empirical

The presented list is not exhaustive. DORAs=dual orexin receptor antagonists. EDS=excessive daytime sleepiness. HT=hydroxy-tryptamine (serotonin). NMDA=N-methyl-D-aspartate. NMS=neuroleptic malignant syndrome. QTc=corrected Q wave-T wave interval. RCT=randomised clinical trial. REMSBD=rapid eye movement sleep behaviour disorder. SNRIs=serotonin-noradrenaline reuptake inhibitors. SSRIs=selective serotonin reuptake inhibitors.

Table: **Treatment of Alzheimer's disease symptoms**

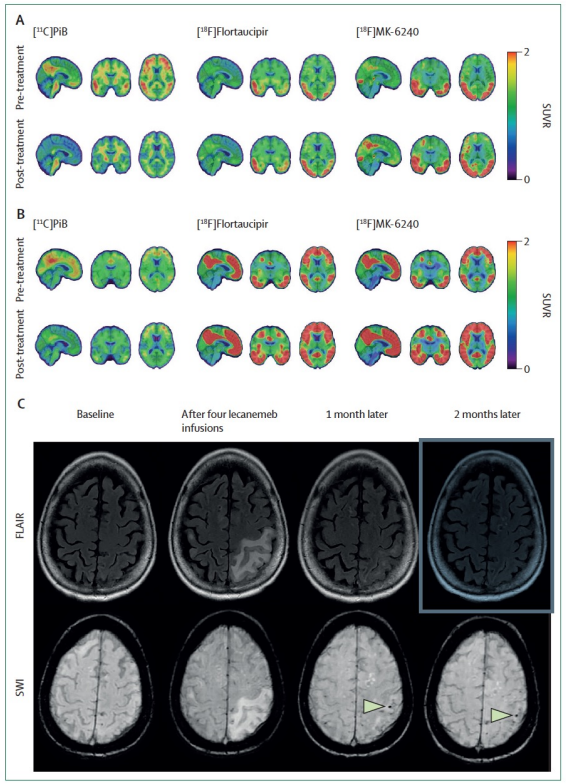

Figure 5: **Effects of anti-Aβ immunotherapy on Alzheimer's disease PET imaging biomarkers and ARIA during anti-Aβ immunotherapy**

(A) Baseline and post-treatment Aβ ([^{11}C]-PiB) and tau ([^{18}F]-Flortaupicir and [^{18}F]-MK-6240) PET scans of an 82-year-old *APOE*ε3/ε4 non-Hispanic white man with an initial diagnosis of mild cognitive impairment due to Alzheimer's disease (CDR global=0·5, CDR-SB=3·5). Note the low tau PET uptake at baseline. After 36 biweekly infusions of lecanemab his Aβ PET scan became negative and his CDR global and CDR-SB scores remained stable. (B) Baseline and post-treatment Aβ ([^{11}C]-PiB) and tau ([^{18}F]-Flortaupicir and [^{18}F]-MK-6240) PET scans of a 50-year-old *APOE*ε3/ε4 white Hispanic woman with a diagnosis of mild cognitive impairment due to Alzheimer's disease (CDR global=0·5, CDR-SB=3·0). Note the high tau PET uptake at baseline. Despite substantial Aβ plaque removal after 32 biweekly infusions of lecanemab, she transitioned to mild dementia (CDR global=1·0, CDR-SB=6·0). (C) Baseline and serial FLAIR and SWI MRI sequences of a female APOEε4/ε4 carrier in her 70s with mild dementia (CDR global=1·0) who presented with right-sided numbness and weakness after her fourth infusion of lecanemab. Brain MRI showed vasogenic parenchymal oedema in left frontal and parietal lobes consistent with radiologically moderate ARIA-E. Lecanemab was discontinued and the patient was admitted to the hospital and treated with intravenous methylprednisolone (1 g daily for 5 days) followed by an oral prednisone taper. Her symptoms resolved completely in the following weeks, and ARIA-E was tracked with monthly serial MRIs until resolution. No ARIA-haemorrhage was initially noted but new lobar microbleeds (arrows) emerged in the territory of ARIA-E upon ARIA-E resolution, a typical phenomenon in the natural history of ARIA. ARIA=amyloid-related imaging abnormality. ARIA-E=amyloid-related imaging abnormality with odema or effusion. CDR=clinical dementia rating. PiB=Pittsburgh compound B. FLAIR=fluid-attenuated inversion recovery. SB=sum of boxes. SUVR=standardised uptake value ratio. SWI=susceptibility weighted imaging.

Panel 2: **Areas of uncertainty, unmet needs, and research priorities**

Genetics and epidemiology

- Large genome-wide association study meta-analyses have identified numerous Alzheimer's disease-linked risk loci; future studies should go beyond case–control studies and prioritise tracking the genetic effects on rate of progression across clinical stages
- The genetic architecture of Alzheimer's disease is highly complex; leveraging machine learning approaches could enable detection of previously unrecognised gene-gene interactions
- Epidemiological evidence highlights multiple modifiable, non-genetic risk factors that might offset the individual's genetic risk and should inform individual-level and population-level dementia preventative strategies
- Gene–environment interactions remain underexplored and should be integrated into Alzheimer's disease risk and progression models, which are urgently needed to explain clinical heterogeneity

Neuropathology and pathophysiology

- Neocortical Aβ plaque deposition appears to facilitate tau neurofibrillary tangle spreading beyond the medial temporal lobe, and Aβ immunotherapy is most effective when neurofibrillary tangles are circumscribed to the medial temporal lobe, yet the molecular links between these two proteinopathies remain poorly understood
- The precise mechanisms underlying selective neuronal vulnerability and resilience remain elusive and will provide crucial insights for prevention and neuroprotection
- Given the near-universal presence of copathologies, such as argyrophilic grain disease, aging-related tau astrogliopathy, cerebral amyloid angiopathy, limbic-predominant age-related TDP43 encephalopathy-neuropathologic change, Lewy body and vascular diseases, their interactions with Alzheimer's disease characteristics and effects on clinical expression, disease progression, and therapeutic response require systematic study
- The contribution of non-neuronal cells, including glia and endothelial cells, is increasingly recognised, but their bidirectional relationships with Alzheimer's disease neuropathological change and neurons remain incompletely defined

Biomarkers

- Current fluid and imaging biomarkers have insufficient sensitivity to the earliest stages of Alzheimer's disease neuropathologic change, underscoring the need for biomarkers that can reliably detect preclinical disease and better reflect the spatiotemporal progression observed in postmortem studies
- Developing PET tracers, as well as cerebrospinal fluid biomarkers and blood-based biomarkers (BBMs), for common copathologies will enhance diagnostic precision and prognostication
- Designing more sensitive cell-type-specific PET tracers capable of distinguishing reactive from homeostatic glia phenotypes and, in the case of BBMs, also discerning between brain from peripheral signals, will help understand the contribution of reactive glia to Alzheimer's disease progression and, perhaps, improve prognosis
- The harmonisation of cerebrospinal fluid and BBM assays and protocols across platforms and laboratories and the standardisation of tau PET quantification across tracers are essential for consistent research and clinical use
- BBM implementation in primary and secondary care settings will require validated cutoffs, adapted clinical workflows, and targeted education to avoid misinterpretation of results by health-care providers and patients
- Increased inclusion of diverse populations in research and clinical settings is an unmet need; development of more accessible sampling approaches (eg, dried blood spot) will facilitate a more equitable deployment of BBMs
- There is a need to accelerate drug development pipelines by reducing the length and size of clinical trials; robust BBMs will not only support participant selection but also serve as pharmacodynamic, predictive markers, and potentially surrogate endpoints

Treatment and prevention

- After more than two decades of learning from unsuccessful trials, anti-Aβ immunotherapy is being refined to improve efficacy, delivery, and safety, particularly regarding amyloid-related imaging abnormality risk in *APOE*ε4 carriers
- Clinical trial research is currently amid the learning curve for tau-directed therapies, including immunotherapy and gene silencing approaches
- Beyond Aβ and tau, there is an urgent need for microglia-directed and astrocyte-directed neuroprotective therapies capable of slowing down Aβ-independent and tau-independent neurodegenerative cascades
- APOE-directed therapies, including gene therapy, are underdeveloped but could hold the key to complete prevention in *APOE*ε4 carriers
- Consortia, such as the Dominantly Inherited Alzheimer Network–Trial Unit and the Alzheimer's Clinical Trials Consortium–Down Syndrome, are accelerating drug development for autosomal dominant Alzheimer's disease and Down syndrome-associated Alzheimer's disease
- Multimodal lifestyle interventions targeting modifiable risk factors could substantially reduce dementia prevalence, but implementation requires sustained and comprehensive public health policies

Conclusions

After decades of sustained research progress,[262] the field of Alzheimer's disease is seeing transformative advances that are beginning to reshape clinical practice. These efforts have yielded a clearer understanding of modifiable and genetic risk factors, refined clinical–pathological correlations, provided an array of diagnostic imaging and fluid biomarkers (including blood-based assays), crystallised in the approval of the first DMTs, and reinforced the importance of evidence-based preventative strategies. Much more needs to be done (panel 2), but this momentum is fuelling new avenues of research into Alzheimer's disease that hold promise to flatten the trajectory of this devastating and complex neurodegenerative disease at both individual and societal levels.

DMTs steht für Disease-Modifying Therapies.

NIH, NASA place limits on foreign co-authors

Grants managers at two of the U.S. government's largest funders of scientific research have recently placed unprecedented limitations on the ability of U.S. scientists to publish with co-authors from other countries, researchers say. Units of the National Institutes of Health (NIH) are privately directing grantees to request permission in advance for any co-authorship with a scholar affiliated with a foreign institution, even if all the work was done in the United States. NASA, meanwhile, is reportedly telling some grantees that papers coauthored with researchers in China may have violated its rules.

Neither agency has publicly issued new formal guidance describing these requirements. Instead, officials are informing grantees individually, leaving researchers confused and concerned. In several cases, NIH grantees say they have been asked to leave out published papers with foreign co-authors from progress reports. Observers say the policy creates an incentive to preemptively remove foreign coauthors from forthcoming papers.

Trump appointees push $250 banknote with his portrait

Trump administration officials have pressed the office responsible for printing the nation's money to design a $250 bill featuring the president's portrait, according to four current and former employees, in what would be the first appearance of a living person on U.S. currency in more than 150 years.

Starting last year, two political appointees at the Treasury Department — U.S. Treasurer Brandon Beach and his senior adviser, Mike Brown — repeatedly urged staff at the agency's Bureau of Engraving and Printing to prepare prototypes of the note, according to the employees, who said the move raised concerns because federal law currently allows only deceased people to appear on bills.